MOLECULAR ORIENTATION AND RELAXATION PHENOMENA

IN POLYMER SOLIDS

STUDIED BY ANALYSIS OF FLUORESCENCE POLARIZATION

YOSHIYUKI NISHIO

DEPARTMENT OF POLYMER CHEMISTRY

KYOTO UNIVERSITY

1 9 8 1

CONTENTS

LIST OF SYMBOLS

The symbols used in this thesis are listed below.

Symbols introduced in <u>Chap. 2.</u>

O-KLM	Coordinate system fixed in a fluorescent molecule.
A_i	Absorbing oscillator of a fluorescent molecule.
F_i	Emitting oscillator of a fluorescent molecule.
δ, ε	Polar and azimuthal angles, respectively, specifying the direction of A_i in the molecular coordinate system O-KLM.
η, ξ	Polar and azimuthal angles, respectively, specifying the direction of F_i in the O-KLM system.
$g(\delta, \varepsilon)$	Probability function of finding A_i in the direction (δ, ε) in the O-KLM system.
$h(\eta, \xi)$	Probability function of finding F_i in the direction (η, ξ) in the O-KLM system.
O-abc	Sample coordinate system fixed in a specimen.
$\omega, \varphi, \chi \ (= \Omega)$	Three Euler angles specifying the orientation of a fluorescent molecule (O-KLM) in the sample coordinate system O-abc.
$m(\omega, \varphi, \chi)$	Orientation distribution function of fluores-

cent molecules in the O-abc system.

Δ, E Polar and azimuthal angles, respectively, specifying the orientation of $\mathbb{A}_i$ in the O-abc system.

H, Ξ Polar and azimuthal angles, respectively, specifying the orientation of $\mathbb{F}_i$ in the O-abc system.

$q(\Delta, E)$ Orientation distribution function of $\mathbb{A}_i$ in the O-abc system.

$r(H, \Xi | A)$ Orientation distribution function of $\mathbb{F}_i$ in the O-abc system.

$Y_{\ell m}$ Spherical harmonics.

$\Phi_{\ell m n}$ Generalized spherical harmonics.

P_ℓ^m Normalized associated Legendre function.

$Z_{\ell m n}$ Generalized associated Legendre function.

D_{mn}^ℓ Wigner rotation matrix.

$G_{\ell n}$ Coefficient for the expansion of $g(\delta, \varepsilon)$ in a series of spherical harmonics $Y_{\ell n}(\delta, \varepsilon)$, characterizing the intrinsic anisotropy of light absorption of a fluorescent molecule.

$H_{\ell' n'}$ Coefficient for the expansion of $h(\eta, \xi)$ in a series of spherical harmonics $Y_{\ell' n'}(\eta, \xi)$, characterizing the intrinsic anisotropy of emission of a fluorescent molecule.

$M_{\ell' m' n'}^{\ell \, m \, n}$ Coefficient for the series expansion of $m(\omega, \varphi, \chi)$ expressed in terms of the product of two gener-

alized spherical harmonics, $\Phi_{\ell mn}(\Omega)\,\Phi_{\ell'm'n'}(\Omega)$, characterizing the molecular orientation distribution.

$\mathbb{P}_1$ Transmission axis of polarizer.

$\mathbb{P}_2$ Transmission axis of analyzer.

α_1,β_1 Polar and azimuthal angles, respectively, specifying the direction of $\mathbb{P}_1$ in the O-abc system.

α_2,β_2 Polar and azimuthal angles, respectively, specifying the direction of $\mathbb{P}_2$ in the O-abc system.

i_a Excitation probability of fluorescent molecule by the incident exciting light.

i_f Detection probability of the fluorescence emitted from $\mathbb{F}_i$ through the analyzer.

$I\binom{\mathbb{P}_1}{\mathbb{P}_2}$ Polarized component of fluorescence intensity.

$S_{\ell m}$ Coefficient for the expansion of i_a in a series of spherical harmonics $Y_{\ell m}{}^*(\Delta,E)$, characterizing the excitation probability.

$T_{\ell'm'}$ Coefficient for the expansion of i_f in a series of spherical harmonics $Y_{\ell'm'}{}^*(H,\Xi)$, characterizing the detection probability.

$\mathbb{E}_i$ Electric field of the exciting light at a position 1 of a fluorescent molecule in the

	anisotropic medium.
E_{i1}, E_{i2}	Two components of E_i, divided in the directions of privileged axes of the medium.
T_i	Period of oscillation of the exciting light E_i.
a_{i1}, a_{i2}	Amplitudes of E_{i1} and E_{i2}, respectively.
P_{1-1}, P_{1-2}	Vibration axes of E_{i1} and E_{i2}, respectively.
δ_i	Phase difference between the two components E_{i1} and E_{i2}.
α_1', β_1'	Polar and azimuthal angles, respectively, specifying the direction of P_{1-1} in the O-abc system.
α_1'', β_1''	Polar and azimuthal angles, respectively, specifying the direction of P_{1-2} in the O-abc system.
E_1, E_2	Electric fields of two detected fluorescence rays coming to the air from F_i in the anisotropic medium.
T_f	Period of oscillation of detected fluorescence light.
a_1, a_2	Amplitudes of E_1 and E_2, respectively.
j_1, j_2	Vibration axes of E_1 and E_2, respectively.
δ_f	Phase difference between E_1 and E_2.
$E_1^{(1)}$, $E_2^{(2)}$	Electric fields of two fluorescence rays in the anisotropic medium, corresponding to E_1 and E_2, respectively, in the air.

$\mathbb{p}_{2-1}$ $(= \mathbb{j}_1^{(1)})$,
$\mathbb{p}_{2-2}$ $(= \mathbb{j}_2^{(2)})$ $\Big\}$ Vibration axes of $\mathbb{E}_1^{(1)}$ and $\mathbb{E}_2^{(2)}$, respectively.

a_{f1}, a_{f2} Scalar products $(\mathbb{p}_2 \cdot \mathbb{j}_1)$ and $(\mathbb{p}_2 \cdot \mathbb{j}_2)$, respectively.

α_2', β_2' Polar and azimuthal angles, respectively, specifying the direction of $\mathbb{p}_{2-1}$ in the O-abc system.

α_2'', β_2'' Polar and azimuthal angles, respectively, specifying the direction of $\mathbb{p}_{2-2}$ in the O-abc system.

D   Thickness of a sample.

$[\ ]_{int}$ in   Refers to the birefringence effect, and

$[S_{\ell m} T_{\ell' m'}]_{int}$ denotes $\int_0^D \sim dl/D$.

Symbols introduced in <u>Chap. 3</u>.

Δn Birefringence.

n_a, n_b, n_c Refractive indices along the principal axes, a, b, and c, of the optically anisotropic medium.

λ_i, λ_f Wavelengths of exciting light and fluorescence, respectively, in the air.

R   Fluorescence anisotropy ratio.

R_0 Fluorescence anisotropy ratio obtained for the rigid matrix in which fluorescent molecules orient randomly.

$\langle\cos^2\delta\rangle,$
$\langle\cos^2\eta\rangle$ } Photophysical anisotropy factors of fluorescent molecules.

$\langle\cos^2\omega\rangle,$
$\langle\cos^4\omega\rangle$ } Second and fourth moments, respectively, about the c-axis of the molecular orientation distribution.

$\langle\sin^2\omega\cos^2\varphi\rangle,$
$\langle\sin^4\omega\cos^4\varphi\rangle$ } Second and fourth moments, respectively, about the a-axis of the molecular orientation distribution.

$\langle\sin^4\omega\cos^2\varphi\rangle$ Another fourth order moment of the molecular orientation distribution.

θ_i Angle between the normal of film surface and an incident beam.

θ_j Angle between the normal of film surface and a direction of fluorescence observation.

θ_{i1}, θ_{i2} Refractive angles of two exciting lights oscillating parallel (I) and perpendicular (II) to the plane of incidence, when they enter the anisotropic medium from the air.

n_{s1}, n_{s2} Refractive indices of the anisotropic medium for the two exciting rays -I and -II.

θ_{i1}' Refractive angle of the normal of light wave front corresponding to the exciting ray-I.

t_1, t_2 Amplitude transmission coefficients of the two rays -I and -II, respectively.

T_1, T_2 Transmittances of light energy of the two

                rays -I and -II, respectively.

θ_1, θ_2 Incident angles of two fluorescence rays whose

                electric fields are parallel (I) and perpen-

                dicular (II) to the plane of incidence, when

                they enter the air from the anisotropic medium.

$n_{s(1)}$, $n_{s(2)}$ Refractive indices of the anisotropic medium

                for the two fluorescence rays.

θ_1' Angle between the normal of film surface and

                the normal of light wave front corresponding

                to the ray whose electric vector lies on the

                plane of incidence.

t_1', t_2' Amplitude transmission coefficients of the two

                fluorescence rays.

T_1', T_2' Transmittances of light energy of the two

                fluorescence rays.

Symbols introduced in Chap. 5.

O-K'L'M'   Coordinate system fixed in a rotating molecule

                in the excited state at $t' = t + u$.

t   time

u   time when used as an order comparable with

                the fluorescence lifetime (nanosecond).

$\mathbb{F}_i'$ — Emitting oscillator of an excited fluorescent molecule with the O-K'L'M' frame.

ω',φ',χ' (= Ω') — Three Euler angles specifying the orientation of the O-K'L'M' frame in the sample coordinate system O-abc.

H',Ξ' — Polar and azimuthal angles, respectively, specifying the direction of $\mathbb{F}_i'$ in the O-abc system.

γ,ψ,ζ (= Γ) — Three Euler angles specifying the rotation of an excited molecule.

$q(\Delta,E,t)$ — Orientation distribution function of absorbing oscillators $\mathbb{A}_i$ with respect to the O-abc system at time t.

$r(H',\Xi',t'|A)$ — Probability function of finding an emitting oscillator $\mathbb{F}_i'$ of fluorescent probes excited at time t in the direction (H',Ξ') at $t'= t + u$.

$m(\Omega,t)$ — Orientation distribution function of fluorescent probes in the O-abc system at time t.

$P(\Omega,t|\Omega',t')$ = $P(\Omega,t|\Gamma,u)$ — Transition probability from orientation angle Ω to Ω' in a period of u (= $t' - t$).

$K(\Omega,t|\Omega',t')$ = $K(\Omega,t|\Gamma,u)$ — Probability function of finding a fluorescent probe oriented at Ω at time t in the direction Ω' at time t'.

$M^{\ell\,m\,n}_{\ell'm'n'}(t|t')$ — Coefficient for the series expansion of

$K(\Omega,t|\Omega',t')$ expressed in terms of the product of two generalized spherical harmonics, $\Phi_{\ell mn}(\Omega)\,\Phi_{\ell'm'n'}(\Omega')$, characterizing the molecular orientation and motion.

τ — Fluorescence lifetime.

$[\ \ ]_s$ in $[M^{\ell\ m\ n}_{\ell'm'n'}(t|t')]_s$ — Denotes the time average, $\int_0^\infty e^{-u/\tau}du/\tau$, for stationary irradiation of a sample specimen.

$\langle(3\cos^2\omega - 1)/2\rangle$ — Orientation factor.

$\langle(3\cos^2\gamma - 1)/2\rangle_s$ — Mobility factor.

$\left.\begin{array}{l}\langle(3\cos^2\omega - 1)/2 \\ \cdot(3\cos^2\gamma - 1)/2\rangle_s \\ \langle(5\cos^4\omega - 1)/4 \\ \cdot(3\cos^2\gamma - 1)/2\rangle_s\end{array}\right\}$ Orientation-mobility factors.

CHAPTER 1

General Introduction

1-1. Introduction

Molecular Orientation

    Mechanical, optical, and other physical properties of

polymer solids are strongly influenced by the orientation of

polymer molecules because of the intrinsic anisotropy of polymer

chains. Practical properties of polymer films and fibers can

only be manifested by the molecular orientation due to drawing

and other processes. Furthermore, in many biological systems,

molecular orientation behaviors have a close relationship to the

biological functions of polymer molecules. Therefore, it is

very important in the fields of polymer science and engineering

to know the molecular orientation characteristics to understand

the relationship between the structure of polymer solids and

their properties.

    There are various methods employed for the measurements of

molecular orientation in polymer solids.[1-3]

    Wide angle X-ray diffraction method is employed to estimate

the orientation of crystalline regions in polymer solids.[4] This

method provides the complete orientation distribution function

of crystallites.[5-8]   The measurements of birefringence, infrared

dichroism, and visible and ultraviolet dichroism are also em-

ployed to estimate the molecular orientation in polymer systems,

however these methods provide information only about the extent

of orientation.

   The application of the fluorescence polarization for molec-

ular orientation measurements enabled us to obtain the information

about the type of molecular orientation in the non-crystalline

region of polymer solids. Nishijima et al. proposed this

method.[9,10]   Experimental works[11-13] have since been carried

out by analyzing the angular distributions of polarized components

of fluorescence intensity, which depend on the second and fourth

moments of the orientation distribution of fluorescent probes in

polymer solid and thus reflect the orientation patterns of

polymer segments in amorphous regions.

   Laser-Raman[14-17] and broad-line NMR[18-22] techniques have

also been remarkably developed recently as new spectroscopic

methods which are capable of obtaining moments of orientation

distribution higher than the second order.

   The initial purpose of this thesis is to develop the

general description of the fluorescence polarization method.

The theoretical treatment is carried out by modifying the

spherical-harmonic expansion technique[7,8,23] which has been

applied for determination of the crystallite orientation by
X-ray diffraction method. The author aims to clarify the
relationship between the polarized fluorescence intensity and
the molecular orientation distribution in order to establish
the method for the quantitative estimations of molecular orien-
tation behaviors.

Molecular Orientation Relaxation

It is also important to examine the molecular orientation
relaxation mechanism in polymer systems for the detailed under-
standing of their properties. The analysis of the molecular
orientation and its relaxation is essential in the investigation
of the structural change in drawn polymer solid by its heat-
treatment and in the further elucidation of the transformation
of the structure during and after the drawing.

The fluorescence polarization technique can also be applied
to the orientation relaxation studies. The effect of molecular
motions of fluorescent probes must be taken into consideration
in order to study molecular orientation and its relaxation
mechanism. This effect affects the polarized components of
fluorescence intensity, when the polymer medium is in the glass-
transition region or in the rubbery state. The anisotropic
mobility of molecules in oriented systems can also be estimated
by analyzing the polarized components of fluorescence intensity.

Recently Jarry et al. have also reported this effect.[24]

The main purpose of this thesis is to give the general

theory of fluorescence polarization in the oriented system in

which the effects of anisotropic rotational motions of fluores-

cent molecules are included. Moreover, the author aims to

apply the result of this theoretical analysis to the experiment

in polymer solids, and to discuss molecular orientation and

its relaxation phenomena in relation to the solid state

properties.

1-2. Outline of This Thesis

The author wishes here to give accounts of the outline of

this thesis.

This thesis consists of eight chapters and two appendixes.

Chapters 2-4 and Appendix I are included in Part I, and Chapters

5-8 and Appendix II are included in Part II.

Chapter 1 is the general introduction of this thesis. The

importance of the studies on molecular orientation and its

relaxation phenomena is emphasized. The outline of this thesis

is also briefly mentioned.

Part I presents the theoretical analysis of fluorescence

polarization in the anisotropic rigid system, in which the

motions of fluorescent molecules are negligible. Applications

of the theoretical analysis to the study of molecular orientation characteristics in polymer solids are also discussed. In Chapter 2, the theory of fluorescence polarization in oriented systems is given. This theory includes the intrinsic photophysical anisotropy of fluorescent molecules, the molecular orientation distribution, and the optical anisotropy of the medium. The polarized component of fluorescence intensity from the oriented system is thus formulated. In Chapter 3, the equation of polarized component of fluorescence intensity provided in Chapter 2 is applied to uniaxially and biaxially oriented systems. The angular distributions of the polarized components of fluorescence intensity are derived for uniaxial and biaxial orientation distributions. The theoretically derived angular distributions of polarized components of fluorescence intensity are examined experimentally, using uniaxially and biaxially stretched polymer films. In Chapter 4, the molecular orientation characteristics are fully discussed for poly(vinyl alcohol) films stretched in four ways (free width uniaxial stretching, simultaneous biaxial stretching, successive biaxial stretching, and fixed width uniaxial stretching) by a stilbene derivative molecule as the fluorescent probe. The estimation of molecular orientation is carried out quantitatively from two moments (the second and fourth moments of the distribution) in the case of free width uniaxial stretching and five moments

(two kinds of second moments and three kinds of fourth order moments) in the other cases of stretching. In Appendix I, the generalized spherical harmonics used for the theoretical treatment in Chapter 2 is shown in a condensed form and some symmetrical properties of this function are also given. Moreover, various optical quantities required to analyze the molecular orientation in biaxially anisotropic systems are represented in plain forms.

Part II presents the theoretical analysis of fluorescence polarization in the anisotropic system, in which the motions of fluorescent molecules are measurable during the fluorescence lifetime, and also deals with the applications of the result of theoretical analysis to the studies on molecular orientation and its relaxation phenomena in polymer systems. In Chapter 5, the polarized component of fluorescence intensity is generally described by introducing a function characterizing the rotational motions of fluorescent molecules. In order to analyze the molecular orientation and motion in uniaxially oriented systems, the simplified equations are also discussed. In Chapter 6, a method to estimate the anisotropy of molecular mobility in a uniaxially symmetrical system is developed. In this chapter, an apparatus is also designed in order to study the molecular orientation and its relaxation mechanism in polymer films. In Chapters 7 and 8, the fluorescence polari-

zation technique proposed in Chapters 5 and 6 is applied to the
experiments in polymer solids. The molecular orientation and
its relaxation mechanism are discussed in relation to molecular
mobility. The anisotropy of molecular mobility in stretched
polymer films is also discussed in terms of the angular factors
characterizing molecular orientation and motion. Chapter 7
deals with the uniaxial stretching of poly(vinyl chloride) films,
and Chapter 8 deals with the uniaxial stretching of natural
rubber films. In Appendix II, some useful equations are derived
for the theoretical treatments in Chapters 5 and 6.

References

1) R. S. Stein and B. E. Read, Appl. Polym. Symp., 8, 255 (1969).

2) G. L. Wilkes, Adv. Polym. Sci., 8, 91 (1971).

3) I. M. Ward, J. Polym. Sci., Polym. Symp., 58, 1 (1977).

4) L. E. Alexander, "X-ray Diffraction Method in Polymer
    Science", New York, John Wiley & Sons, Inc., 1969, Chap. 4.

5) R. J. Roe and W. R. Krigbaum, J. Chem. Phys., 40, 2608 (1964).

6) W. R. Krigbaum and R. J. Roe, J. Chem. Phys., 41, 737 (1964).

7) R. J. Roe, J. Appl. Phys., 36, 2024 (1965).

8) S. Nomura, H. Kawai, I. Kimura, and M. Kagiyama, J. Polym.
    Sci., A-2, 8, 383 (1970).

9) Y. Nishijima, Y. Onogi, and T. Asai, Repts. Progr. Polym.

Phys. Japan, $\underline{8}$, 131 (1965).

10) Y. Nishijima, Y. Onogi, and T. Asai, J. Polym. Sci., C, $\underline{15}$, 237 (1966).

11) Y. Nishijima, Y. Onogi, and T. Asai, Repts. Progr. Polym. Phys. Japan, $\underline{10}$, 461 (1967). Y. Nishijima, Y. Onogi, and T. Asai, ibid., $\underline{11}$, 391 (1968). Y. Nishijima, Y. Onogi, R. Yamazaki, and K. Kawakami, ibid., $\underline{11}$, 407 (1968). Y. Nishijima, Y. Onogi, and R. Yamazaki, ibid., $\underline{11}$, 415 (1968). T. Asai, Y. Onogi, and Y. Nishijima, ibid., $\underline{12}$, 433 (1969).

12) Y. Nishijima, J. Polym. Sci., C, $\underline{31}$, 353 (1970).

13) Y. Nishijima, "Fluorescence Methods in Polymer Research", in "Progress in Polymer Science, Japan", (Eds. S. Onogi and K. Uno), vol. 6, Kodansha, Tokyo, John Wiley, New York, 1973, pp. 199-251.

14) S. W. Cornell and J. L. Koenig, J. Appl. Phys., $\underline{39}$, 4883 (1968).

15) D. I. Bower, J. Polym. Sci., Polym. Phys. Ed., $\underline{10}$, 2135 (1972).

16) J. Purvis and D. I. Bower, Polymer, $\underline{15}$, 645 (1974).

17) J. Purvis and D. I. Bower, J. Polym. Sci., Polym. Phys. Ed., $\underline{14}$, 1461 (1976).

18) V. J. McBrierty and I. M. Ward, Brit. J. Appl. Phys. (J. Phys. D), $\underline{1}$, 1529 (1968).

19) V. J. McBrierty, I. R. McDonald, and I. M. Ward, Brit. J. Appl. Phys. (J. Phys. D), $\underline{4}$, 88 (1971).

20) M. Kashiwagi, M. J. Folkes, and I. M. Ward, Polymer, $\underline{12}$, 697 (1971).

21) M. Kashiwagi and I. M. Ward, Polymer, $\underline{13}$, 145 (1972).

22) M. Kashiwagi, A. Cunningham, A. J. Manuel, and I. M. Ward, Polymer, $\underline{14}$, 111 (1973).

23) R. J. Roe, J. Polym. Sci., A-2, $\underline{8}$, 1187 (1970).

24) J. P. Jarry and L. Monnerie, J. Polym. Sci., Polym. Phys. Ed., $\underline{16}$, 443 (1978).

PART I

FLUORESCENCE POLARIZATION IN THE ANISOTROPIC RIGID SYSTEM

AND

ITS APPLICATION TO CHARACTERIZATION OF ORIENTED POLYMER SOLIDS

CHAPTER 2

Theory of Polarization of Fluorescence

in the Oriented Rigid System

2-1. Introduction

When fluorescent molecules absorb the energy of polarized

light, they are excited photoselectively. The probability of

excitation is determined by the angular alignments of the

molecular axes with respect to the direction of the electric

vector of the exciting light. The polarization characteristic

of fluorescence from the system is indicative of the spatial

distribution of the molecular axes of excited molecules.[1-3]

Such a polarization characteristic of fluorescence is one of

the several properties[4-6] which can be utilized for the study

of molecular orientation behavior.

This chapter deals with the generalization of fluorescence

polarization in the anisotropic rigid system. In order to

clarify the polarization characteristics of fluorescence inten-

sity in relation to the intrinsic photophysical anisotropy of

fluorescent molecules and the molecular orientation distribution,

the equation of polarized component of fluorescence intensity

will be given in the generalized form. The features of the

theoretical analysis are as follows: 1) The photophysical
anisotropy of a fluorescent molecule is treated with a model of
"ellipsoidal" dipoles for the absorption of light and the
emission of fluorescence. 2) The fluorescent molecules are
dispersed in a birefringent rigid medium. Finally, 3) the
relationship between the polarized component of fluorescence
intensity and the molecular orientation distribution is repre-
sented in terms of the coefficients of the series expansions in
spherical harmonics.

2-2. Oscillator Model for Light Absorption and Emission
      of Fluorescent Molecules

     First of all, let us define the transition moments of the
light absorption and emission in terms of the probability
functions $g(\delta,\varepsilon)$ and $h(\eta,\xi)$. These functions are the proba-
bilities of finding the absorbing and emitting oscillators $\mathbb{A}_i$
and $\mathbb{F}_i$, respectively, and given in the molecular coordinate
system O-KLM, as shown in Fig. 2-1. In this figure, the K- and
M- axes lie on a molecular plane formed by the conjugated
double bonds, and the M-axis is on the main axis of the fluo-
rescent molecule. The directions of $\mathbb{A}_i$ and $\mathbb{F}_i$ are specified by
a set of polar and azimuthal angles with respect to the molecular
coordinate system O- KLM, (δ,ε) and (η,ξ), respectively. The
functions $g(\delta,\varepsilon)$ and $h(\eta,\xi)$ are normalized as follows;
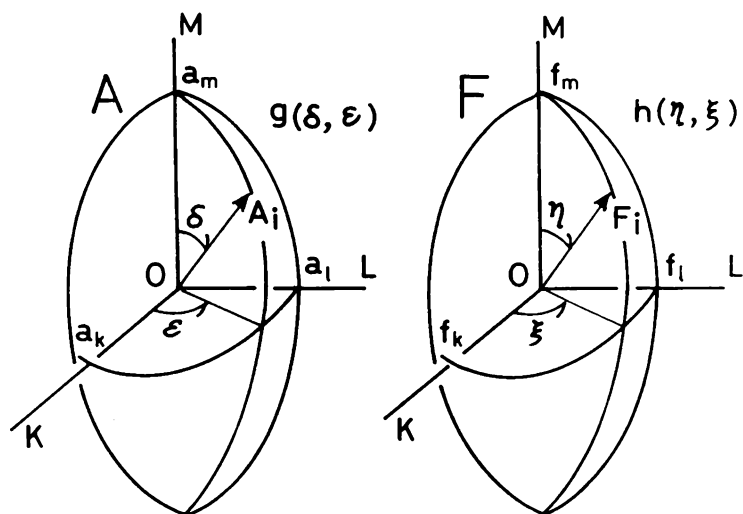
Fig. 2-1. Oscillator model for the characterization of the photophysical anisotropy of a fluorescent molecule. The functions, $g(\delta,\varepsilon)$ and $h(\eta,\xi)$, are the probabilities of finding the absorbing and emitting oscillators, A_i and F_i, respectively, in the coordinate system O-KLM fixed in the fluorescent molecule.

$$\int_{\delta,\varepsilon} g(\delta,\varepsilon) \; d(\delta,\varepsilon) = 1 \qquad\qquad (2-1)$$

$$\int_{\eta,\xi} h(\eta,\xi) \; d(\eta,\xi) = 1 \; , \qquad\qquad (2-2)$$

where

$$\int_{\delta,\varepsilon} d(\delta,\varepsilon) = \int_0^{2\pi} \int_0^{\pi} \sin\delta d\delta d\varepsilon$$

$$\int_{\eta,\xi} d(\eta,\xi) = \int_0^{2\pi} \int_0^{\pi} \sin\eta d\eta d\xi \; .$$

In the case of the general "ellipsoidal" dipoles as shown in Fig. 2-1, $g(\delta,\varepsilon)$ and $h(\eta,\xi)$ can be represented as

$$g(\delta,\varepsilon) = \frac{1}{3} \left\{ \left(\frac{\cos^2\varepsilon}{a_k^2} + \frac{\sin^2\varepsilon}{a_l^2} \right) \sin^2\delta + \frac{\cos^2\delta}{a_m^2} \right\}^{-3/2} \qquad (2-3)$$

$$h(\eta,\xi) = \frac{1}{3} \left\{ \left(\frac{\cos^2\xi}{f_k^2} + \frac{\sin^2\xi}{f_l^2} \right) \sin^2\eta + \frac{\cos^2\eta}{f_m^2} \right\}^{-3/2} \; . \qquad (2-4)$$

The institution of such a model is based on the following reasons: (a) The absorption and emission transition moments are essentially independent of each other. (b) Plural types of electronic transitions may take place simultaneously on the occasion of the absorption of the incident light by fluorescent molecules.[7-9] (c) A thermal effect may be included in the function $h(\eta,\xi)$. This effect signifies a limited libration of the molecular axis of excited molecule. The time scale of this

kind of vibration is much shorter than that of molecular
rotational diffusion.

2-3. Angular Specification of Orientation Axes and

        Relationship among Various Angular Functions

    The orientation of the molecular frame O-KLM with respect
to the coordinate system O-abc fixed in the specimen (e.g., a
stretched polymer film) can be specified by using three Euler
angles, ω, φ, and χ, as shown in Fig. 2-2. The orientation of
the axes A_i and F_i, lying in the directions (δ,ε) and (η,ξ) in
the molecular coordinate system O-KLM, can also be given by
using a set of polar and azimuthal angles, (Δ,E) and (H,Ξ), with
respect to the sample coordinate system O-abc, as shown in
Fig. 2-3.

    Secondly, let us define $m(\omega,\varphi,\chi)$ as the orientation distri-
bution function of the fluorescent probes within the coordinate
system O-abc. Similarly, let the orientation distribution
function of the absorbing oscillator A_i with respect to the
sample coordinate system O-abc be $q(\Delta,E)$. Moreover, let us
introduce the function $r(H,\Xi|A)$ as the probability of finding
the emitting oscillator F_i in the direction (H,Ξ). Since the
emitting oscillator F_i is only produced on the excitation of
the particular fluorescent molecules, the orientation distri-
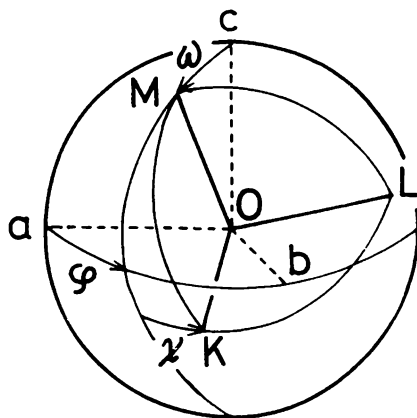bution function of F_i is denoted as $r(H,\Xi|A)$. In the ideal case

Fig. 2-2. Euler angles, ω, φ, and χ, specifying the orientation of the molecular coordinate system O-KLM with respect to the coordinate system O-abc fixed in the specimen.
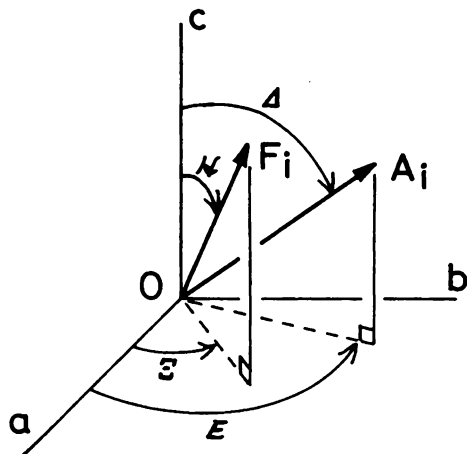

Fig. 2-3. Polar and azimuthal angles specifying the orientations of the axes, A_i and F_i, in the sample coordinate system O-abc.

in which the emitting oscillator $\mathbf{F}_i$ can be identified with the absorbing oscillator $\mathbf{A}_i$, $r(H,\Xi|A)$ equals to $\underline{\delta}(H-\Delta)\underline{\delta}(\Xi-E)$. ($\underline{\delta}$ denotes the Dirac delta function.) Three functions $m(\omega,\varphi,\chi)$, $q(\Delta,E)$, and $r(H,\Xi|A)$ are normalized as

$$\int_\Omega m(\omega,\varphi,\chi)\ d\Omega = 1 \tag{2-5}$$

$$\int_{\Delta,E} q(\Delta,E)\ d(\Delta,E) = 1 \tag{2-6}$$

$$\int_{H,\Xi} r(H,\Xi|A)\ d(H,\Xi) = 1\ , \tag{2-7}$$

where

$$\int_\Omega d\Omega = \int_0^{2\pi}\int_0^{2\pi}\int_0^\pi \sin\omega d\omega d\varphi d\chi$$

and the representations, $\int_{\Delta,E} d(\Delta,E)$ and $\int_{H,\Xi} d(H,\Xi)$, have the same notation as previously used for $\int_{\delta,\varepsilon} d(\delta,\varepsilon)$.

By application of the expanded Legendre addition theorem,[10] the transformation relations among the three sets of angles (Δ,E), (δ,ε), and (ω,φ,χ) and among the three sets of angles (H,Ξ), (η,ξ), and (ω,φ,χ) are given by the following equations in terms of the spherical harmonics $Y_{\ell m}$ and the generalized spherical harmonics $\Phi_{\ell m n}$.

$$Y_{\ell m}^*(\Delta,E) = 2\pi\left(\frac{2}{2\ell+1}\right)^{1/2}\sum_{n=-\ell}^{\ell} \Phi_{\ell m n}^*(\Omega)Y_{\ell n}^*(\delta,\varepsilon) \tag{2-8}$$

$$(\ell = 0,1,2,\ldots\ ,\ m = -\ell,\ldots,0,\ldots,\ell)$$

$$Y_{\ell'm'}^*(H,\Xi) = 2\pi \left(\frac{2}{2\ell'+1}\right)^{1/2} \sum_{n'=-\ell'}^{\ell'} \Phi_{\ell'm'n'}^*(\Omega) Y_{\ell'n'}^*(\eta,\xi) \quad (2\text{-}9)$$

$$(\ell' = 0,1,2,\ldots \, , \; m' = -\ell',\ldots,0,\ldots,\ell'\,),$$

where * denotes the complex conjugate, and

$$Y_{\ell m}(\Delta,E) = P_{\ell}^m(\cos\Delta) \; e^{-imE}/(2\pi)^{1/2} \, ,\ldots \qquad (2\text{-}10)$$

$$\Phi_{\ell mn}(\Omega) = Z_{\ell mn}(\cos\omega) \; e^{-i(m\varphi+n\chi)}/(2\pi) \, . \qquad (2\text{-}11)$$

The function P_{ℓ}^m is the normalized associated Legendre function, and $Z_{\ell mn}$ is a generalization of the associated Legendre function. These functions were used by Roe,[10] and were also described by Nomura et al.[11] and Bower[12]. The generalized spherical harmonics $\Phi_{\ell mn}(\Omega)$ defined by eq. (2-11) can also be related to the Wigner rotation matrix $D_{mn}^{\ell}(\Omega)$, as follows:

$$\Phi_{\ell mn}(\Omega) = (-1)^{m-n} \left(\frac{2\ell+1}{8\pi^2}\right)^{1/2} D_{mn}^{\ell}(\Omega) \, , \qquad (2\text{-}12)$$

in which D_{mn}^{ℓ} is the rotation operator following the convention of Rose[13] and that of Yamanouchi[14]. The explicit form of $\Phi_{\ell mn}$ is shown in Appendix I. The spherical harmonics $Y_{\ell m}$ defined by eq. (2-10) can also be represented as

$$Y_{\ell m} = (2\pi)^{1/2} \; \Phi_{\ell m0} \qquad (2\text{-}13)$$

-20-

and is somewhat different from $Y_{\ell m}$ used in References (13) and
(14) (see Note (15)).

Multiplying both sides of the equation obtained by the
product of eqs. (2-8) and (2-9) by all the defined angular func-
tions, $m(\omega,\varphi,\chi)$, $q(\Delta,E)$, $r(H,\Xi|A)$, $g(\delta,\varepsilon)$, and $h(\eta,\xi)$, and
integrating over the whole ranges of all the angles, one can
derive the following relationship by using the normalization
conditions given by eqs. (2-1), (2-2), and (2-5)-(2-7).

$$\int_{\Delta,E}\int_{H,\Xi} Y_{\ell m}{}^{*}(\Delta,E)Y_{\ell'm'}{}^{*}(H,\Xi)q(\Delta,E)r(H,\Xi|A)\ d(H,\Xi)d(\Delta,E)$$

$$= 8\pi^{2}\{(2\ell+1)(2\ell'+1)\}^{-1/2} \sum_{n,n'} G_{\ell n}H_{\ell'n'}M_{\ell'm'n'}^{\ell\ m\ n}\ , \qquad (2-14)$$

where

$$G_{\ell n} = \int_{\delta,\varepsilon} Y_{\ell n}{}^{*}(\delta,\varepsilon)g(\delta,\varepsilon)\ d(\delta,\varepsilon) \qquad (2-15)$$

$$H_{\ell'n'} = \int_{\eta,\xi} Y_{\ell'n'}{}^{*}(\eta,\xi)h(\eta,\xi)\ d(\eta,\xi) \qquad (2-16)$$

$$M_{\ell'm'n'}^{\ell\ m\ n} = \int_{\Omega} \Phi_{\ell mn}{}^{*}(\Omega)\Phi_{\ell'm'n'}{}^{*}(\Omega)m(\omega,\varphi,\chi)\ d\Omega\ . \qquad (2-17)$$

Here $G_{\ell n}$ and $H_{\ell'n'}$ are the coefficients for the expansions of
$g(\delta,\varepsilon)$ and $h(\eta,\xi)$ in a series of spherical harmonics $Y_{\ell n}(\delta,\varepsilon)$
and $Y_{\ell'n'}(\eta,\xi)$, respectively, and characterize the intrinsic
photophysical anisotropy of the fluorescent molecule. The
coefficient $M_{\ell'm'n'}^{\ell\ m\ n}$ is the angular average characterizing the

-21-

molecular orientation distribution. The left side of eq. (2-14) can be combined with the observed quantity, i.e., the polarized component of fluorescence intensity, as shown in the next section.

2-4. Polarized Component of Fluorescence Intensity

Let i_a be the excitation probability when the fluorescent probe having an oscillator $\mathbb{A}_i$ is excited by the incident polarized light with its electric vector $\mathbb{P}_1$, and i_f be the detection probability of the fluorescence emitted from an oscillator $\mathbb{F}_i$ through the analyzer with its transmission axis $\mathbb{P}_2$. Then, the fluorescence intensity of the polarized component $I\left(\begin{smallmatrix}\mathbb{P}_1\\\mathbb{P}_2\end{smallmatrix}\right)$ can be written as follows,

$$I\left(\begin{smallmatrix}\mathbb{P}_1\\\mathbb{P}_2\end{smallmatrix}\right) = \int_{\Delta,E}\int_{H,\Xi} q(\Delta,E)i_a r(H,\Xi|A)i_f \, d(H,\Xi)d(\Delta,E) \ . \qquad (2-18)$$

If the angular alignments of the vectors $\mathbb{P}_1$ and $\mathbb{P}_2$ with respect to the sample coordinate system O-abc are specified by using a pair of polar and azimuthal angles (α_1,β_1) and (α_2,β_2), respectively, the excitation probability i_a is a function of the angles (α_1,β_1) and (Δ,E), and similarly, i_f is a function of the angles (α_2,β_2) and (H,Ξ). Therefore, when i_a and i_f are formulated in terms of the series expansion in spherical harmonics, as shown by

$$i_a = k \sum_{\ell=0}^{\infty} \sum_{m=-\ell}^{\ell} S_{\ell m} Y_{\ell m}{}^*(\Delta, E) \qquad (2\text{-}19)$$

and

$$i_f = \phi \sum_{\ell'=0}^{\infty} \sum_{m'=-\ell'}^{\ell'} T_{\ell' m'} Y_{\ell' m'}{}^*(H, \Xi) \;, \qquad (2\text{-}20)$$

the coefficients $S_{\ell m}$ and $T_{\ell' m'}$ depend on only the angular alignments of $\mathbb{P}_1$ and $\mathbb{P}_2$, respectively, and they can be obtained by the following equations:

$$S_{\ell m} = \frac{1}{k} \int_{\Delta, E} i_a Y_{\ell m}(\Delta, E) \; d(\Delta, E) \qquad (2\text{-}21)$$

$$T_{\ell' m'} = \frac{1}{\phi} \int_{H, \Xi} i_f Y_{\ell' m'}(H, \Xi) \; d(H, \Xi) \;. \qquad (2\text{-}22)$$

For example, in the simplest case, that is, in optically isotropic media, i_a and i_f can be written as

$$i_a = k \, (\, \mathbb{P}_1 \cdot \mathbb{A}_i \,)^2 \qquad (2\text{-}23)$$

$$i_f = \phi \, (\, \mathbb{P}_2 \cdot \mathbb{F}_i \,)^2 \;. \qquad (2\text{-}24)$$

Hence, substituting eqs. (2-23) and (2-24) into eqs. (2-21) and (2-22), respectively, one can calculate as follows:

$$S_{00} = (4\pi/9)^{1/2} \qquad (2\text{-}25a)$$

$$S_{20} = (4\pi/45)^{1/2} \, (3\cos^2\alpha_1 - 1) \qquad (2\text{-}25b)$$

$$S_{21} = -S_{2\bar{1}}^* = (2\pi/15)^{1/2} \sin 2\alpha_1 \, e^{-i\beta_1} \qquad (2\text{-}25c)$$

$$S_{22} = S_{2\bar{2}}^* = (2\pi/15)^{1/2} \sin^2\alpha_1 \, e^{-2i\beta_1} \qquad (2\text{-}25d)$$

$$S_{\ell m} = 0 \qquad \text{for } \ell = \text{odd or } \ell > 2 \ , \qquad (2\text{-}25e)$$

and similarly, for $T_{\ell'm'}$, the above set of equations is applicable by substituting (α_2, β_2) for (α_1, β_1).

Now, substituting eqs. (2-19) and (2-20) into eq. (2-18) and using eq. (2-14) derived in the preceding section, we find the relationship between the polarized component of fluorescence intensity and the molecular orientation distribution.

$$I\binom{\mathbb{P}_1}{\mathbb{P}_2} = 8\pi^2 \, k\phi \sum_{\substack{\ell \, m \, n \\ \ell'm'n'}} \{(2\,\ell+1)(2\,\ell'+1)\}^{-1/2} \, S_{\ell m} T_{\ell'm'}$$
$$\times \, G_{\ell n} H_{\ell'n'} M_{\ell'm'n'}^{\ell \, m \, n} \ . \qquad (2\text{-}26)$$

Equation (2-26) is the fundamental equation for the polarized component of fluorescence intensity. In this derivation, however, we have not considered the effect of the optical anisotropy of the medium (i.e. birefringence effect) on the polarized component of fluorescence intensity. In order to treat this effect, the excitation probability of fluorescent probes and the polarization characteristics of fluorescence must be considered in the birefringent medium, in other words, i_a and i_f defined

above need to be described in more general forms than those shown by eqs. (2-23) and (2-24).

Light Absorption of Fluorescent Probe in Birefringent Medium:

When the incident linearly polarized light enters an optically anisotropic medium, it propagates as two polarized components whose vibration axes and velocities of the propagation are different from each other. Let $\mathbb{E}_i$ be the electric field of the exciting light at the position of a fluorescent molecule. The electric field $\mathbb{E}_i$ can be divided into two components, $\mathbb{E}_{i1}$ and $\mathbb{E}_{i2}$, whose vibration axes are in the directions of privileged axes of the medium, as given in eq. (2-27).

$$\mathbb{E}_i = \mathbb{E}_{i1} + \mathbb{E}_{12} , \qquad (2\text{-}27)$$

in which

$$\mathbb{E}_{i1} = a_{i1} \, \mathbb{P}_{1-1} \, \cos(\frac{2\pi}{T_i} t - \delta_{i1}) \qquad (2\text{-}28a)$$

$$\mathbb{E}_{i2} = a_{i2} \, \mathbb{P}_{1-2} \, \cos(\frac{2\pi}{T_i} t - \delta_{i2}) , \qquad (2\text{-}28b)$$

where T_i is the period of oscillation of the exciting light in the medium. Then, the excitation probability i_a may be given in the following way:

$$i_a \propto \int_0^{T_i} (\mathbb{E}_i \cdot \mathbb{A}_i)^2 \, dt/T_i . \qquad (2\text{-}29)$$

Substitution of eqs. (2-27) and (2-28) into eq. (2-29) leads to

$$i_a = k \{ a_{i1}{}^2 (\mathbb{P}_{1-1} \cdot \mathbb{A}_i)^2 + a_{i2}{}^2 (\mathbb{P}_{1-2} \cdot \mathbb{A}_i)^2$$

$$+ 2 a_{i1} a_{i2} (\mathbb{P}_{1-1} \cdot \mathbb{A}_i) (\mathbb{P}_{1-2} \cdot \mathbb{A}_i) \cos \delta_i \}, \qquad (2\text{-}30)$$

where δ_i is the phase difference $\delta_{i1} - \delta_{i2}$ between the two compo-
nents $\mathbb{E}_{i1}$ and $\mathbb{E}_{i2}$.

Equation (2-29) is based on the following concepts: (a) The excitation of a molecule by the incident light takes place along the absorbing dipole within 10^{-15} second order corresponding to the period of the light wave.[16] (b) The energy of an electro-magnetic wave passing across a unit area in the medium per unit time is given by the Poynting vector $\mathbb{S}$ ($= \mathbb{E} \times \mathbb{H}$), and the inten-sity of light is the time-averaged value of the magnitude of $\mathbb{S}$, i.e., $\int_0^T |\mathbb{S}| dt/T$ ($\propto \int_0^T |\mathbb{E}|^2 dt/T$).

Fluorescence Emission from Fluorescent Probe in Birefringent Medium:

The electric field of fluorescence light at a distance r from the emitting oscillator $\mathbb{F}_i$ can be represented as follows:

$$\mathbb{E}_f = a_f \, \mathbb{j} \, \cos (\frac{2\pi}{T_f} t - \mathbb{k} \cdot \mathbb{r}) \qquad (2\text{-}31)$$

and

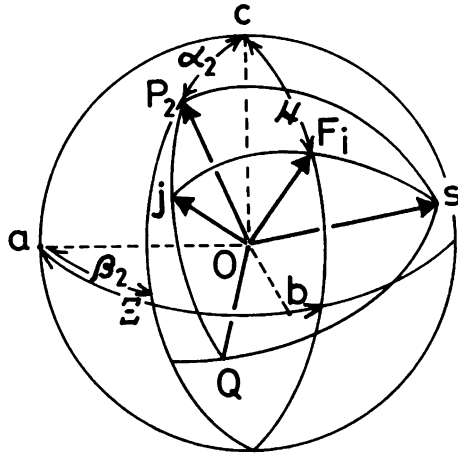$$\mathbb{j} \propto \mathbb{s} \times (\mathbb{F}_i \times \mathbb{s}) , \qquad (2\text{-}32)$$

Fig. 2-4. Diagram illustrating the angular alignments
of unit vectors, $\mathbb{F}_i$, $\mathbb{j}$, $\mathbb{s}$, and $\mathbb{p}_2$, in the sample coor-
dinate system O-abc. The vector $\mathbb{s}$ is normal to the
plane of analyzer, $\overparen{\mathbb{p}_2\mathbb{Q}}$.

where $\mathbb{s}$ is the unit vector which indicates the observed direc-
tion and is equal to $\mathbb{r}/r$. and T_f is the period of oscillation of
the fluorescence emission. When we observe such fluorescence
through the analyzer with its transmission axis $\mathbb{p}_2$ perpendicular
to the vector $\mathbb{s}$ (see the angular alignments in Fig. 2-4), the
detection probability i_f may be given by

$$i_f \propto \int_0^{T_f} (\mathbb{p}_2 \cdot \mathbb{E}_f)^2 \, dt/T_f = \frac{1}{2} a_f^2 (\mathbb{p}_2 \cdot \mathbb{j})^2 . \qquad (2\text{-}33)$$

Using eq. (2-32) and ($\mathbb{p}_2 \cdot \mathbb{s}$) = 0, we find that eq. (2-33)

-27-

coincides with eq. (2-24).

If two rays of fluorescence emitted from $\mathbb{F}_i$ are detected and their electric fields are given by

$$\mathbb{E}_1 = a_1 \, \mathbf{j}_1 \, \cos(\frac{2\pi}{T_f} \, t - \delta_{f1}) \tag{2-34a}$$

and

$$\mathbb{E}_2 = a_2 \, \mathbf{j}_2 \, \cos(\frac{2\pi}{T_f} \, t - \delta_{f2}) \, , \tag{2-34b}$$

then i_f can be written in a way similar to eq. (2-30), as follows:

$$i_f = \phi \, \{ a_1^2 (\mathbb{P}_2 \cdot \mathbf{j}_1)^2 + a_2^2 (\mathbb{P}_2 \cdot \mathbf{j}_2)^2$$
$$+ 2a_1 a_2 (\mathbb{P}_2 \cdot \mathbf{j}_1) (\mathbb{P}_2 \cdot \mathbf{j}_2) \cos\delta_f \} \, , \tag{2-35}$$

where $\delta_f = \delta_{f1} - \delta_{f2}$.

In the anisotropic medium, however, the two rays $\mathbb{E}_1$ and $\mathbb{E}_2$ should propagate in the directions which are different from the observed direction $\mathbf{s}$, and their vibration axes should also be different from $\mathbf{j}_1$ and $\mathbf{j}_2$. Suppose that $\mathbb{E}_1$ corresponds to one component, $\mathbb{E}_1^{(1)}$, of the electric vector $\mathbb{E}^{(1)}$ of the fluorescence which propagates in the direction $\mathbf{s}^{(1)}$ in the medium, as shown in Fig. 2-5. The amplitude a_1 of the detected fluorescence $\mathbb{E}_1$ can be related to the amplitude $a_1^{(1)}$ of $\mathbb{E}_1^{(1)}$ in the medium in the following way,

-28-
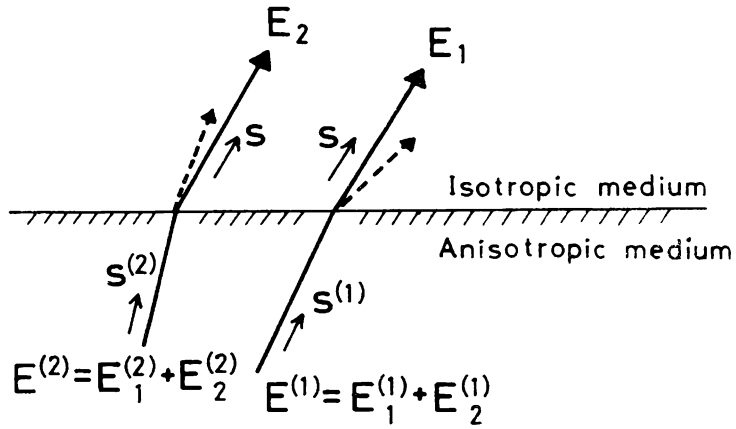
Fig. 2-5. Observed fluorescence rays, E_1 and E_2, coming from a fluorescent probe in the anisotropic medium.

$$a_1 = a^{(1)} (\; \mathtt{j}_1^{(1)} \cdot \mathtt{j}^{(1)}) \; , \qquad\qquad (2\text{-}36)$$

where $\mathtt{j}^{(1)}$ and $\mathtt{j}_1^{(1)}$ are the vibration axes of $E^{(1)}$ and $E_1^{(1)}$, respectively. By using the relations that $\mathtt{j}^{(1)} \propto s^{(1)} \times (F_i \times s^{(1)})$ and $(\mathtt{j}_1^{(1)} \cdot s^{(1)}) = 0$, eq. (2-36) can be rewritten as follows,

$$a_1 \propto a^{(1)} (\; \mathtt{j}_1^{(1)} \cdot F_i) \; . \qquad\qquad (2\text{-}37)$$

In the same manner, the amplitude of E_2 can be represented, by properly changing the numbers of suffixes used for E_1, as follows,

$$a_2 \propto a^{(2)} (\, \mathbf{j}_2^{(2)} \cdot \mathbb{F}_i \,) \; . \qquad\qquad (2\text{-}38)$$

By substituting eqs. (2-37) and (2-38) into eq. (2-35) and by altering the notations $\mathbf{j}_1^{(1)}$ and $\mathbf{j}_2^{(2)}$ to new notations $\mathbb{P}_{2\text{-}1}$ and $\mathbb{P}_{2\text{-}2}$, respectively, eq. (2-35) can be rewritten in the following form.

$$i_f = \phi \, \{ a_{f1}{}^2 (\, \mathbb{P}_{2\text{-}1} \cdot \mathbb{F}_i \,)^2 + a_{f2}{}^2 (\, \mathbb{P}_{2\text{-}2} \cdot \mathbb{F}_i \,)^2$$

$$+ \, 2 a_{f1} a_{f2} (\, \mathbb{P}_{2\text{-}1} \cdot \mathbb{F}_i \,)(\, \mathbb{P}_{2\text{-}2} \cdot \mathbb{F}_i \,) \cos\delta_f \} \; , \quad (2\text{-}39)$$

where

$$a_{f1} = (\, \mathbb{P}_2 \cdot \mathbf{j}_1 \,) \qquad\qquad (2\text{-}40a)$$

$$a_{f2} = (\, \mathbb{P}_2 \cdot \mathbf{j}_2 \,) \; . \qquad\qquad (2\text{-}40b)$$

Polarized Component of Fluorescence Intensity in the Optically Anisotropic Medium:

Both equations (2-30) and (2-39) consist of the sum of three terms. Accordingly, the coefficients, $S_{\ell m}$ and $T_{\ell' m'}$, of the series expansions given by eqs. (2-19) and (2-20) can be expressed in the following forms which consist of the three terms.

$$S_{\ell m} = a_{i1}^2 \, S_{\ell m}^{(1)} + a_{i2}^2 \, S_{\ell m}^{(2)} + 2a_{i1}a_{i2}\cos\delta_i \, S_{\ell m}^{(3)} \qquad (2\text{-}41)$$

$$T_{\ell'm'} = a_{f1}^2 \, T_{\ell'm'}^{(1)} + a_{f2}^2 \, T_{\ell'm'}^{(2)} + 2a_{f1}a_{f2}\cos\delta_f \, T_{\ell'm'}^{(3)} \, . \qquad (2\text{-}42)$$

Then the coefficients $S_{\ell m}^{(j)}$ and $T_{\ell'm'}^{(j)}$ (j=1,2,3) can be determined by the following equations:

$$S_{\ell m}^{(j)} = \int_{\Delta,E} (\, \mathbb{P}_{1-j} \cdot \mathbb{A}_i \,)^2 \, Y_{\ell m}(\Delta,E) \, d(\Delta,E) \qquad (j = 1,2) \quad (2\text{-}43)$$

$$S_{\ell m}^{(3)} = \int_{\Delta,E} (\, \mathbb{P}_{1-1} \cdot \mathbb{A}_i \,)(\, \mathbb{P}_{1-2} \cdot \mathbb{A}_i \,) \, Y_{\ell m}(\Delta,E) \, d(\Delta,E) \qquad (2\text{-}44)$$

$$T_{\ell'm'}^{(j)} = \int_{H,\Xi} (\, \mathbb{P}_{2-j} \cdot \mathbb{F}_i \,)^2 \, Y_{\ell'm'}(H,\Xi) \, d(H,\Xi) \qquad (j = 1,2) \quad (2\text{-}45)$$

$$T_{\ell'm'}^{(3)} = \int_{H,\Xi} (\, \mathbb{P}_{2-1} \cdot \mathbb{F}_i \,)(\, \mathbb{P}_{2-2} \cdot \mathbb{F}_i \,) \, Y_{\ell'm'}(H,\Xi) \, d(H,\Xi) . \quad (2\text{-}46)$$

On the other hand, i_a and i_f should depend on the distance l from the surface to the fluorescent molecule in the medium of thickness D, since the phase differences δ_i and δ_f are the functions of the optical path difference between the two components of each light wave. Hence, the polarized component of fluorescence intensity obtained from the anisotropic system can be written as

$$I(\begin{matrix}\mathbb{P}_1 \\ \mathbb{P}_2\end{matrix}) = \int_0^D \int_{\Delta,E} \int_{H,\Xi} q(\Delta,E) i_a r(H,\Xi|A) i_f \, d(H,\Xi)d(\Delta,E)dl/D \, . \quad (2\text{-}47)$$

One can derive the following equation from eq. (2-47) by the

-31-

same procedure as eq. (2-26) was derived from eq. (2-18).

$$I\binom{\mathbb{P}_1}{\mathbb{P}_2} = 8\pi^2 k\phi \sum_{\substack{\ell\ m\ n \\ \ell'm'n'}} \{(2\ell+1)(2\ell'+1)\}^{-1/2} [S_{\ell m}T_{\ell'm'}]_{int}$$
$$\times\ G_{\ell n}H_{\ell'n'}M_{\ell'm'n'}^{\ell\ m\ n}\ , \qquad (2\text{-}48)$$

where

$$[S_{\ell m}T_{\ell'm'}]_{int} = \int_0^D (a_{i1}^2 S_{\ell m}^{(1)} + a_{i2}^2 S_{\ell m}^{(2)} + 2a_{i1}a_{i2}\cos\delta_i\ S_{\ell m}^{(3)})$$
$$\times\ (a_{f1}^2 T_{\ell'm'}^{(1)} + a_{f2}^2 T_{\ell'm'}^{(2)} + 2a_{f1}a_{f2}\cos\delta_f\ T_{\ell'm'}^{(3)})dl/D\ . \quad (2\text{-}49)$$

2-5. Explicit Formulation of Coefficients

The coefficients $S_{\ell m}^{(j)}$, $T_{\ell'm'}^{(j)}$ (j=1,2,3), $G_{\ell n}$, $H_{\ell'n'}$, and $M_{\ell'm'n'}^{\ell\ m\ n}$ in eqs. (2-48) and (2-49) can be given in more explicit form as shown below.

$S_{\ell m}^{(j)}$ and $T_{\ell'm'}^{(j)}$ (j=1,2,3): In order to calculate these coefficients by eqs. (2-43)-(2-46), let the polar and azimuthal angles of $\mathbb{P}_{1-1}$, $\mathbb{P}_{1-2}$, $\mathbb{P}_{2-1}$, and $\mathbb{P}_{2-2}$, with respect to the sample coordinate system O-abc, be given by (α_1',β_1'), (α_1'',β_1''), (α_2',β_2'), and (α_2'',β_2''), respectively. Then the result of the calculations is given as follows,

$$S_{00}^{(1)} = (4\pi/9)^{1/2} \qquad\qquad (2\text{-}50a)$$

$$S_{20}^{(1)} = (4\pi/45)^{1/2} \, (3\cos^2\alpha_1' - 1) \tag{2-50b}$$

$$S_{21}^{(1)} = -S_{2\bar{1}}^{(1)}* = (2\pi/15)^{1/2} \, \sin 2\alpha_1' \, e^{-i\beta_1'} \tag{2-50c}$$

$$S_{22}^{(1)} = S_{2\bar{2}}^{(1)}* = (2\pi/15)^{1/2} \, \sin^2\alpha_1' \, e^{-2i\beta_1'} \tag{2-50d}$$

$$S_{\ell m}^{(1)} = 0 \qquad \text{for } \ell = \text{odd or } \ell > 2 \, . \tag{2-50e}$$

Equations (2-50a)-(2-50e) are also applicable to $S_{\ell m}^{(2)}$, $T_{\ell'm'}^{(1)}$, and $T_{\ell'm'}^{(2)}$, by substituting (α_1', β_1') by (α_1'', β_1''), (α_2', β_2'), and (α_2'', β_2''), respectively. (Equations (2-50a)-(2-50e) are, in fact, equivalent to eqs. (2-25a)-(2-25e).) The coefficients $S_{\ell m}^{(3)}$ can be given by

$$S_{00}^{(3)} = (4\pi/9)^{1/2}\{ \cos\alpha_1' \, \cos\alpha_1''$$
$$+ \sin\alpha_1' \, \sin\alpha_1'' \, \cos(\beta_1' - \beta_1'') \} \tag{2-51a}$$

$$S_{20}^{(3)} = (4\pi/45)^{1/2}\{ 2\cos\alpha_1' \, \cos\alpha_1''$$
$$- \sin\alpha_1' \, \sin\alpha_1'' \, \cos(\beta_1' - \beta_1'') \} \tag{2-51b}$$

$$S_{21}^{(3)} = -S_{2\bar{1}}^{(3)}* = (2\pi/15)^{1/2}(\sin\alpha_1' \, \cos\alpha_1'' \, e^{-i\beta_1'}$$
$$+ \cos\alpha_1' \, \sin\alpha_1'' \, e^{-i\beta_1''}) \tag{2-51c}$$

$$S_{22}^{(3)} = S_{2\bar{2}}^{(3)}* = (2\pi/15)^{1/2} \, \sin\alpha_1' \, \sin\alpha_1'' \, e^{-i(\beta_1' + \beta_1'')} \tag{2-51d}$$

$$S_{\ell m}^{(3)} = 0 \qquad \text{for } \ell = \text{odd or } \ell > 2 \, . \tag{2-51e}$$

As for $T^{(3)}_{\ell'm'}$, eqs. (2-51a)-(2-51e) are applicable by substituting (α_2, β_2) for (α_1, β_1).

$\underline{G_{\ell n} \text{ and } H_{\ell'n'}}$: These coefficients can be calculated by eqs. (2-15) and (2-16). Some of them can be written in the explicit form as shown by

$$G_{00} = (4\pi)^{-1/2} \qquad (2\text{-}52a)$$

$$G_{20} = (16\pi/5)^{-1/2} (3\langle\cos^2\delta\rangle - 1) \qquad (2\text{-}52b)$$

$$G_{22} = G_{2\bar{2}}{}^* = (32\pi/15)^{-1/2} \langle[\sin^2\delta\, e^{2i\varepsilon}]\rangle \;, \quad (2\text{-}52c)$$

where the sign $\langle[\;\;]\rangle$ denotes the operator that

$$\langle[X]\rangle = \langle\text{Re } X\rangle + i \langle\text{Im } X\rangle \qquad (2\text{-}53)$$

(Re X : real part of X , Im X : imaginary part of X).

As for $H_{\ell'n'}$, eqs. (2-52a)-(2-52c) are applicable by substituting (η, ξ) for (δ, ε).

$\underline{M^{\ell\; m\; n}_{\ell'm'n'}}$: The coefficients $M^{\ell\; m\; n}_{\ell'm'n'}$ are given by eq. (2-17). Their apparent forms can be obtained as a function of several angular averages, i.e., the moments of molecular orientation distribution, as follows,

$$M^{000}_{000} = 1/\ 8\pi^2 \tag{2-54a}$$

$$M^{200}_{000} = (\sqrt{5}/\ 16\pi^2)(3<\cos^2\omega> -1) \tag{2-54b}$$

$$M^{200}_{200} = (5/\ 32\pi^2)(9<\cos^4\omega> - 6<\cos^2\omega> + 1) \tag{2-54c}$$

$$M^{210}_{2\bar{1}0} = (15/\ 16\pi^2)(<\cos^4\omega> - <\cos^2\omega>) \tag{2-54d}$$

$$M^{220}_{2\bar{2}0} = (15/\ 64\pi^2)(<\cos^4\omega> - 2<\cos^2\omega> + 1) \tag{2-54e}$$

$$M^{220}_{220} = (15/\ 64\pi^2)\ <[\ \sin^4\omega\ e^{4i\varphi}\ ]> \tag{2-54f}$$

$$M^{210}_{210} = (15/\ 16\pi^2)\ <[\ (\sin^2\omega - \sin^4\omega)\ e^{2i\varphi}\ ]> \tag{2-54g}$$

$$M^{220}_{000} = (\sqrt{15/2}/\ 16\pi^2)\ <[\ \sin^2\omega\ e^{2i\varphi}\ ]> \tag{2-54h}$$

$$M^{220}_{200} = \sqrt{3/2}\ (5/\ 32\pi^2)\ <[\ (2\sin^2\omega - 3\sin^4\omega)\ e^{2i\varphi}\ ]> \tag{2-54i}$$

etc.

References and Note

1) Y. Nishijima, Y. Onogi, and T. Asai, J. Polym. Sci., C, 15, 237 (1966).

2) Y. Nishijima, J. Polym. Sci., C, 31, 353 (1970).

3) Y. Nishijima, "Fluorescence Methods in Polymer Research", in "Progress in Polymer Science, Japan", (Eds. S. Onogi and K. Uno), vol. 6, Kodansha, Tokyo, John Wiley, New York,

1973, pp. 199-251.

4) R. S. Stein and B. E. Read, Appl. Polym. Symp., $\underline{8}$, 255 (1969).

5) G. E. Wilkes, Adv. Polym. Sci., $\underline{8}$, 91 (1971).

6) I. M. Ward, J. Polym. Sci., Polym. Symp., $\underline{58}$, 1 (1977).

7) Y. Tanizaki and H. Hiratsuka, Journal of the Spectroscopical Society of Japan, $\underline{25}$, 205 (1976).

8) T. Hoshi, Kagaku no Ryoiki, $\underline{31}$, 91 (1977).

9) E. W. Thulstrup, J. Michl, and J. H. Eggers, J. Phys. Chem., $\underline{74}$, 3868 (1970).

10) R. J. Roe, J. Appl. Phys., $\underline{36}$, 2024 (1965).

11) S. Nomura, H. Kawai, I. Kimura, and M. Kagiyama, J. Polym. Sci., A-2, $\underline{8}$, 383 (1970).

12) D. I. Bower, J. Polym. Sci., Polym. Phys. Ed., $\underline{10}$, 2135 (1972).

13) M. E. Rose, "Elementary Theory of Angular Momentum", John Wiley & Sons, Inc., New York, 1957, Chap. 4.

14) T. Yamanouchi, "Kaiten-gun To Sono Hyogen", Iwanami, Tokyo, 1957, Chap. 3, §. 12.

15) The spherical harmonics $Y_{\ell m}$ used in this thesis is equivalent to $Y_{\ell,-m}$ and $(-1)^m Y_{\ell m}^*$ used in Refs. (13) and (14).

16) C. A. Parker, "Photoluminescence of Solutions", Elsevir Pub. Co., London, 1968, Chap. 1.

CHAPTER 3

Application to Uniaxially and Biaxially Oriented Systems

3-1. Introduction

In the preceding chapter, the theoretical analysis of

polarized fluorescence was carried out by considering the photo-

physical anisotropy of a fluorescent probe and the birefringence

effect of optically anisotropic medium on the polarized component

of fluorescence intensity. Consequently, the equation for the

polarized component of fluorescence intensity in the optically

anisotropic system was derived in the form as shown by eq. (2-48).

In this chapter, the equation (2-48) is applied to the

cases of uniaxially and biaxially oriented systems and checked

experimentally using uniaxially and biaxially stretched polymer

films in which fluorescent probes are partially oriented.

3-2. Fluorescence Polarization in Uniaxially Oriented Systems

Let us apply eq. (2-48) to the study of uniaxial orientation

distribution.

When the orientation distribution of fluorescent probes,

referred to the sample coordinate system O-abc, is rotationally

symmetrical about the c-axis and the orientation of fluorescent

probes themselves is also rotationally symmetrical around the M-axis, the distribution function $m(\omega,\varphi,\chi)$ depends on only the angle ω. Then the coefficient $M^{\ell\ m\ n}_{\ell'm'n'}$ has the symmetrical property,

$$M^{\ell\ m\ n}_{\ell'm'n'} = 0 \qquad \text{for } m+m'\neq0 \text{ or } n+n'\neq0 \ . \qquad (3-1)$$

Furthermore, when the fluorescent probes treated here have a quite high photophysical anisotropy, one can reasonably assume that the both transition moments of absorption and emission are uniaxially symmetrical prolate ellipsoidal dipoles. Then $g(\delta,\varepsilon)$ and $h(\eta,\xi)$ defined in Chapter 2 are independent of ε and ξ, respectively, and hence the following conditions are satisfied.

$$G_{\ell n} = 0 \qquad \text{for } n\neq0 \qquad (3-2)$$

$$H_{\ell'n'} = 0 \qquad \text{for } n'\neq0 \ . \qquad (3-3)$$

Using eq. (2-48) under the above mentioned conditions, the polarized fluorescence intensity can be represented as follows:

$$I\binom{\mathbb{P}_1}{\mathbb{P}_2} = 8\pi^2\, k\phi \sum_{\ell\ \ell'\ m} \{(2\ell+1)(2\ell'+1)\}^{-1/2}\ [S_{\ell m}T_{\ell'\overline{m}}]_{\text{int}}$$

$$\times\ G_{\ell0}H_{\ell'0}M^{\ell\ \ \ m\ \ 0}_{\ell'\overline{m}\ 0} \qquad (3-4)$$

$$(\ -\min(\ell,\ell')\ \leq\ m\ \leq\ \min(\ell,\ell'),\quad \ell \text{ and } \ell' = 0,2\ )\ .$$

-38-

Here we find that the orientation factors in the right side of eq. (3-4) are the coefficients given by eqs. (2-54a)-(2-54e) and hence they are the functions of the second and fourth moments of molecular orientation distribution about the c-axis, $\langle\cos^2\omega\rangle$ and $\langle\cos^4\omega\rangle$. Moreover, we find from eqs. (2-52a) and (2-52b) that the photophysical anisotropy factors in eq. (3-4) are $\langle\cos^2\delta\rangle$ and $\langle\cos^2\eta\rangle$.

On the other hand, $[S_{\ell m}T_{\ell'm'}]_{int}$ depends on the alignment of optical system for the measurement. For the alignment in which the planes of polarizer and analyzer are parallel to the ca-plane of the oriented sample as shown in Fig. 3-1, the incident exciting polarized light and the fluorescence can both be divided into two components, that is, one is parallel to the c-axis and the other is parallel to the a-axis. Then one can give the following equations for the amplitudes and the vibration directions of the two components, using the symbols defined in Chapter 2.

For the incident exciting light,

$$\left\{ \begin{array}{ll} a_{i1} = \cos\alpha_1 & \text{(3-5a)} \\ \\ a_{i2} = \sin\alpha_1 & \text{(3-5b)} \end{array} \right.$$

and

$$\left\{ \begin{array}{ll} \mathbb{P}_{1-1} = (\alpha_1',\beta_1') = (0,0) & \text{(3-6a)} \\ \\ \mathbb{P}_{1-2} = (\alpha_1'',\beta_1'') = (\pi/2,0) \ . & \text{(3-6b)} \end{array} \right.$$

-39-
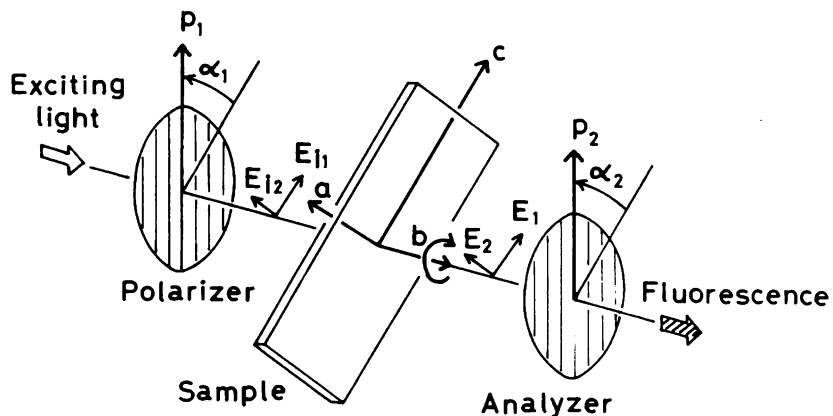
Fig. 3-1. Optical system for measuring the polarized components of fluorescence intensity from a uniaxially oriented sample.

For the fluorescence,

$$\left\{ \begin{array}{ll} a_{f1} = \cos\alpha_2 & \text{(3-7a)} \\ \\ a_{f2} = \sin\alpha_2 & \text{(3-7b)} \end{array} \right.$$

and

$$\left\{ \begin{array}{ll} \mathbb{P}_{2-1} = (\alpha_2', \beta_2') = (0,0) & \text{(3-8a)} \\ \\ \mathbb{P}_{2-2} = (\alpha_2'', \beta_2'') = (\pi/2, 0) \ . & \text{(3-8b)} \end{array} \right.$$

Therefore, using eqs. (2-49), (2-50), and (2-51), we have

$$[S_{00}T_{00}]_{int} = 4\pi/9 \tag{3-9a}$$

$$[S_{20}T_{00}]_{int} = (4\pi/\ 9\sqrt{5})(3\cos^2\alpha_1 - 1) \tag{3-9b}$$

$$[S_{00}T_{20}]_{int} = (4\pi/\ 9\sqrt{5})(3\cos^2\alpha_2 - 1) \tag{3-9c}$$

$$[S_{20}T_{20}]_{int} = (4\pi/45)(3\cos^2\alpha_1 - 1)(3\cos^2\alpha_2 - 1) \tag{3-9d}$$

$$[S_{21}T_{2\bar{1}}]_{int} = [S_{2\bar{1}}T_{21}]_{int} = -(2\pi/15)\sin2\alpha_1\sin2\alpha_2$$
$$\times \int_0^D \cos\delta_i\cos\delta_f \ dl/D \tag{3-9e}$$

$$[S_{22}T_{2\bar{2}}]_{int} = [S_{2\bar{2}}T_{22}]_{int} = (2\pi/15)\sin^2\alpha_1\sin^2\alpha_2 \ . \tag{3-9f}$$

The birefringence effect due to the optical anisotropy of the medium is expressed in the term, $[S_{21}T_{2\bar{1}}]_{int}$, and this term is ineffective when p_1 and/or p_2 coincides with one of the principal axes of the anisotropic medium.

Let us write the birefringence term $\int_0^D\cos\delta_i\cos\delta_f dl/D$ in a more condensed form. For the wavelength of exciting light, λ_i, and that of fluorescence, λ_f, the relative phase differences δ_i and δ_f between the two components of each light are given by

$$\delta_i = 2\pi \ \Delta n_i l/\lambda_i \tag{3-10}$$

$$\delta_f = 2\pi \ \Delta n_f (D - 1)/\lambda_f \ , \tag{3-11}$$

where Δn_i and Δn_f are the birefringences ($n_c - n_a$) for the wavelengths λ_i and λ_f, respectively (n_c, n_a: refractive indices in the directions of the principal axes c and a). Therefore the birefringence term can be calculated as

$$\int_0^D \cos\delta_i \cos\delta_f \, dl/D = (\Delta_i \sin\Delta_i - \Delta_f \sin\Delta_f)/(\Delta_i^2 - \Delta_f^2) \ , \quad (3\text{-}12)$$

where

$$\Delta_i = 2\pi \, \Delta n_i D/\lambda_i \quad\quad\quad\quad (3\text{-}13)$$

$$\Delta_f = 2\pi \, \Delta n_f D/\lambda_f \ . \quad\quad\quad\quad (3\text{-}14)$$

3-3. Experimental Verification for Uniaxially Stretched
       Polymer Films

In order to verify the validity of the equation for the polarized fluorescence intensity in the uniaxially oriented system, the experiment was carried out by using uniaxially stretched polymer films in which fluorescent molecules were dispersed.

Poly(vinyl alcohol) (PVA; average degree of polymerization 500) was dissolved in water containing a fluorescent stilbene derivative (Whtex RP; Sumitomo Chem. Co.) as shown in Fig. 3-2. The film specimen (PVA-RP) was prepared by casting the solution onto a glass plate at 50 °C. The concentration of the fluo-
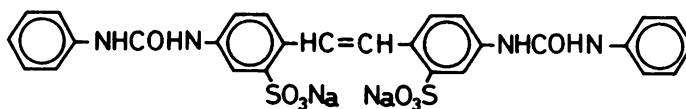
Fig. 3-2. Fluorescent compound of stilbene derivative (RP).
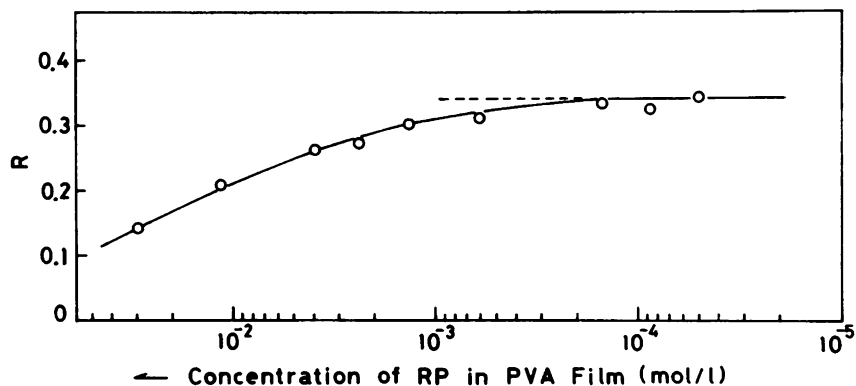
Fig. 3-3. Fluorescence anisotropy ratio[*) versus concentration of RP in PVA film. (* See eq. (3-17) and Note 2).)

rescent molecule in the film was controlled at about 1×10^{-4} mol/l. (It was confirmed that the fluorescence depolarization by energy migration due to high concentration effect was not caused at this concentration. See Fig. 3-3.) The sample of uniaxially symmetrical orientation was prepared by the free width uniaxial stretching in which it was drawn at 100 °C in heated air and cooled quickly to room temperature.

-43-

Now, let the c- and the b- axes of the sample coordinate system O-abc be the stretched axis and the axis perpendicular to the plane of film surface, respectively. Then, using the optical system shown in Fig. 3-1, one can observe many polarized components of fluorescence intensity by rotating the oriented sample about the b-axis for various angular alignments of the transmission axes of polarizer ($\mathbb{P}_1$) and analyzer ($\mathbb{P}_2$). When the oriented sample is rotated about the b-axis from the initial position where the c-axis is parallel to $\mathbb{P}_1$, the angle of rotation is equal to α_1. Let I_{cc} be the polarized component of fluorescence intensity when the axes $\mathbb{P}_1$ and $\mathbb{P}_2$ are both parallel to the c-axis, i.e., $\alpha_1=\alpha_2=0$, and I_{ca} be the component when $\mathbb{P}_1$ and $\mathbb{P}_2$ are parallel to the c- and the a- axes, respectively, i.e., $\alpha_1=0$ and $\alpha_2=\pi/2$. I_{aa} and I_{ac} can be similarly defined.

The fluorescent molecules were excited by the 365 nm line of a mercury arc lamp, and the fluorescence was detected through a cut-off filter (SC-42, Fuji Film Co.) with a cut-off wavelength of 420 nm.

In order to verify the applicability of eq. (3-4) to uniaxially oriented system, let us take the following procedures:
1) The photophysical anisotropy factors, $\langle\cos^2\delta\rangle$ and $\langle\cos^2\eta\rangle$, of the fluorescent molecule RP were estimated. 2) The estimation of the second and fourth moments, $\langle\cos^2\omega\rangle$ and $\langle\cos^4\omega\rangle$, of molecular orientation distribution was carried out in terms of

-44-

eq. (3-4) by using the observed values of the three principal

components of fluorescence intensity (I_{cc}, I_{ca}, and I_{aa}).

3) The birefringence was measured by means of a polarizing

microscope (Nikon POH, Nihon Kogaku Co.), and the value of

$\int_0^D \cos\delta_i \cos\delta_f \, dl/D$ was calculated from eqs. (3-12)-(3-14). For

this calculation, the following values were adopted; λ_i=365 nm,

and λ_f=435 nm since the maximum peak of the fluorescence spec-

trum of the compound RP in PVA film was at 435 nm. The wave-

length dispersion of birefringence was disregarded. 4) Many

components of observed polarized fluorescence intensity were

compared with the corresponding values calculated from eq. (3-4)

by using the values estimated in the procedures 1)-3).

When a prameter B[1)] defined by

$$B = (I_{cc} + 2I_{ca})/(I_{cc} + 2I_{ac}) \qquad (3-15)$$

was estimated for PVA-RP films stretched at various draw ratios,

it was independent of the extent of elongation and nearly equal

to unity. Equation (3-15) can be rewritten by using eq. (3-4),

as follows;

$$B = (\frac{1}{2} + \frac{16\pi^{5/2}}{5} G_{20}M_{000}^{200})/(\frac{1}{2} + \frac{16\pi^{5/2}}{5} H_{20}M_{200}^{000})$$

$$= (\frac{1}{2} + \frac{3\langle\cos^2\delta\rangle -1}{2} \frac{3\langle\cos^2\omega\rangle -1}{2})/(\frac{1}{2} + \frac{3\langle\cos^2\eta\rangle -1}{2} \frac{3\langle\cos^2\omega\rangle -1}{2}).$$

$$(3-16)$$

Hence, from the result of $B \simeq 1$, the anisotropy of light absorption and emission of the fluorescent molecule RP can be considered to be nearly equal. Then the photophysical anisotropy factors were evaluated as $\langle \cos^2 \delta \rangle = \langle \cos^2 \eta \rangle = 0.951$ from the fluorescence anisotropy ratio[2] of unstretched PVA-RP film, R_0, which is defined by

$$R_0 = (I_{cc} - I_{ca})/(I_{cc} + 2I_{ca})$$

$$= \frac{2}{5} \frac{3\langle \cos^2 \delta \rangle -1}{2} \frac{3\langle \cos^2 \eta \rangle -1}{2} . \qquad (3-17)$$

Figure 3-4 shows the result of measurement of the polarized components of fluorescence intensity for the PVA-RP film stretched uniaxially to 20 % elongation with free width. The birefringence, Δn, of this film is 0.196×10^{-2} for the Sodium-D line. The thickness of the film, D, is 0.123 mm. The value of $\int_0^D \cos\delta_i \cos\delta_f \, dl/D$ was estimated to be -0.457 from the retardation, 242 nm ($= \Delta nD$). The second and fourth moments were estimated as follows: $\langle \cos^2 \omega \rangle = 0.400$ and $\langle \cos^4 \omega \rangle = 0.258$. Figures 3-4a, 3-4b, and 3-4c show the results of the verification for the three cases; a) $\alpha_2 = \alpha_1$, b) $\alpha_2 = \alpha_1 + \pi/2$, and c) $\alpha_2 = \alpha_1 + \pi/4$, respectively. Observed fluorescence intensity is in good agreement with the curve calculated by eq. (3-4) according to the above mentioned procedures. In these figures, the calculated
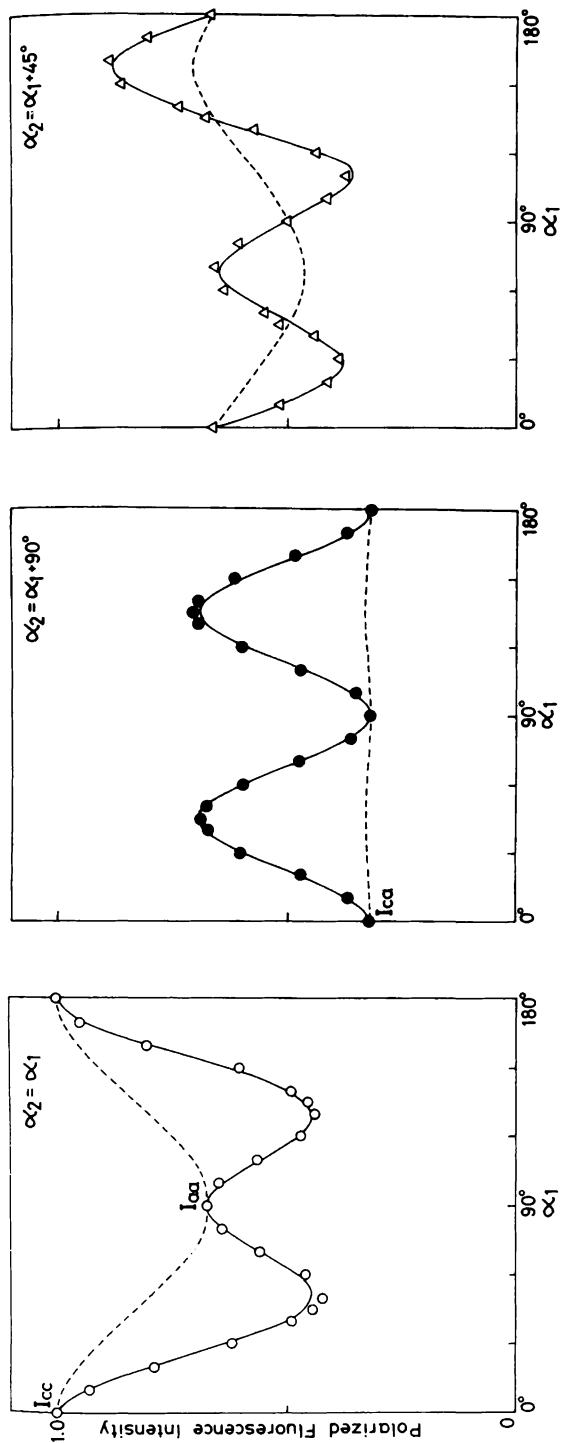
Fig. 3-4. Polarized components of fluorescence intensity obtained from uniaxially stretched PVA-RP film (20 % elongation with free width) as a function of the angle of rotation (= α_1) of the specimen about the b-axis. (O), (●), (△): Observed fluorescence intensities; (———): Calculated curve by eq. (3-4); (— — —): Calculated curve disregarding the birefringence effect.

(a) $\alpha_2 = \alpha_1$

(b) $\alpha_2 = \alpha_1 + \pi/2$

(c) $\alpha_2 = \alpha_1 + \pi/4$

curves disregarding the birefringence effect due to the optical

anisotropy of the polymer medium are also shown by the broken

lines, in order to clarify the birefringence effect. It is

clear that the polarized fluorescence intensity is affected very

remarkably by the optical anisotropy of the medium.

Similar experimental verifications were carried out for

other uniaxially oriented PVA-RP films stretched to higher

elongation, and the results were also explained reasonably.

Moreover, such verifications were carried out for uniaxially

stretched poly(vinyl chloride) (PVC) films containing stilbene

derivative -SW.[3] The observed polarized components of fluo-

rescence intensity from the oriented PVC-SW film were also in

good agreement with those according to eq. (3-4), as shown in

Fig. 3-5.

It can be concluded from these results that the equation

of the polarized component of fluorescence intensity is valid

for the application to the optically anisotropic system of

uniaxial symmetry and that the obtained values of the moments

of molecular orientation distribution are also reliable.

From the fact that the observed fluorescence intensity is

in agreement with the one given by eq. (3-4), the broken line

curves shown in Figs. 3-4 and 3-5 characterize distinctly the

true type of molecular orientation. Accordingly, when we esti-

mate the molecular orientation from the angular distribution of
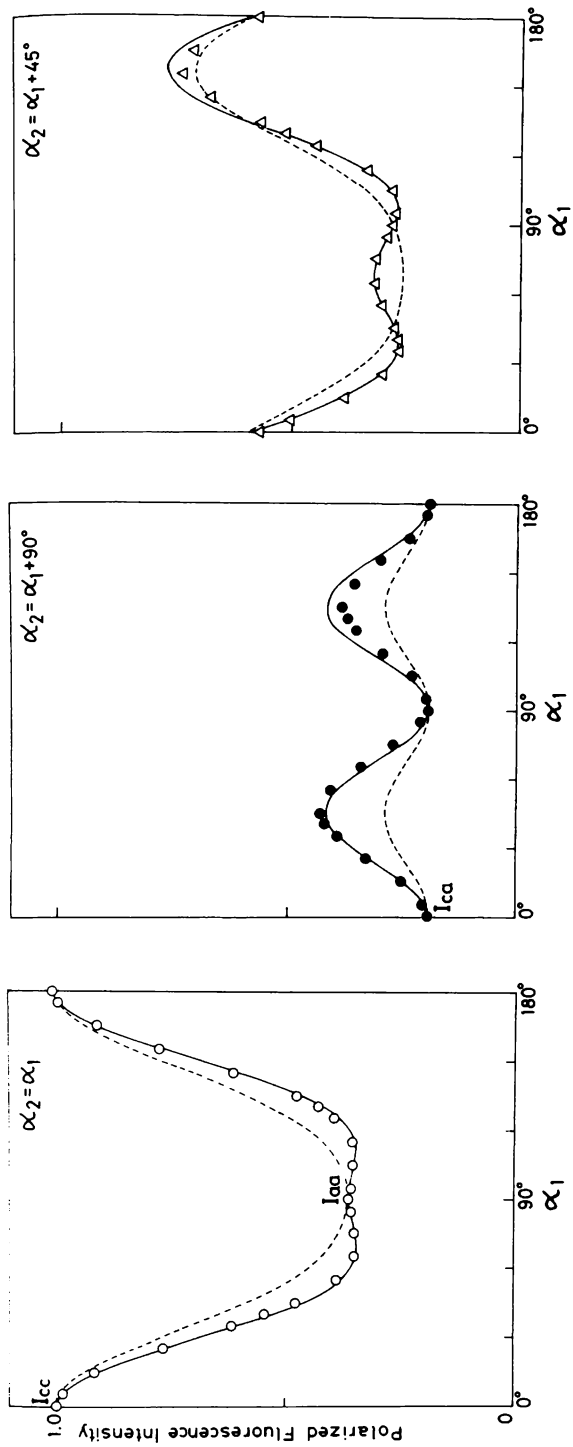
Fig. 3-5. The same as Fig. 3-4, but for PVC-SW sample (340 % elongation with free

width, $\langle \cos^2 \omega \rangle = 0.511$, $\langle \cos^4 \omega \rangle = 0.389$, $\Delta nD = 486$ nm, $\int_0^D \cos \delta_i \cos \delta_f \, dl/D = 0.146$ for

$\lambda_i = 365$ nm and $\lambda_f = 442$ nm).

the polarized components of fluorescence intensity, we should

remove the contribution due to the effect of the optical aniso-

tropy of the medium from the observed intensity according to

the theoretical formula derived in this discussion.

Effect of Wavelength Distribution of Detected Fluorescence:

For the calculation of $\int_0^D \cos\delta_i \cos\delta_f \, dl/D$ in the above men-

tioned experimental verifications, one representative wavelength

of fluorescence (i.e., λ_f = 435 nm for PVA-RP, 442 nm for PVC-

SW) was used disregarding the wavelength distribution of detected

fluorescence light. The deviation from the calculated curves

(i.e., solid lines as shown in Figs. 3-4 and 3-5) due to such an

effect was taken into account for PVA-RP and PVC-SW samples

given in Figs. 3-4 and 3-5, respectively.

The fluorescence spectra of PVA-RP and PVC-SW films through

the sharp cut-off filter (SC-42) are shown in Figs. 3-6a and

3-6b. For the oriented samples having the retardations (ΔnD) of

242 nm and 486 nm, the birefringence term $\int_0^D \cos\delta_i \cos\delta_f \, dl/D$ for

the fluorescence wavelength (λ_f) is calculated and plotted

against λ_f in Fig. 3-6c. The right vertical axis shows the

maximum differences between $I\left(\begin{smallmatrix}\alpha_1\\\alpha_2\end{smallmatrix}\right)_{\lambda_f}$ and $I\left(\begin{smallmatrix}\alpha_1\\\alpha_2\end{smallmatrix}\right)_{435}$, and between

$I\left(\begin{smallmatrix}\alpha_1\\\alpha_2\end{smallmatrix}\right)_{\lambda_f}$ and $I\left(\begin{smallmatrix}\alpha_1\\\alpha_2\end{smallmatrix}\right)_{442}$, where $I\left(\begin{smallmatrix}\alpha_1\\\alpha_2\end{smallmatrix}\right)_{\lambda_f}$ is the polarized fluorescence

intensity obtained when measured monochromatically at the wave-

length λ_f. (Here, let $I\left(\begin{smallmatrix}0\\0\end{smallmatrix}\right)$, i.e., I_{cc} be unity.) The maximum
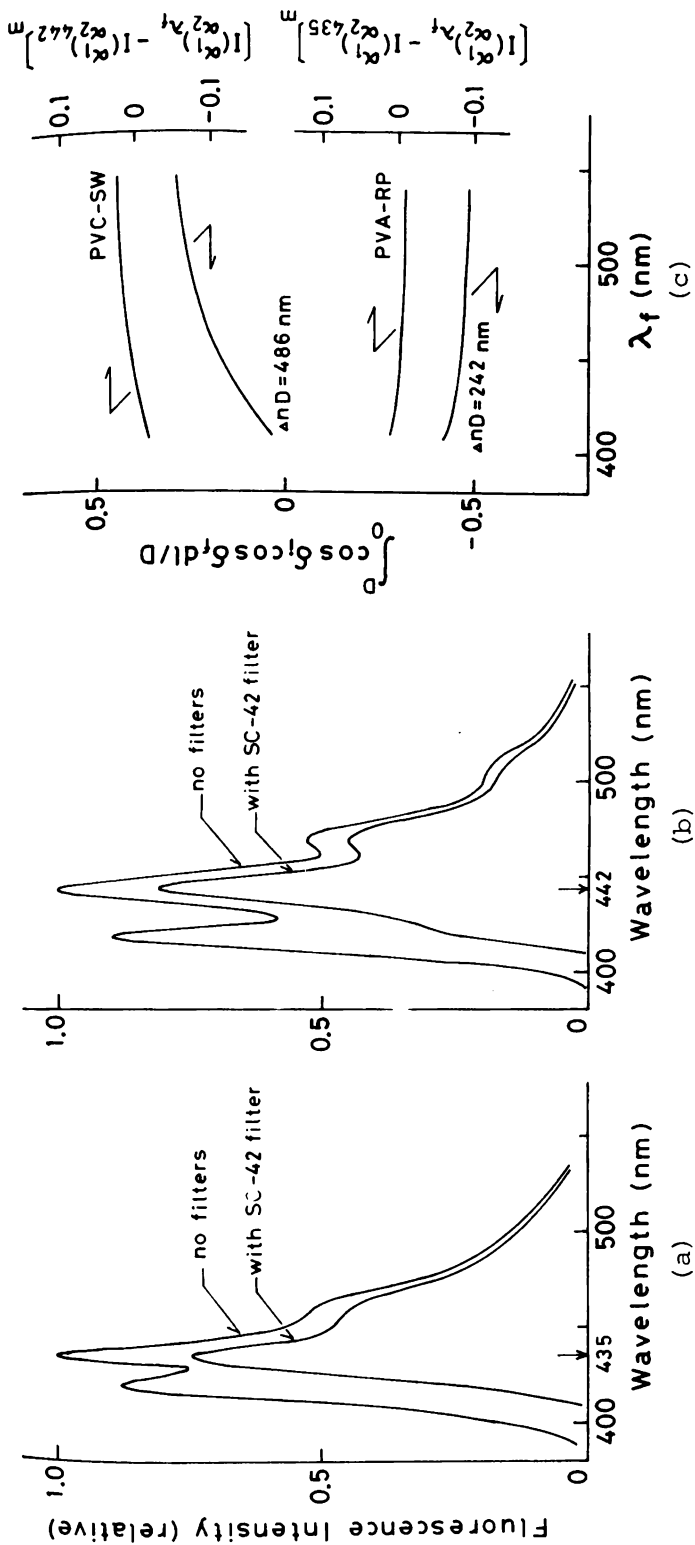
Fig. 3-6. (a) Fluorescence spectra of RP in PVA film with SC-42 filter and without the filter. (b) Fluorescence spectra of SW in PVC film with SC-42 filter and without the filter. (c) Birefringence term $\int_0^D \cos\delta_i\cos\delta_f dl/D$ versus wavelength of detected fluorescence (λ_f), and maximum differences $[I({}^{\alpha_1}_{\alpha_2})_{\lambda_f} - I({}^{\alpha_1}_{\alpha_2})_{435}]_m$ and $[I({}^{\alpha_1}_{\alpha_2})_{\lambda_f} - I({}^{\alpha_1}_{\alpha_2})_{442}]_m$ versus λ_f, estimated for the oriented samples PVA-RP (Fig. 3-4) and PVC-SW (Fig. 3-5).

differences are given by the set of $\alpha_1 = \alpha_2 = \pi/4$ (see eq. (3-9e)).

It is noted in Fig. 3-6 that the deviation caused by neglecting the effect of the wavelength distribution is less than a few percent and in practice the angular distribution of polarized components of fluorescence intensity can be treated with the wavelength at the maximum peak of detected fluorescence spectrum.

3-4. Fluorescence Polarization in Biaxially Oriented Systems

Let us apply eq. (2-48) to the case of biaxial orientation distribution.

Now, let the orientation distributions of the K-, L-, and M- axes of fluorescent probes in the sample coordinate system O-abc have a symmetrical property of the point group D_{2h}. Then the ab-, bc-, and ca- planes of the sample are three mutually perpendicular mirror planes. Such a molecular orientation distribution may be found when polymer films are deformed in orthogonally biaxial stretching.

When the molecular orientation distribution has such a symmetry, the coefficient $M_{\ell'm'n'}^{\ell\ m\ n}$ characterizing the molecular orientation has the following relationships,

$$M_{\ell'm'n'}^{\ell\ m\ n} = 0 \qquad \text{for } m+m' \neq \text{even} \qquad (3\text{-}18)$$

and

$$M^{\ell\ m\ n}_{\ell'm'n'} \begin{cases} = M^{\ell\ m\ \bar{n}}_{\ell'm'\bar{n}'} = M^{\ell\ \bar{m}\ n}_{\ell'\bar{m}'n'}{}^* \\[2mm] = M^{\ell\ \bar{m}\ \bar{n}}_{\ell'\bar{m}'n'} = M^{\ell\ m\ n}_{\ell'm'n'}{}^* \\[2mm] = M^{\ell\ \bar{m}\ n}_{\ell'\bar{m}'n'} = M^{\ell\ m\ \bar{n}}_{\ell'm'\bar{n}'}{}^* \; . \end{cases} \qquad (3\text{-}19)$$

The above equations can be derived by utilizing the symmetrical properties of the generalized spherical harmonics $\Phi_{\ell mn}(\Omega)$. (See eqs. (AI-2) and (AI-3) in Appendix I.)

If the photophysical anisotropy of fluorescent probes used here is quite high and the coefficients $G_{\ell n}$ and $H_{\ell'n'}$ have the symmetry given by eqs. (3-2) and (3-3) as treated in the uni-axially oriented system, then the general equation (2-48) for the polarized fluorescence intensity can be simplified as follows;

$$I\binom{\mathbb{P}_1}{\mathbb{P}_2} = 8\pi^2 k\phi \sum_{\substack{\ell\ m \\ \ell'm'}} \{(2\ell+1)(2\ell'+1)\}^{-1/2} [S_{\ell m}T_{\ell'm'}]_{int}$$
$$\times\ G_{\ell 0}H_{\ell'0}M^{\ell\ m\ 0}_{\ell'm'0} \qquad (3\text{-}20)$$

$$(\ m + m' = \text{even}, \quad \ell \text{ and } \ell' = 0,2\ ) \; .$$

Since the imaginary part of $M^{\ell\ m\ n}_{\ell'm'n'}$ must be zero from eq. (3-19), the orientation factors constituting eq. (3-20) are the coefficients given by eqs. (2-54a)-(2-54i) and are the functions of

the five angular averages, $\langle\cos^2\omega\rangle$, $\langle\cos^4\omega\rangle$, $\langle\sin^2\omega\cos2\varphi\rangle$, $\langle\sin^4\omega\cos2\varphi\rangle$, and $\langle\sin^4\omega\cos4\varphi\rangle$. The angular averages $\langle\sin^2\omega\cdot\cos2\varphi\rangle$, $\langle\sin^4\omega\cos2\varphi\rangle$, and $\langle\sin^4\omega\cos4\varphi\rangle$ can be rewritten as

$$\langle\sin^2\omega\cos2\varphi\rangle = 2\langle\sin^2\omega\cos^2\varphi\rangle + \langle\cos^2\omega\rangle - 1 \qquad (3\text{-}21a)$$

$$\langle\sin^4\omega\cos2\varphi\rangle = 2\langle\sin^4\omega\cos^2\varphi\rangle - \langle\cos^4\omega\rangle + 2\langle\cos^2\omega\rangle - 1 \quad (3\text{-}21b)$$

$$\langle\sin^4\omega\cos4\varphi\rangle = 8\langle\sin^4\omega\cos^4\varphi\rangle - 8\langle\sin^4\omega\cos^2\varphi\rangle + \langle\cos^4\omega\rangle$$

$$- 2\langle\cos^2\omega\rangle + 1 \ , \quad (3\text{-}21c)$$

so that the polarized component of fluorescence intensity from the biaxially oriented system depends on the second and fourth moments about the c-axis ($\langle\cos^2\omega\rangle$ and $\langle\cos^4\omega\rangle$), the second and fourth moments about the a-axis ($\langle\sin^2\omega\cos^2\varphi\rangle$ and $\langle\sin^4\omega\cos^4\varphi\rangle$), and another fourth order average $\langle\sin^4\omega\cos^2\varphi\rangle$.

The coefficient $[S_{\ell m}T_{\ell'm'}]_{int}$ is dependent on the optical system employed for the measurement. In this treatment of biaxially oriented system, the polarized components of fluorescence intensity are calculated in an optical system as shown in Fig. 3-7, where the directions of incident beam and fluorescence observation are at angles θ_i and θ_j, respectively, from the c-axis. These directions are in a horizontal plane perpendicular to the surface of the sample (ab-plane). When the
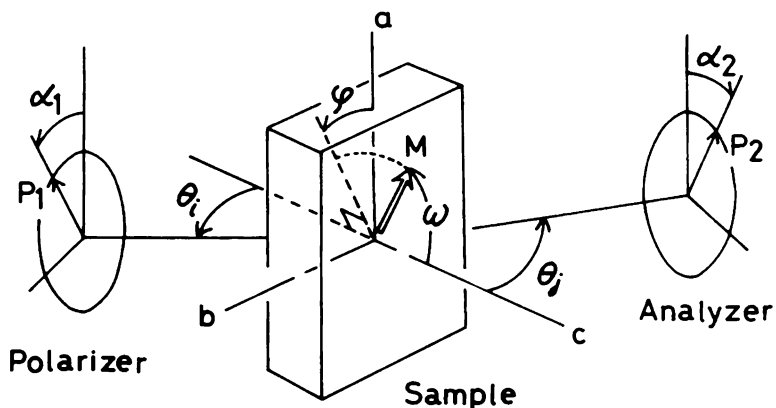
Fig. 3-7. Optical system for measuring the polarized
components of fluorescence intensity from a biaxially
oriented sample. (A)-set: the a-axis is parallel to the
vertical axis, (B)-set: the b-axis is parallel to the
vertical axis.

a-axis of the sample is vertical to the horizontal plane, the

alignment of the sample is defined as (A)-set. In the alignment

for (B)-set, the b-axis is vertical to the horizontal plane.

For such an optical system, both the incident exciting light and

the emitted fluorescence light are divided into the horizontal

and vertical components in the optically anisotropic sample.

The amplitudes and the vibration axes of the two components

of the exciting light which propagates in the anisotropic medium

can be given by the following equations, using the same notations

as defined in Chapter 2.

$$\begin{cases} a_{i1} = \sin\alpha_1 & \text{(3-22a)} \\ \\ a_{i2} = \cos\alpha_1 & \text{(3-22b)} \end{cases}$$

and

$$\begin{cases} \mathbb{p}_{1-1} = (\alpha_1', \beta_1') \begin{cases} = (\pi/2 - \theta_{i1},\ \pi/2) & \text{for (A)-set} \\ = (\pi/2 - \theta_{i1},\ \pi) & \text{for (B)-set} \end{cases} & \text{(3-23a)} \\ \\ \mathbb{p}_{1-2} = (\alpha_1'', \beta_1'') \begin{cases} = (\pi/2,\ 0) & \text{for (A)-set} \\ = (\pi/2,\ \pi/2) & \text{for (B)-set ,} \end{cases} & \text{(3-23b)} \end{cases}$$

where the subscripts 1 and 2 of a_i and $\mathbb{p}_1$ denote the horizontal and the vertical components, respectively, and θ_{i1} is the refraction angle for the horizontal component of incident light from the air into the anisotropic medium.

Similarly, the following relations can be given for the two components of the fluorescence coming from the anisotropic medium into the air.

$$\begin{cases} a_{f1} = \sin\alpha_2 & \text{(3-24a)} \\ \\ a_{f2} = \cos\alpha_2 & \text{(3-24b)} \end{cases}$$

and

$$\begin{cases} \mathbb{P}_{2-1} = (\alpha_2', \beta_2') \begin{cases} = (\pi/2 - \theta_1, \ \pi/2) & \text{for (A)-set} \\ = (\pi/2 - \theta_1, \ \pi) & \text{for (B)-set} \end{cases} & (3\text{-}25a) \\ \\ \mathbb{P}_{2-2} = (\alpha_2'', \beta_2'') \begin{cases} = (\pi/2, \ 0) & \text{for (A)-set} \\ = (\pi/2, \ \pi/2) & \text{for (B)-set ,} \end{cases} & (3\text{-}25b) \end{cases}$$

where θ_1 is the incident angle for the horizontal component when fluorescence beams enter the air from the anisotropic medium.

Using eqs. (3-23) and (3-25), one can calculate the coefficients $S_{\ell m}^{(j)}$ and $T_{\ell'm'}^{(j)}$, ($j = 1,2,3$) from eqs. (2-50) and (2-51). Moreover, by substituting the result of these calculations and eqs. (3-22) and (3-24) into eq. (2-49), $[S_{\ell m}T_{\ell'm'}]_{int}$ can be calculated in an explicit form. In the case of oblique incidence of a light beam, however, the effect of the transmittance or the reflectance of light energy must be considered, since the proportion of light energy transmitted through the surface of the sample is, in general, different between the horizontal and the vertical components. Therefore, in order to correct such an effect, the following equation should be utilized here instead of eq. (2-49).

$$[S_{\ell m}T_{\ell'm'}]_{int}$$

$$= \int_0^D (T_1 a_{i1}^2 \ S_{\ell m}^{(1)} + T_2 a_{i2}^2 \ S_{\ell m}^{(2)} + 2T_{av} a_{i1} a_{i2} \cos\delta_i \ S_{\ell m}^{(3)})$$

$$\times (T_1' a_{f1}^2 \ T_{\ell'm'}^{(1)} + T_2' a_{f2}^2 \ T_{\ell'm'}^{(2)} + 2T_{av}' a_{f1} a_{f2} \cos\delta_f \ T_{\ell'm'}^{(3)}) \, dl/D \ ,$$

$$(3\text{-}26)$$

where

$$
\begin{cases}
T_1 = \dfrac{\cos\{(\theta_{i1}+\theta_{i2})/2\}}{\cos\theta_i}\, n_{s1} t_1^{\,2} & \text{(3-27a)} \\[3mm]
T_2 = \dfrac{\cos\{(\theta_{i1}+\theta_{i2})/2\}}{\cos\theta_i}\, n_{s2} t_2^{\,2} & \text{(3-27b)} \\[3mm]
T_{av} = \dfrac{\cos\{(\theta_{i1}+\theta_{i2})/2\}}{\cos\theta_i}\, \dfrac{n_{s1}+n_{s2}}{2}\, t_1 t_2 & \text{(3-27c)}
\end{cases}
$$

and

$$
\begin{cases}
T_1' = \dfrac{\cos\theta_j}{\cos\{(\theta_1+\theta_2)/2\}}\, \dfrac{1}{n_{s(1)}}\, t_1'^{\,2} & \text{(3-28a)} \\[3mm]
T_2' = \dfrac{\cos\theta_j}{\cos\{(\theta_1+\theta_2)/2\}}\, \dfrac{1}{n_{s(2)}}\, t_2'^{\,2} & \text{(3-28b)} \\[3mm]
T_{av}' = \dfrac{\cos\theta_j}{\cos\{(\theta_1+\theta_2)/2\}}\, \dfrac{1/n_{s(1)}+1/n_{s(2)}}{2}\, t_1' t_2' \ . & \text{(3-28c)}
\end{cases}
$$

The notations $(\theta_{i1},\theta_{i2})$, (n_{s1},n_{s2}), (t_1,t_2), and (T_1,T_2) denote, in turn, the refractive angles, the refractive indices of the anisotropic medium, the amplitude transmission coefficients, and the transmittances of light energy for the two components of incident exciting light. Similarly, (θ_1,θ_2), $(n_{s(1)},n_{s(2)})$, (t_1',t_2'), and (T_1',T_2') denote, in turn, the incident angles, the refractive indices of the anisotropic medium, the amplitude transmission coefficients, and the transmittances of light energy

-58-

for the two rays of fluorescence from an emitting oscillator F_i in the anisotropic medium. These values can be determined by the principal refractive indices, n_a, n_b, and n_c, of the anisotropic medium, as shown in Appendix I.

The result of the calculation of $[S_{\ell m} T_{\ell' m'}]_{int}$ for the case of (A)-set can be given as follows:

$$[S_{00}T_{00}]_{int} = (4\pi/9)(T_1 \sin^2\alpha_1 + T_2 \cos^2\alpha_1)$$

$$\times (T_1' \sin^2\alpha_2 + T_2' \cos^2\alpha_2) \qquad (3\text{-}29a)$$

$$[S_{20}T_{00}]_{int} = (4\pi/9\sqrt{5})\{T_1 \sin^2\alpha_1 (3\sin^2\theta_{i1} - 1) - T_2 \cos^2\alpha_1\}$$

$$\times (T_1' \sin^2\alpha_2 + T_2' \cos^2\alpha_2) \qquad (3\text{-}29b)$$

$$[S_{00}T_{20}]_{int} = (4\pi/9\sqrt{5})(T_1 \sin^2\alpha_1 + T_2 \cos^2\alpha_1)$$

$$\times \{T_1' \sin^2\alpha_2 (3\sin^2\theta_1 - 1) - T_2' \cos^2\alpha_2\} \qquad (3\text{-}29c)$$

$$[S_{20}T_{20}]_{int} = (4\pi/45)\{T_1 \sin^2\alpha_1 (3\sin^2\theta_{i1} - 1) - T_2 \cos^2\alpha_1\}$$

$$\times \{T_1' \sin^2\alpha_2 (3\sin^2\theta_1 - 1) - T_2' \cos^2\alpha_2\} \qquad (3\text{-}29d)$$

$$[S_{21}T_{2\bar{1}}]_{int} = [S_{2\bar{1}}T_{21}]_{int}^{*}$$

$$= (-2\pi/15)\{(T_1 T_1' \sin^2\alpha_1 \sin^2\alpha_2 \sin 2\theta_{i1} \sin 2\theta_1$$

$$+ \ T_{av}T'_{av}\sin 2\alpha_1 \sin 2\alpha_2 \sin\theta_{il}\sin\theta_l \int_0^D \cos\delta_i \cos\delta_f \, dl/D)$$

$$+ \ i \ (T_{av}T'_1 \sin 2\alpha_1 \sin^2\alpha_2 \sin\theta_{il}\sin 2\theta_l \int_0^D \cos\delta_i \, dl/D$$

$$- \ T_1 T'_{av}\sin^2\alpha_1 \sin 2\alpha_2 \sin 2\theta_{il}\sin\theta_l \int_0^D \cos\delta_f \, dl/D) \ \} \qquad (3\text{-}29e)$$

$$[S_{22}T_{2\bar2}]_{int} \ = \ [S_{2\bar2}T_{22}]_{int}{}^*$$

$$= \ (2\pi/15) \ [\{ \ (T_1 \sin^2\alpha_1 \cos^2\theta_{il} \ - \ T_2 \cos^2\alpha_1)$$

$$\times \ (T'_1 \sin^2\alpha_2 \cos^2\theta_{il} \ - \ T'_2 \cos^2\alpha_2)$$

$$+ \ T_{av}T'_{av}\sin 2\alpha_1 \sin 2\alpha_2 \cos\theta_{il}\cos\theta_l \int_0^D \cos\delta_i \cos\delta_f \, dl/D\}$$

$$+ \ i \ \{T_{av}\sin 2\alpha_1 \cos\theta_{il}(T'_1 \sin^2\alpha_2 \cos^2\theta_l \ - \ T'_2 \cos^2\alpha_2)\int_0^D \cos\delta_i \, dl/D$$

$$- \ T'_{av}\sin 2\alpha_2 \cos\theta_l(T_1 \sin^2\alpha_1 \cos^2\theta_{il} \ - \ T_2 \cos^2\alpha_1)\int_0^D \cos\delta_f \, dl/D\}]$$

$$(3\text{-}29f)$$

$$[S_{22}T_{22}]_{int} \ = \ [S_{2\bar2}T_{2\bar2}]_{int}{}^*$$

$$= \ (2\pi/15) \ [\{ \ (T_1 \sin^2\alpha_1 \cos^2\theta_{il} \ - \ T_2 \cos^2\alpha_1)$$

$$\times \ (T'_1 \sin^2\alpha_2 \cos^2\theta_l \ - \ T'_2 \cos^2\alpha_2)$$

$$- \ T_{av}T'_{av}\sin 2\alpha_1 \sin 2\alpha_2 \cos\theta_{il}\cos\theta_l \int_0^D \cos\delta_i \cos\delta_f \, dl/D\}$$

$$+ \ i \ \{T_{av}\sin 2\alpha_1 \cos\theta_{il}(T'_1 \sin^2\alpha_2 \cos^2\theta_l \ - \ T'_2 \cos^2\alpha_2)\int_0^D \cos\delta_i \, dl/D$$

$$+ \ T'_{av}\sin 2\alpha_2 \cos\theta_l(T_1 \sin^2\alpha_1 \cos^2\theta_{il} \ - \ T_2 \cos^2\alpha_1)\int_0^D \cos\delta_f \, dl/D\}]$$

$$(3\text{-}29g)$$

$$[S_{21}T_{21}]_{int} = [S_{2\bar{1}}T_{2\bar{1}}]_{int}{}^*$$

$$= (-2\pi/15)\,\{(T_1 T_1' \sin^2\alpha_1 \sin^2\alpha_2 \sin2\theta_{i1} \sin2\theta_1$$

$$- T_{av}T_{av}' \sin2\alpha_1 \sin2\alpha_2 \sin\theta_{i1} \sin\theta_1 \int_0^D \cos\delta_i \cos\delta_f \,dl/D)$$

$$+ i\,(T_{av}T_1' \sin2\alpha_1 \sin^2\alpha_2 \sin\theta_{i1} \sin2\theta_1 \int_0^D \cos\delta_i \,dl/D$$

$$+ T_1 T_{av}' \sin^2\alpha_1 \sin2\alpha_2 \sin2\theta_{i1} \sin\theta_1 \int_0^D \cos\delta_f \,dl/D)\,\} \qquad \text{(3-29h)}$$

$$[S_{22}T_{00}]_{int} = [S_{2\bar{2}}T_{00}]_{int}{}^*$$

$$= (-2\pi/3)\,\sqrt{2/15}\,(T_1' \sin^2\alpha_2 + T_2' \cos^2\alpha_2)$$

$$\times (T_1 \sin^2\alpha_1 \cos^2\theta_{i1} - T_2 \cos^2\alpha_1 + i\,T_{av}\sin2\alpha_1 \cos\theta_{i1}\int_0^D \cos\delta_i \,dl/D)$$

$$\text{(3-29i)}$$

$$[S_{00}T_{22}]_{int} = [S_{00}T_{2\bar{2}}]_{int}{}^*$$

$$= (-2\pi/3)\,\sqrt{2/15}\,(T_1 \sin^2\alpha_1 + T_2 \cos^2\alpha_1)$$

$$\times (T_1' \sin^2\alpha_2 \cos^2\theta_1 - T_2' \cos^2\alpha_2 + i\,T_{av}' \sin2\alpha_2 \cos\theta_1 \int_0^D \cos\delta_f \,dl/D)$$

$$\text{(3-29j)}$$

$$[S_{22}T_{20}]_{int} = [S_{2\bar{2}}T_{20}]_{int}{}^*$$

$$= (-2\pi/15)\,\sqrt{2/3}\,\{T_1' \sin^2\alpha_2 (3\sin^2\theta_1 - 1) - T_2' \cos^2\alpha_2\}$$

$$\times (T_1 \sin^2\alpha_1 \cos^2\theta_{i1} - T_2 \cos^2\alpha_1 + i\,T_{av}\sin2\alpha_1 \cos\theta_{i1}\int_0^D \cos\delta_i \,dl/D)$$

$$\text{(3-29k)}$$

$$[S_{20}T_{22}]_{int} = [S_{20}T_{2\bar{2}}]_{int}{}^*$$

$$= (-2\pi/15)\sqrt{2/3}\ \{T_1\sin^2\alpha_1(3\sin^2\theta_{i1}-1) - T_2\cos^2\alpha_1\}$$

$$\times\ (T_1'\sin^2\alpha_2\cos^2\theta_1 - T_2'\cos^2\alpha_2 + i\ T_{av}'\sin2\alpha_2\cos\theta_1\int_0^D\cos\delta_f dl/D)\ .$$

$$(3-291)$$

Equations (3-29a)-(3-291) are also applicable to the case of (B)-set, except that the sign of $[S_{\ell m}T_{\ell'm'}]_{int}$ for $m+m'=2$ and -2 is opposite for the case of (B)-set, that is, $[S_{\ell m}T_{\ell'm'}]_{int}$ ((B)-set) $= -[S_{\ell m}T_{\ell'm'}]_{int}$ ((A)-set) for $m+m'=2$ and -2.

Practically, we need only the real part of $[S_{\ell m}T_{\ell'm'}]_{int}$, since the imaginary part of the coefficient $M_{\ell'm'0}^{\ell m 0}$ should be equal to zero from eq. (3-19). Therefore, we can find the birefringence term, $\int_0^D\cos\delta_i\cos\delta_f dl/D$, in $[S_{21}T_{2\bar{1}}]_{int}$, $[S_{22}T_{2\bar{2}}]_{int}$, $[S_{22}T_{22}]_{int}$, and $[S_{21}T_{21}]_{int}$. The birefringence effect is absent when the transmission axis of polarizer and/or that of analyzer coincides with the vertical or the horizontal direction. $\int_0^D\cos\delta_i\cdot\cos\delta_f dl/D$ can be given by using eqs. (AI-13) and (AI-14) in Appendix I, in the following way:

$$\int_0^D\cos\delta_i\cos\delta_f\ dl/D = (\Delta_i\sin\Delta_i - \Delta_f\sin\Delta_f)/(\Delta_i^2 - \Delta_f^2)\ ,\quad (3-12)$$

where for (A)-set,

$$\Delta_i = \frac{2\pi D}{\lambda_i} \frac{1}{n_c} \left(n_c \sqrt{n_a^2 - \sin^2\theta_i} - n_b \sqrt{n_c^2 - \sin^2\theta_i} \right) \qquad (3\text{-}30)$$

$$\Delta_f = \frac{2\pi D}{\lambda_f} \frac{1}{n_c} \left(n_c \sqrt{n_a^2 - \sin^2\theta_j} - n_b \sqrt{n_c^2 - \sin^2\theta_j} \right) , \qquad (3\text{-}31)$$

and for (B)-set, the principal refractive indices, n_a and n_b, must be exchanged.

3-5. Experimental Verification for Biaxially Stretched

     Polymer Films

     In order to verify the validity of the equation of polarized fluorescence intensity in the biaxially oriented system, the experiment was carried out by using a biaxially stretched poly(vinyl alcohol) film in which fluorescent probes RP were dispersed. The PVA-RP film was prepared by casting the solution in the same way as described in the previous section. The biaxial stretching was carried out at 100 °C by the apparatus for orthogonally biaxial stretching (Iwamoto Seisakusho Co., Ltd.). The sample film was stretched uniaxially with fixed width, then it was subjected to a secondary stretching along the axis perpendicular to the first stretching axis. Here, let the axis with the larger refractive index of the two stretching axes of the film be the a-axis and the other be the b-axis. Accordingly, the c-axis is defined as the axis normal to the surface

of the film. The measurement of the polarized components of fluorescence intensity were carried out for two kinds of alignments of the optical axes with respect to the surface of the film, that is, $\theta_i = \theta_j = 0°$ and $\theta_i = \theta_j = 60°$ in the optical system shown in Fig. 3-7. On the other hand, the principal refractive indices (n_a, n_b, and n_c) were measured by using an Abbe refractometer, and a polarizing microscope was also used for the measurement of the birefringence in the ab-plane, i.e., $n_a - n_b$.

The equation of polarized fluorescence intensity in the optically anisotropic system of biaxial orientation can be verified experimentally in the same manner for uniaxially oriented films. The five moments of molecular orientation distribution, $<\cos^2\omega>$, $<\cos^4\omega>$, $<\sin^2\omega\cos^2\varphi>$, $<\sin^4\omega\cos^4\varphi>$, and $<\sin^4\omega\cos^2\varphi>$, were determined from eq. (3-20) by using the observed values of several components of fluorescence intensity unaffected by the birefringence effect. In those cases the transmission axes of polarizer and analyzer were either in the vertical or the horizontal direction, i.e., $\alpha_1 = 0$ or $\pi/2$ and $\alpha_2 = 0$ or $\pi/2$. For the calculation, 0.951 was adopted as the factors of photophysical anisotropy of the fluorescent probe RP, i.e., $<\cos^2\delta> = <\cos^2\eta> = 0.951$. Many components of observed polarized fluorescence intensity were compared with their corresponding values calculated from eq. (3-20) by using the previously estimated five moments. For this purpose, the bire-

fringence term $\int_0^D \cos\delta_i \cos\delta_f \, dl/D$ must be determined beforehand

from eqs. (3-12), (3-30), and (3-31) by using the values of

principal refractive indices.

Figure 3-8 shows the result of measurement of polarized

components of fluorescence intensity for PVA-RP film which was

stretched to 76 % elongation on the first stretching and to 26 %

elongation on the second stretching. The first and second

stretching axes of this film correspond to the a- and b- axes,

respectively, and three principal refractive indices for the

Sodium-D line are n_a = 1.5263, n_b = 1.5202, and n_c = 1.5155.

The thickness of the film, D, is 0.120 mm. The values of five

moments were determined as follows; $\langle\cos^2\omega\rangle$ = 0.166, $\langle\cos^4\omega\rangle$ =

0.060, $\langle\sin^2\omega\cos^2\varphi\rangle$ = 0.539, $\langle\sin^4\omega\cos^4\varphi\rangle$ = 0.399, and $\langle\sin^4\omega$

$\cdot\cos^2\varphi\rangle$ = 0.481.

Figure 3-8a shows the verification for the case of the

oriented sample which was rotated about the c-axis at every 10°

angle from the initial position where the a-axis was parallel to

the transmission axis of polarizer ($\mathbb{P}_1$) in the optical system

of $\theta_i = \theta_j = 0°$. In this figure, the open circle (O) and the

filled circle (●) represent the observed polarized components

of fluorescence intensity for the sets of parallel Nicols (α_2 =

α_1) and crossed Nicols ($\alpha_2 = \alpha_1 + \pi/2$), respectively.

Figure 3-8b shows the result of the verification for the

case in which the polarizer was rotated about its normal at

I(α_1)

I(α_1+90°)

Polarized Fluorescence Intensity

Rotation Angle of Sample

(a)

I(α_1)A$_{45°}$

I(α_1)B$_{45°}$

Rotation Angle of Polarizer

(b)

-66-
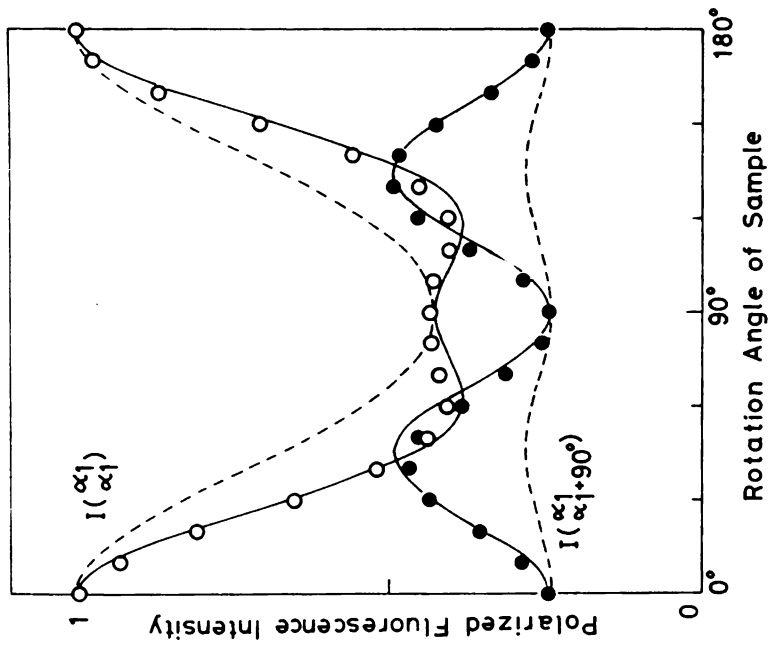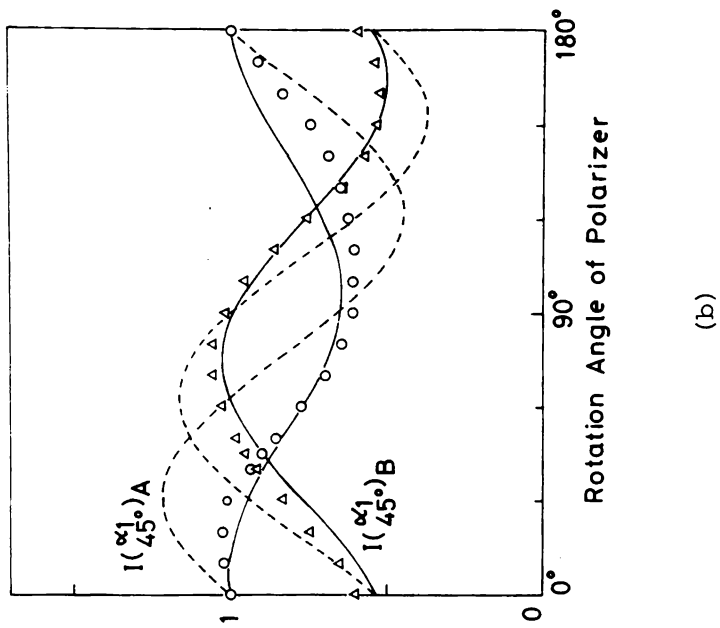
Fig. 3-8. Polarized components of fluorescence intensity obtained from biaxially stretched PVA-RP film (76 % elongation along the first stretching axis, 26 % elongation along the second stretching axis), (a) as a function of the angle of rotation of the specimen about the c-axis in the case of $\theta_i=\theta_j=0°$ ($\bigcirc$: $\alpha_2=\alpha_1$, $\bullet$: $\alpha_2=\alpha_1+\pi/2$) and (b) as a function of the angle of rotation of the polarizer in the case of $\theta_i=\theta_j=60°$ and $\alpha_2=\pi/4$ ($\bigcirc$: (A)-set, $\triangle$: (B)-set). (——): Calculated curve by eq. (3-20). (— —): Calculated curve disregarding the birefringence effect.

every 10° angle from the intial state where the transmission axis of polarizer (p_1) was parallel to the vertical axis, while the transmission axis of analyzer (p_2) was kept at an angle of $\pi/4$ to the vertical axis in the optical system of $\theta_i = \theta_j = 60°$. In this figure, the open circle (O) and the triangle ($\triangle$) represent the observed polarized components of fluorescence intensity for (A)-set (the a-axis of the sample is kept parallel to the vertical axis) and (B)-set (the b-axis of the sample is kept parallel to the vertical axis), respectively.

In Figs. 3-8a and 3-8b, the solid lines are the curves calculated according to the procedure mentioned previously. The observed fluorescence intensities are in good agreement with these solid lines. The curves calculated disregarding the birefringence effect due to the optical anisotropy of the polymer medium are also shown by the broken lines in order to clarify the effect of birefringence.

Similar experimental verifications were carried out for other biaxially stretched PVA-RP films, and the results were obtained reasonably.

It can be concluded from these results that the equation of polarized fluorescence intensity is valid also for the biaxially anisotropic system and that the obtained values of the five moments of molecular orientation are also reliable.

References and Notes

1) Y. Onogi and Y. Nishijima, Repts. Progr. Polym. Phys. Japan, 19, 411 (1976).

2) The fluorescence anisotropy ratio[*], R, can be compared with the degree of polarization of fluorescence[**], P, as follows:

$$R = 2P/(3 - P) \ ,$$

where
$$P = (I_{\parallel} - I_{\perp})/(I_{\parallel} + I_{\perp})$$

in which $I_{\parallel}$ and $I_{\perp}$ are the polarized components of fluorescence intensity parallel and perpendicular, respectively, to the electric vector of the exciting light.

*) A. Jablonski, Bull. Acad. Polon. Sci. Ser. Math. Phys., 8, 259 (1960).

**) F. Perrin, J. Phys., 7, 390 (1926).

   G. Weber, Biochem. J., 51, 145 (1952).

3) The fluorescent molecule SW is used in Chapter 8, too. Its molecular structure is shown in Fig. 8-1. The PVC-SW film was prepared by casting the solution of PVC (SG-1100, Nihon Carbide Co.) in cyclohexanone containing fluorescent probe SW onto a glass plate at about 50 °C. The maximum peak of the fluorescence spectrum of SW in PVC film is at 442 nm. For the photophysical anisotropy factors of this probe, the value of $\langle\cos^2\delta\rangle=\langle\cos^2\eta\rangle=0.957$ was adopted, which was

estimated from the fluorescence anisotropy ratio of un-

stretched PVC-SW film.

CHAPTER 4

Estimation of Molecular Orientation Distribution

from Its Moments

in Polymer Films Stretched in Various Ways

4-1. Introduction

The polarized component of fluorescence intensity is, in
general, dependent on not only the molecular orientation distri-
bution but also the optical anisotropy of the medium. Hence,
when the molecular orientation behavior is estimated from the
polar diagram representation of the angular distribution of
polarized components of fluorescence intensity,[1] the bire-
fringence effect due to the optical anisotropy of the medium
must be taken into consideration, as mentioned in section 3-3
in Chapter 3. In addition, Hibi et al. reported the effect of
absorption of light by the anisotropic medium as another effect
on the angular distribution of polarized components of fluo-
rescence intensity.[2] The estimation of molecular orientation
behavior from the polar diagram representation of observed
fluorescence intensity is very powerful for the recognition of
the type of orientation distribution at sight, providing that
crrections for the anisotropic medium are properly made.

In Chapter 3, it was verified that the equation of the

polarized component of fluorescence intensity is reasonably

applicable to the anisotropic systems of both uniaxial and

biaxial orientations and that the moments of molecular orien-

tation distribution can also be evaluated reliably. In this

chapter, the characterization of molecular orientation is

carried out quantitatively from the several moments of molecular

orientation distribution, for PVA-RP films stretched in various

ways.

The estimation of molecular orientation distribution from

its moments was carried out for oriented PVA-RP films which were

stretched to various draw ratios in four ways; 1) free width

uniaxial stretching, 2a) simultaneous biaxial stretching, 2b)

successive biaxial stretching, and 2c) fixed width uniaxial

stretching. In the case of 1), the stretching axis of the film

is the c-axis and therefore the orientation distribution of the

molecular axis (M-axis) can be estimated from the second and

fourth moments about the c-axis, $<\cos^2\omega>$ and $<\cos^4\omega>$, determined

from eq. (3-4) by using the observed components of fluorescence

intensity which are not affected by the birefringence effect.

In the cases of 2a), 2b), and 2c), the axis normal to the film

surface is the c-axis and the stretching axes are the a- and b-

axes. Therefore, the molecular orientation distribution can be

estimated from the five moments, $\langle\cos^2\omega\rangle$, $\langle\cos^4\omega\rangle$, $\langle\sin^2\omega\cos^2\varphi\rangle$, $\langle\sin^4\omega\cos^4\varphi\rangle$, and $\langle\sin^4\omega\cos^2\varphi\rangle$, determined from eq. (3-20) by using the observed components of fluorescence intensity which are not affected by the birefringence effect.

4-2. Free Width Uniaxial Stretching

The molecular orientation in the case of free width uni-axial stretching of PVA-RP films has already been estimated by Onogi from the second and fourth moments.[3,4] In order to compare with the cases of biaxial stretching and fixed width uniaxial stretching which are discussed in the next section, let us summarize the result of free width uniaxial stretching.

The relationships between $\langle\cos^2\omega\rangle$, $\langle\cos^4\omega\rangle$, and per cent elongation of oriented PVA-RP films stretched uniaxially with free width are shown in Fig. 4-1. The per cent elongation of a stretched sample was determined from the positions of marks on the film. The solid lines in this figure show the theoretical curves according to the Kratky type affine deformation model.[5] The theoretical curve of $\langle\cos^4\omega\rangle$ against $\langle\cos^2\omega\rangle$ coincides with the relationship assuming the type of orientation distribution to be the prolate ellipsoid of revolution.

The plots of observed values of $\langle\cos^2\omega\rangle$ and $\langle\cos^4\omega\rangle$ against per cent elongation fit the theoretical curves assuming the affine deformation at the initial stage of elongation, whereas
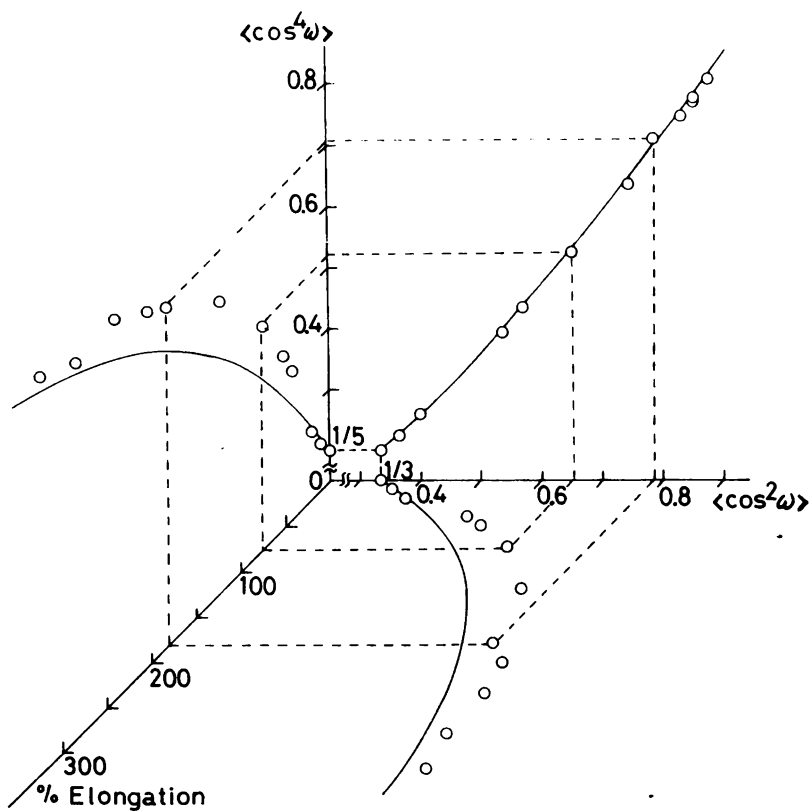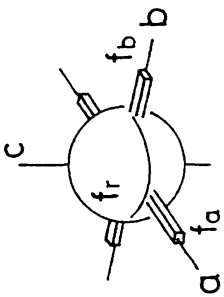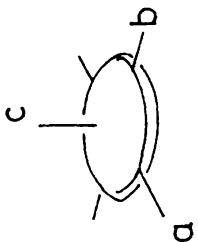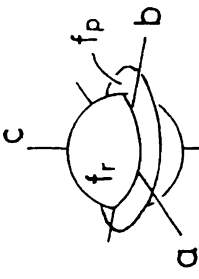
Fig. 4-1. Relationships between $\langle\cos^2\omega\rangle$, $\langle\cos^4\omega\rangle$, and per cent elongation for PVA-RP film uniaxially stretched with free width. (———): Theoretical curve assuming the Kratky type affine deformation mechanism.

at larger elongation the molecular orientation seems to exceed the orientation theoretically expected by the affine deformation. However, the plots of the fourth moment against the second moment fit the solid line curve . Therefore, the type of orientation distribution of molecular axes of fluorescent probes RP in PVA film can be explained to be a prolate ellipsoidal distribution, though the deformation mechanism is not exactly the same as the affine transformation mechanism. This result also suggests that the orientation of polymer chains in the amorphous region of uniaxially stretched PVA film is not a peculiar type.

4-3. Biaxial Stretching and Fixed Width Uniaxial Stretching

In Table 4-1, three kinds of basic models of the molecular orientation distribution in the biaxial stretching are shown together with the corresponding orientation distribution functions. Model A is a combination model of three-dimensional random orientation and two perpendicular axial orientations. In this case, while a portion of the molecules orients along the two perpendicular stretching axes, the other portion remains unoriented as it was. Model B is a model of oblate ellipsoidal orientation distribution. In this model, k_{ac}, k_{bc}, and k are defined as the axial ratios of ellipsoid, i.e., $k_{ac} = c/a$, $k_{bc} = c/b$, and k = b/a (= k_{ac}/k_{bc}). Model C is a combination model of three-dimensional random orientation and planar orien-

Table 4-1. Basic types of the molecular orientation distribution for biaxial stretching of polymer films. $m(\omega,\varphi)$: Orientation distribution function of the molecular axis (M-axis). δ: Dirac delta function.

TYPE OF ORIENTATION	ORIENTATION DISTRIBUTION FUNCTION $m(\omega, \varphi)$	KIND OF OPTICAL ANISOTROPY	
		I	II
A	$= (1/4\pi)f_r + \delta\left(\omega - \dfrac{\pi}{2}\right) \displaystyle\sum_{n=0,1} \left[\dfrac{f_a}{2}\,\delta(\varphi - n\pi) + \dfrac{f_b}{2}\,\delta\left(\varphi - \dfrac{2n+1}{2}\pi\right) \right]$ $(\ f_r + f_a + f_b = 1\ )$	A_I $f_a = f_b$	A_{II} $f_a \neq f_b$
B	$= (1/4\pi)k k_{bc}^2 \left[k_{bc}^2(k^2-1)\sin^2\omega\cos^2\varphi + (1-k_{bc}^2)\cos^2\omega + k_{bc}^2 \right]^{-3/2}$ $(\ k = b/a,\ k_{bc} = c/b,\ k_{ac} = c/a\ )$	B_I $k = 1$	B_{II} $k \neq 1$
C	$= (1/4\pi)f_r + f_p\,\delta\left(\omega - \dfrac{\pi}{2}\right)$ $\times\ \dfrac{1}{2\pi}\ \dfrac{k}{\sin^2\varphi + k^2\cos^2\varphi}$ $(\ f_r + f_p = 1,\ k = b/a\ )$	C_I $k = 1$	C_{II} $k \neq 1$

tation. In this case, while a portion of the molecules orients parallel to the ab-plane, the other portion remains unoriented as it was. A_I, B_I, and C_I are the models corresponding to the simultaneous biaxial stretching and A_{II}, B_{II}, and C_{II} are the models corresponding to the successive biaxial stretching and uniaxial stretching with fixed width. The first set is the model for optically anisotropic systems of uniaxial orientation and the second set is the model for optically anisotropic systems of biaxial orientation.

Figure 4-2 shows the comparison of the relationships between the observed values of the second and fourth order moments with those obtained by using the models A, B, and C. In Fig. 4-2a, the fourth moment about the c-axis, $\langle \cos^4\omega \rangle$, is plotted against the second moment about the c-axis, $\langle \cos^2\omega \rangle$. In Fig. 4-2b, the fourth moment about the a-axis, $\langle \sin^4\omega\cos^4\varphi \rangle$, is plotted against the second moment about the a-axis, $\langle \sin^2\omega\cos^2\varphi \rangle$. In Fig. 4-2c, the other fourth order moment, $\langle \sin^4\omega\cos^2\varphi \rangle$, is plotted against $\langle \sin^2\omega\cos^2\varphi \rangle$. In thse figures, the plots of observed values ($\bigcirc$: simultaneous biaxial stretching, $\bullet$: successive biaxial stretching, and $\triangle$: fixed width uniaxial stretching) fit the theoretical curves assuming the orientation distribution of type B. Accordingly, it can be concluded that when PVA film is biaxially stretched or uniaxially stretched with fixed width, the orientation distribution of molecular axes does not obey the

-77-
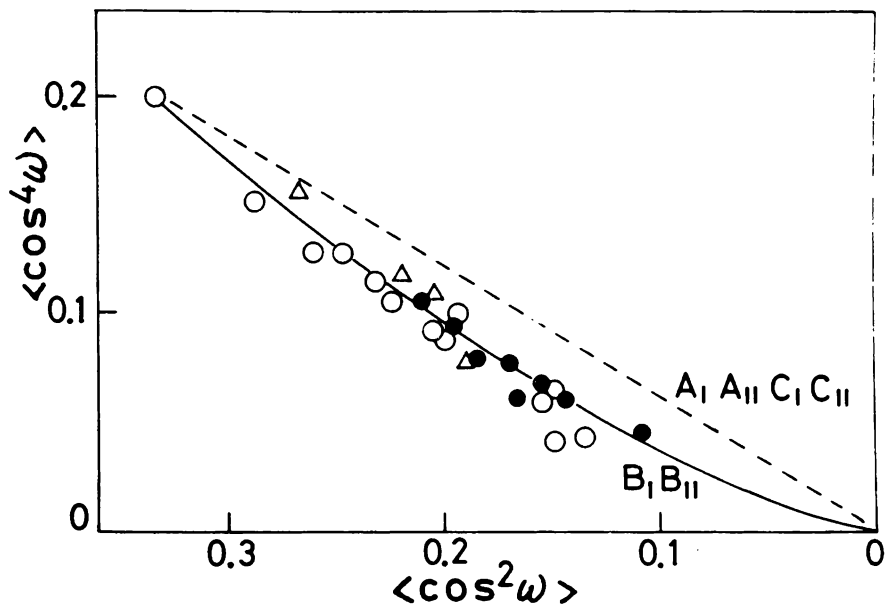
(a) $\langle \cos^4 \omega \rangle$ vs. $\langle \cos^2 \omega \rangle$.
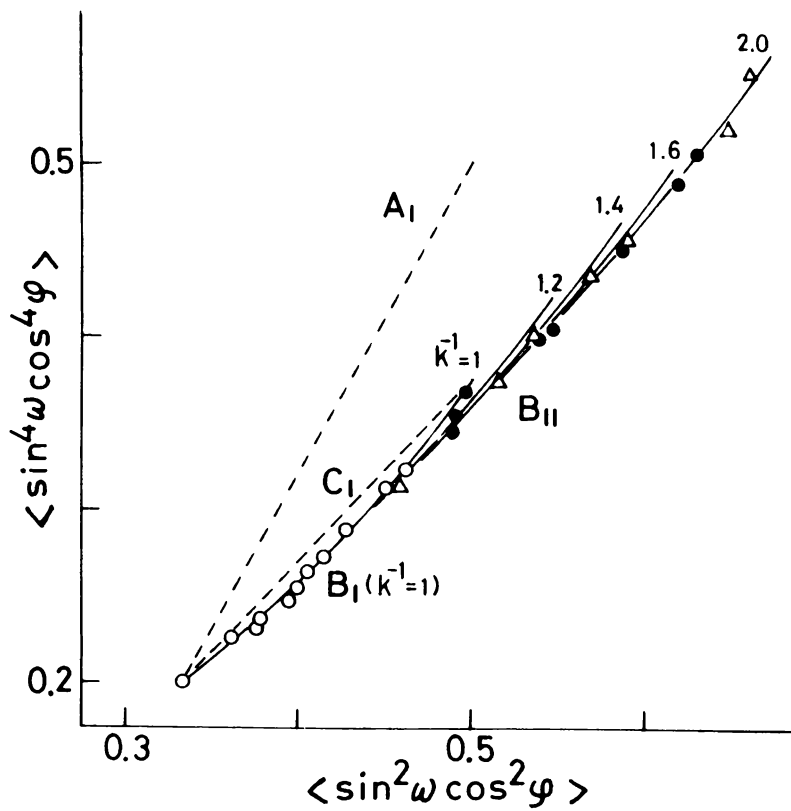
(b) $\langle \sin^4 \omega \cos^4 \varphi \rangle$ vs. $\langle \sin^2 \omega \cos^2 \varphi \rangle$.
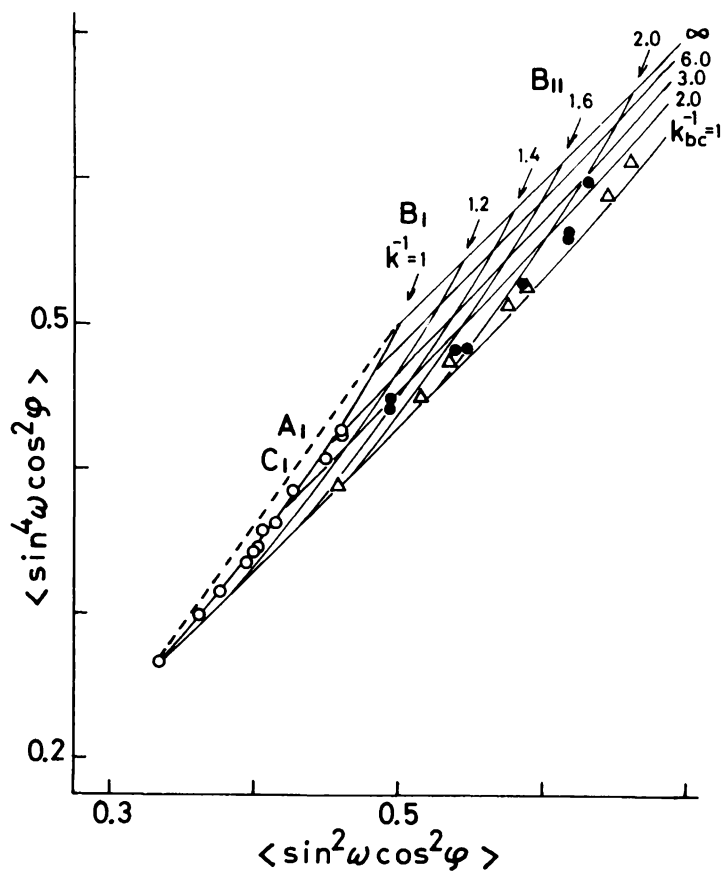
(c) $\langle \sin^4 \omega \cos^2 \varphi \rangle$ vs. $\langle \sin^2 \omega \cos^2 \varphi \rangle$.

Fig. 4-2. Comparison of relationships between observed values of the second and fourth order moments with those obtained by using the models of molecular orientation distribution shown in Table 4-1. (◯): simultaneous biaxial stretching, (●): successive biaxial stretching, (△): fixed width uniaxial stretching.

types A and C which are the extreme cases of molecular orientation.

In order to estimate quantitatively the orientation of molecular axes with respect to the sample coordinate system O-abc, the second moment about the a-axis, $<\sin^2\omega\cos^2\varphi>$, is plotted against the second moment about the c-axis, $<\cos^2\omega>$, in Fig. 4-3. The degree of molecular orientation parallel to the ab-plane increases with decreasing value of $<\cos^2\omega>$, and the degree of molecular orientation along the a-axis increases with increasing value of $<\sin^2\omega\cos^2\varphi>$. The solid lines are the theoretical curves for the ellipsoidal orientation distribution, and they are illustrated by varying the axial ratios, k_{bc} and k, of the ellipsoid. One can easily estimate the degree of molecular orientation with respect to the sample coordinate system O-abc, from the position plotted in this figure. The values in the brackets beside the points plotted in this figure show the per cent elongations which were determined by using the square lattice pattern printed on the film surface. In the case of successive biaxial stretching, the per cent elongation of the first stretching is shown at the top in a bracket and that of the second stretching is shown at the bottom. The axis having the larger extent of elongation was always defined as the a-axis in the sample. In the case of fixed width uniaxial stretching along the a-axis, the observed values are plotted near the
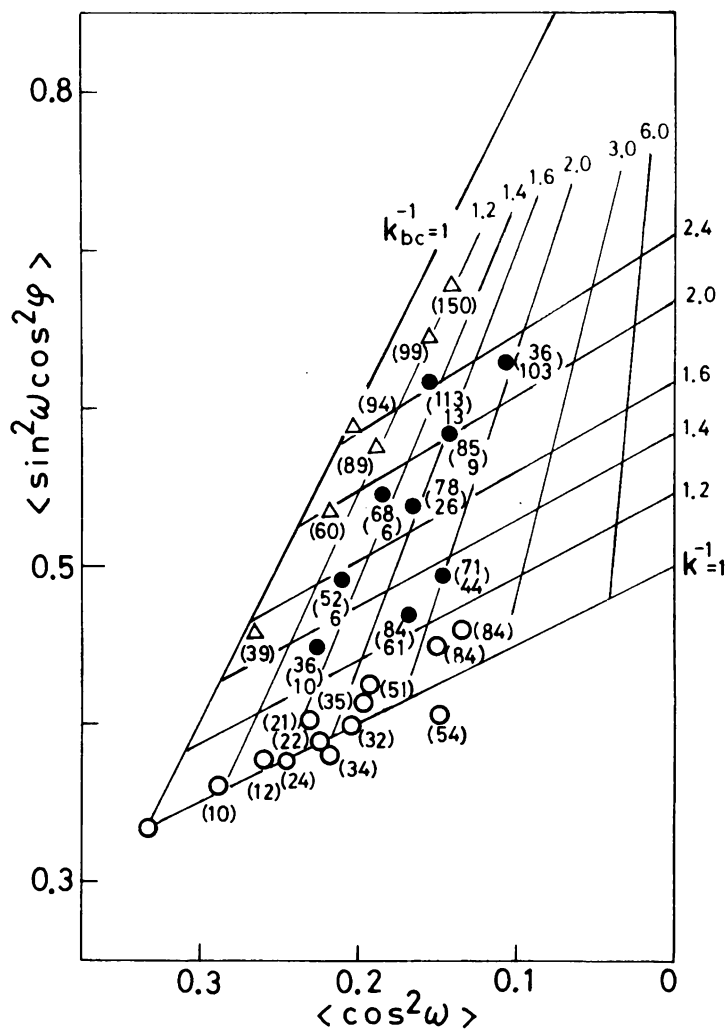
Fig. 4-3. Plot of $\langle \sin^2\omega\cos^2\varphi \rangle$ against $\langle \cos^2\omega \rangle$.

($\bigcirc$): simultaneous biaxial stretching, ($\bullet$): successive biaxial stretching, ($\triangle$): fixed width uniaxial stretching. The lines indicate the ellipsoidal orientation distribution by varying the axial ratios of the ellipsoid.

theoretical line of $k_{bc}^{-1} = 1$ corresponding to the uniaxial

stretching with free width. This result can be explained from

the fact that the center of the film specimen tended to shrink

to some extent along the direction perpendicular to the

stretching axis. (The samples for the measurement were always

prepared by cutting out from the center of stretched film.)

Figure 4-4 shows the plots of $<\cos^2\omega>$ and $<\sin^2\omega\cos^2\varphi>$

against the per cent elongation in direction of the a-axis.

The solid and broken lines are the theoretical curves assuming

the affine transformation mechanism of the ellipsoidal orien-

tation distribution. They are illustrated by varying the value

of λ_a/λ_b (λ_a: draw ratio of the a-axis, λ_b: draw ratio of the

b-axis). The lines L_2, L_1, and L_1' are the theoretical curves

corresponding to the simultaneous biaxial stretching, the uni-

axial stretching along the a-axis with free width, and the

uniaxial stretching along the a-axis with fixed width, respec-

tively. The L_1 lines are the theoretical curves according to

the Kratky type affine deformation model discussed for the case

of uniaxial stretching with free width. The open circle (O),

the filled circle ($\bullet$), the filled square ($\blacksquare$), and the tri-

angle ($\triangle$) express, respectively, the observed values for the

cases of the simultaneous biaxial stretching, the successive

biaxial stretching of $\lambda_a/\lambda_b \simeq 1.4$, the successive biaxial

stretching of $\lambda_a/\lambda_b \simeq 1.8$, and the uniaxial stretching with fixed

width. The values of $\langle \cos^2 \omega \rangle$ tend to be larger than those expected theoretically by the affine deformation for all the series of samples stretched in the three fifferent ways. This means that fluorescent probes tend to orient parallel to the ab-plane more slowly than they orient in the affine mechanism. On the other hand, the values of $\langle \sin^2 \omega \cos^2 \varphi \rangle$ are plotted closely on the theoretical curves. Considering the result shown in Fig. 4-4 more carefully, in the case of simultaneous biaxial stretching the observed values of $\langle \sin^2 \omega \cos^2 \varphi \rangle$ are smaller than those obtained by assuming the affine deformation mechanism, whereas in the case of successive biaxial stretching, the values of $\langle \sin^2 \omega \cos^2 \varphi \rangle$ tend to become larger than those obtained by assuming the affine deformation as the value of λ_a / λ_b increases. It can be found from this experiment that when PVA films are deformed in biaxial stretching, fluorescent probes orient toward the direction of stretching axis having the larger extent of elongation more easily than expected by the affine mechanism after balancing ($\lambda_a = \lambda_b$). These results of biaxial stretching and uniaxial stretching with fixed width are consistent with the result of uniaxial stretching with free width (Fig. 4-1).
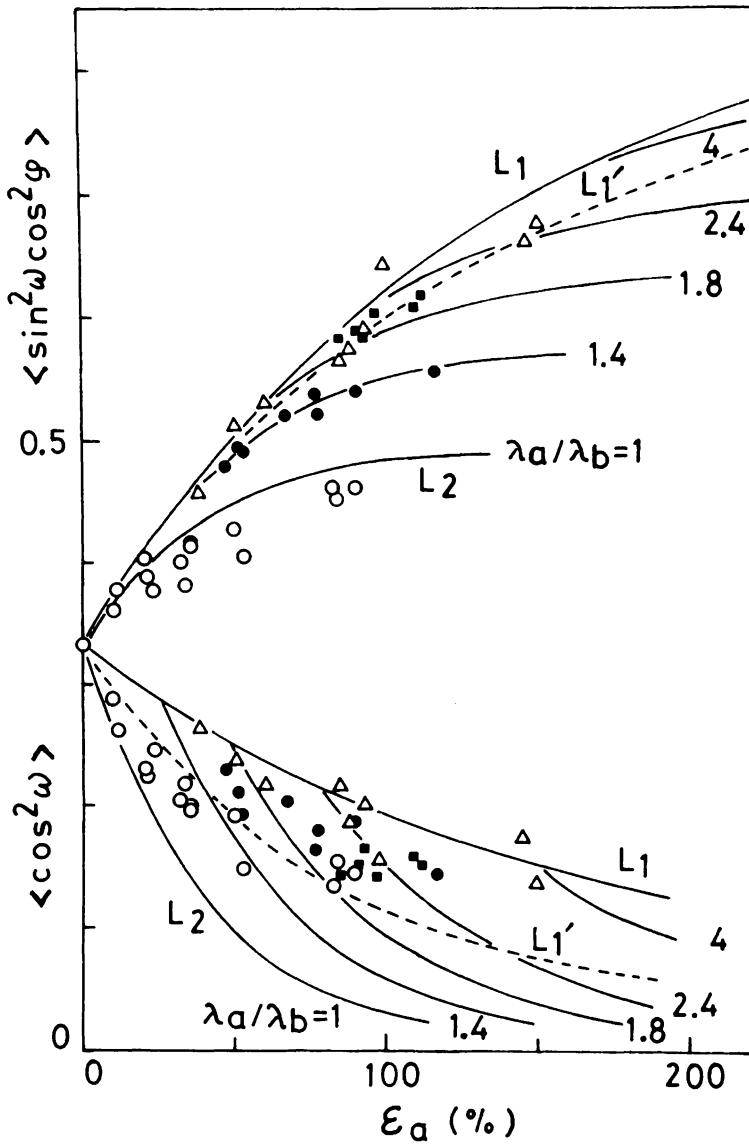
Fig. 4-4. $<\cos^2\omega>$ and $<\sin^2\omega\cos^2\varphi>$ versus per cent

elongation (ε_a) in direction of the a-axis of PVA-RP

film. (O): simultaneous biaxial stretching, (●): suc-

cessive biaxial stretching of $\lambda_a/\lambda_b \simeq 1.4$, (■): suc-

cessive biaxial stretching of $\lambda_a/\lambda_b \simeq 1.8$, and

(△): fixed width uniaxial stretching. L_1: theoretical

curve corresponding to the free width uniaxial stretching

along the a-axis, L_1': theoretical curve corresponding to

the fixed width uniaxial stretching along the a-axis,

and L_2: theoretical curve corresponding to the simul-

taneous biaxial stretching.

4-4. Comparison of Fluorescence Polarization with

   Birefringence

   Let us show a comparison of the second moment obtained from

fluorescence measurement with that from birefringence for PVA-RP

films used in the previous sections.

   Figure 4-5 shows the plot of the second moment ($<\cos^2\omega>$)

obtained by the fluorescence method against birefringence ($\Delta n =$

$n_c - n_a = n_c - n_b$) for PVA-RP films stretched uniaxially with

free width. The lines (a) and (b) show the relationship between

the second moment ($<\cos^2\omega>_{\Delta n}$) and Δn, according to the following

equation:

$$\Delta n = \frac{3<\cos^2\omega>_{\Delta n} - 1}{2} \Delta n° \ , \qquad (4-1)$$

where $\Delta n°$ is the intrinsic birefringence for the perfect uni-

axial orientation of polymer chains and $<\cos^2\omega>_{\Delta n}$ is the second

moment for the orientation of anisotropic units of polariz-

ability. In this figure, the value for intrinsic birefringence

of 44.3×10^{-3}, which was estimated by Nomura et al.[6] for the

crystalline phase in PVA film, and that of 42.2×10^{-3}, which

was estimated by Kobayashi et al.[7] for PVA-Congo Red system,

are taken as the reference values of $\Delta n°$. The observed value

of $<\cos^2\omega>$ rapidly increases linearly with an increase of bire-

fringence in the range of $0 < \Delta n < 1.5 \times 10^{-2}$ and then gradually
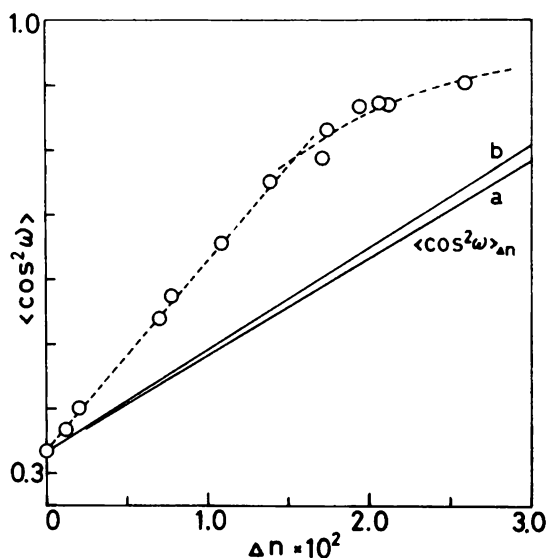
Fig. 4-5. Relationship between the second moment ($<\cos^2\omega>$)

obtained from fluorescence measurement and birefringence

for uniaxially stretched PVA-RP films (free width).

Line (a): second moment from birefringence using $\Delta n° =$

44.3×10^{-3}. Line (b): second moment from birefringence

using $\Delta n° = 42.2 \times 10^{-3}$.

increases beyond $\Delta n = 1.5 \times 10^{-2}$. Moreover, the second moment

$<\cos^2\omega>$ from fluorescence measurement is larger than $<\cos^2\omega>_{\Delta n}$

estimated from birefringence data.

Figure 4-6 shows the results of PVA-RP samples stretched

biaxially and those stretched uniaxially with fixed width, i.e.,

the second moment about the c-axis, $<\cos^2\omega>$, is plotted against

$(\Delta n_{ac} + \Delta n_{bc})/2$ and the second moment about the a-axis,

-87-
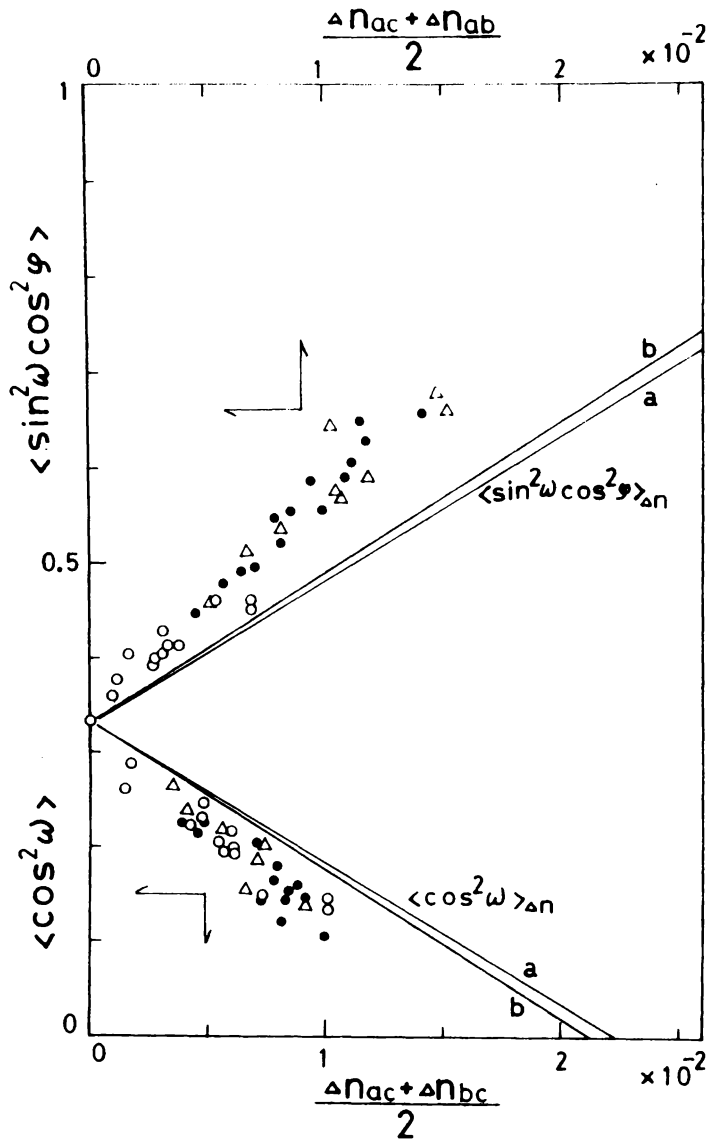
Fig. 4-6. Relationships between the second moments ($<\sin^2\omega$

$\cdot\cos^2\varphi>$, $<\cos^2\omega>$) obtained from fluorescence measurement

and birefringence for stretched PVA-RP films.

(○): simultaneous biaxial stretching, (●): successive

biaxial stretching, and (△): fixed width uniaxial

stretching. Lines (a): second moments from birefringences

using $\Delta n° = 44.3 \times 10^{-3}$. Lines (b): second moments from

birefringences using $\Delta n° = 42.2 \times 10^{-3}$.

$<\sin^2\omega\cos^2\varphi>$, is plotted against $(\Delta n_{ac} + \Delta n_{ab})/2$. Here, $\Delta n_{ac} = n_a - n_c$, $\Delta n_{bc} = n_b - n_c$, and $\Delta n_{ab} = n_a - n_b$. The lines (a) and (b) in this firure show the relationships between the second moments and birefringence, which were obtained by assuming the same values of $\Delta n°$ as used in Fig. 4-5 from the following equations:

$$\frac{\Delta n_{ac} + \Delta n_{ab}}{2} = \frac{3<\sin^2\omega\cos^2\varphi>_{\Delta n} - 1}{2} \Delta n° \qquad (4\text{-}2)$$

$$\frac{\Delta n_{ac} + \Delta n_{bc}}{2} = -\frac{3<\cos^2\omega>_{\Delta n} - 1}{2} \Delta n° \ , \qquad (4\text{-}3)$$

where $<\sin^2\omega\cos^2\varphi>_{\Delta n}$ and $<\cos^2\omega>_{\Delta n}$ are the second moments about the a- and c- axes, respectively, for the orientation of rotationally symmetrical anisotropic units of polarizability. In this figure, it can also be seen that the degree of orientation of fluorescent probes tends to precede that of the molecular orientation estimated from birefringence data.

Birefringence derives from the anisotropic orientation of polymer chains which have the intrinsic anisotropy of polarizability. The orientation of polymer chains both in crystalline and non-crystalline regions affects the total birefringence of the system. Hence, the results shown in Figs. 4-5 and 4-6 suggest that the molecular orientation in the non-crystalline regions precedes the crystalline orientation. However, it should

be remembered what follows: The structural unit for orientation
measurement by the birefringence method is not so clear in regard
to its size or form. On the other hand, the structural unit for
orientation measurement by the fluorescence method is a fluores-
cent probe in amorphous regions, and its length is about 25 Å
for RP and may be taken to be larger than that of anisotropic
unit of polarizability.

References

1) Y. Nishijima, Y. Onogi, and T. Asai, J. Polym. Sci., C, 15,
    237 (1966).

    Y. Nishijima, J. Polym. Sci., C, 31, 353 (1970).

    Y. Nishijima, "Fluorescence Methods in Polymer Research",

    in "Progress in Polymer Science, Japan", (Eds. S. Onogi and

    K. Uno), vol. 6, Kodansha, Tokyo, John Wiley, New York,

    1973, pp. 199-251.

2) S. Hibi, M. Maeda, and M. Suzuki, Polymer preprints, Japan,

    26, 382 (1977): Presented at the 26th Annual Meeting of the

    Society of Polymer Science, Japan, Kyoto, May, 1977.

3) Y. Onogi and Y. Nishijima, Repts. Progr. Polym. Phys. Japan,

    19, 415 (1976).

4) Y. Onogi and Y. Nishijima, Ann. Rept. Res. Inst. Chem.

    Fibers, 33, 19 (1976)

5) O. Kratky, Kolloid-Z., <u>64</u>, 213 (1933).

6) S. Nomura and H. Kawai, J. Polym. Sci., A-2, <u>4</u>, 797 (1966).

7) Y. Kobayashi, S. Okajima, and H. Miya, Kogyo Kagaku Zasshi, <u>59</u>, 82 (1956).

AI-1. Generalized Spherical Harmonics $\Phi_{\ell mn}$

As described in Chapter 2, the generalized spherical

harmonics $\Phi_{\ell mn}(\Omega)$ is defined as follows,

$$\Phi_{\ell mn}(\Omega) = \Phi_{\ell mn}(\omega, \varphi, \chi)$$

$$= Z_{\ell mn}(\cos\omega)\, e^{-i(m\varphi + n\chi)}/(2\pi)$$

$$= (-1)^{m-n}\, (\frac{2\ell + 1}{8\pi^2})^{1/2}\, D_{mn}^{\ell}(\Omega)\ .$$

The function $\Phi_{\ell mn}$ can be represented in more condensed form as

given by eq. (AI-1), which is derived from the explicit form of

$Z_{\ell mn}$ [1,2) or that of D_{mn}^{ℓ} . [3,4)

$$\Phi_{\ell mn}(\Omega) = \{\frac{2\ell + 1}{2}\cdot\frac{(\ell + m)!\,(\ell - m)!}{(\ell + n)!\,(\ell - n)!}\}^{1/2}\cdot\frac{(-1)^{\ell - m}}{2^{\ell}(\ell - m)!}$$

$$\times (1 - y)^{-(m-n)/2}\cdot(1 + y)^{-(m+n)/2}$$

$$\times \frac{d^{\ell - m}}{dy^{\ell - m}}\{(1 - y)^{\ell - n}(1 + y)^{\ell + n}\}\cdot e^{-i(m\varphi + n\chi)}/(2\pi), \quad (AI-1)$$

where $\qquad\qquad y = \cos\omega\ .$

Utilizing such symmetry properties [1,5) of $Z_{\ell mn}$ as

$$Z_{\ell mn}(y) = (-1)^{m+n} Z_{\ell\bar{m}\bar{n}}(y) = (-1)^{\ell+m} Z_{\ell m\bar{n}}(-y) \;,$$

we obtain many symmetry properties of $\Phi_{\ell mn}$. Some of them are shown in the following ways:

$$\Phi_{\ell mn}(\omega,\pi-\varphi,-\chi) = (-1)^{n} \Phi_{\ell\bar{m}\bar{n}}(\omega,\varphi,\chi) \tag{AI-2a}$$

$$\Phi_{\ell mn}(\omega,\pi-\varphi,\pi-\chi) = \Phi_{\ell\bar{m}\bar{n}}(\omega,\varphi,\chi) \tag{AI-2b}$$

$$\Phi_{\ell mn}(\omega,-\varphi,-\chi) = (-1)^{m+n} \Phi_{\ell\bar{m}\bar{n}}(\omega,\varphi,\chi) \tag{AI-2c}$$

$$\Phi_{\ell mn}(\omega,-\varphi,\pi-\chi) = (-1)^{m} \Phi_{\ell\bar{m}\bar{n}}(\omega,\varphi,\chi) \tag{AI-2d}$$

$$\Phi_{\ell mn}(\pi-\omega,\varphi,-\chi) = (-1)^{\ell+m} \Phi_{\ell m\bar{n}}(\omega,\varphi,\chi) \tag{AI-2e}$$

$$\Phi_{\ell mn}(\pi-\omega,\varphi,\pi-\chi) = (-1)^{\ell+m+n} \Phi_{\ell m\bar{n}}(\omega,\varphi,\chi) \tag{AI-2f}$$

$$\Phi_{\ell mn}(\omega,\varphi,\chi) = (-1)^{m+n} \Phi_{\ell\bar{m}\bar{n}}^{*}(\omega,\varphi,\chi) \;. \tag{AI-3}$$

It follows that the coefficient $M_{\ell'm'n'}^{\ell\;m\;n}$, given by

$$M_{\ell'm'n'}^{\ell\;m\;n} = \langle [\; \Phi_{\ell mn}^{*}(\Omega)\, \Phi_{\ell'm'n'}^{*}(\Omega) \;] \rangle$$

$$= \int_{\Omega} \Phi_{\ell mn}^{*}(\Omega)\, \Phi_{\ell'm'n'}^{*}(\Omega)\, m(\omega,\varphi,\chi)\; d\Omega$$

should also have some symmetry properties when the molecular orientation distribution function has a high symmetry. For example, as stated in Chapter 3, the coefficient $M_{\ell'm'n'}^{\ell\;m\;n}$ for

the case of biaxially oriented system has the relationships of eqs. (3-18) and (3-19), which can be derived by utilizing eqs. (AI-2) and (AI-3).

AI-2. Refraction and Reflection of Light on the Boundary

between the Isotropic and the Anisotropic Media

Let us consider the refraction and reflection phenomena of exciting light and fluorescence on the plane surfaces of the anisotropic medium, in order to represent the various quantities constituting eqs. (3-27) and (3-28) in plain forms.

Refractive Angles and Refractive Indices:

Figure AI-1 shows the refraction and the reflection of an incident light beam on the interface between the air and the anisotropic medium, whose principal refractive indices are n_a, n_b, and n_c. (Here, let the refractive index of the air be unity.) The incident light can be represented by two linearly polarized lights vibrating orthogonally each other. The directions of vibration are parallel (I) and perpendicular (II) to the plane of incidence which is the bc-plane for (A)-set or the ac-plane for (B)-set.

Through the geometrical analysis based on Huygens' construction, the refractive angles, θ_{i1} and θ_{i2}, of the two rays, I and

Fig. AI-1. Reflection and refraction of an incident beam on the boundary between isotropic and anisotropic media.

II, can be written as a function of the incident angle and the principal refractive indices of the anisotropic medium, as follows,

$$\tan\theta_{i1} = \frac{n_b \sin\theta_i}{n_c \sqrt{n_c^2 - \sin^2\theta_i}} \qquad (AI-4a)$$

(for (A)-set)

$$\sin\theta_{i2} = \frac{\sin\theta_i}{n_a} \quad \text{or} \quad \tan\theta_{i2} = \frac{\sin\theta_i}{\sqrt{n_a^2 - \sin^2\theta_i}} \ . \qquad (AI-4b)$$

(In the case of (B)-set, n_a and n_b must be exchanged mutually, and the similar treatment for (B)-set can be carried out in equations given for (A)-set in this Appendix.) In eqs. (AI-4a) and (AI-4b), θ_{i1} is the refractive angle of ray-I whose electric vector lies on the plane of incidence, and θ_{i2} is the refractive angle of ray-II whose electric vector is normal to the plane of incidence. The former does not coincide with the angle of refraction of the vector normal to the light wave surface, while the latter does so. The refractive angle, θ_{i1}', of the normal of light wave front corresponding to ray-I can be given by

$$\tan\theta_{i1}' = \frac{n_c \sin\theta_i}{n_b \sqrt{n_c^2 - \sin^2\theta_i}} \qquad \text{(for (A)-set) .} \qquad (AI-5)$$

Furthermore, let n_{s1} and n_{s2} be the indices of refraction of ray -I and -II, respectively, for the anisotropic medium, then

$$n_{s1} = \frac{(1 + \tan\theta_{i1} \tan\theta'_{i1})}{\tan\theta'_{i1} \sqrt{1 + \tan^2\theta_{i1}}} \cdot \sin\theta_i \qquad \text{(AI-6a)}$$

$$n_{s2} = \frac{\sin\theta_i}{\sin\theta_{i2}} \qquad . \qquad \text{(AI-6b)}$$

On the other film surface parallel to the surface given in Fig. AI-1, the light emitted from a fluorescent molecule in the medium is also partially reflected and partially transmitted. When two rays of polarized fluorescence vibrating orthogonally transmit through the anisotropic medium into the air, the incident angles, θ_1 and θ_2, of the two rays whose refractive angles are both θ_j are given in the same manners as in eqs. (AI-4a) and (AI-4b). That is,

$$\tan\theta_1 = \frac{n_b \sin\theta_j}{n_c \sqrt{n_c^2 - \sin^2\theta_j}} \qquad \text{(AI-7a)}$$

$$\text{(for (A)-set)}$$

$$\sin\theta_2 = \frac{\sin\theta_j}{n_a} \quad \text{or} \quad \tan\theta_2 = \frac{\sin\theta_j}{\sqrt{n_a^2 - \sin^2\theta_j}} \qquad . \qquad \text{(AI-7b)}$$

The incident angle, θ'_1, of the normal of light wave front corresponding to the ray whose electric vector lies on the plane of incidence can be given by

$$\tan\theta'_1 = \frac{n_c \sin\theta_j}{n_b \sqrt{n_c^2 - \sin^2\theta_j}} \qquad \text{(for (A)-set)} \quad . \qquad \text{(AI-8)}$$

The indices of refraction of the two observed fluorescence rays vibrating orthogonally in the anisotropic medium, $n_{s(1)}$ and $n_{s(2)}$, can be also given in the same manners as in eqs. (AI-6a) and (AI-6b). That is,

$$n_{s(1)} = \frac{(1 + \tan\theta_1 \tan\theta_1')}{\tan\theta_1' \sqrt{1 + \tan^2\theta_1}} \cdot \sin\theta_j \qquad \text{(AI-9a)}$$

$$n_{s(2)} = \frac{\sin\theta_j}{\sin\theta_2} . \qquad \text{(AI-9b)}$$

Amplitude Transmission Coefficients:

Utilizing the continuity of the tangential components of the electric fields and the magnetic fields of incident, reflected, and transmitted lights on either side of the boundary surface between the two dielectric media, we obtain the following equations for the amplitude transmission coefficients.

For the exciting light,

$$t_1 = \frac{2\cos\theta_i \sqrt{1 + \tan^2\theta_{i1}}}{1 + (1/2)\sin2\theta_i (1/\tan\theta_{i1}' + \tan\theta_{i1}')} \qquad \text{(AI-10a)}$$

$$t_2 = \frac{2\tan\theta_{i2}}{\tan\theta_i + \tan\theta_{i2}} = \frac{2\sin\theta_{i2}\cos\theta_i}{\sin(\theta_i + \theta_{i2})} , \qquad \text{(AI-10b)}$$

and for the fluorescence,

$$t_1' = \frac{2\sin\theta_j\ (1/\tan\theta_1' + \tan\theta_1)/\sqrt{1 + \tan^2\theta_1}}{1 + (1/2)\sin2\theta_j\ (1/\tan\theta_1' + \tan\theta_1)} \qquad \text{(AI-11a)}$$

$$t_2' = \frac{2\tan\theta_j}{\tan\theta_j + \tan\theta_2} = \frac{2\sin\theta_j\cos\theta_2}{\sin(\theta_j + \theta_2)}, \qquad \text{(AI-11b)}$$

where the suffixes, 1 and 2 of t and t', serve as reminders that the electric field of the ray is parallel (1) or perpendicular (2) to the plane of incidence. These equations correspnd to Fresnel's equations extended for the refraction and reflection phenomena on the interface between the isotropic and the aniso-tropic media.

Transmittances:

As shown in Fig. AI-1, when an incident exciting light beam irradiates a unit area of the film surface, the cross section of the incident beam is equal to $\cos\theta_i$, and the only fluorescent groups existing within the shaded part in this figure can absorb the two transmitted linearly polarized light vibrating orthogonally. As the difference between the values of θ_{i1} and θ_{i2} is small, the cross section of the shaded part is regarded as $\cos\{(\theta_{i1} + \theta_{i2})/2\}$. Accordingly, the ratio of the cross section of the transmitted beam to that of the incident beam can be approximated by $[\cos\{(\theta_{i1} + \theta_{i2})/2\}]/\cos\theta_i$. Similarly, the change of irradiated area due to the refraction of the fluorescence beam

-100-

on the other surface may be given by $\cos\theta_j/\cos\{(\theta_1+\theta_2)/2\}$.

The transmittance is given by the ratio of transmitted energy (or transmitted flux) to incident energy (or incident flux). The radiant flux density is, in general, given by the Poynting vector and is simply proportional to the product of the refractive index of the medium and the square of amplitude of the electric field of the ray. Therefore, the transmittances of the exciting light and the fluorescence can be represented by eqs. (3-27) and (3-28).

Phase Differences between Two Components of Exciting Light and Fluorescence:

The phase difference, δ_i, between the two rays with their electric fields, $\mathbb{E}_{i1}$ and $\mathbb{E}_{i2}$, of exciting light at the distance l from the film surface, can be given as follows (see Fig. AI-2):

$$\delta_i = \frac{2\pi}{\lambda_i} \{(\overline{RQ} + n_{s2}\overline{QF}) - n_{s1}\overline{PF}\}$$

$$= \frac{2\pi l}{\lambda_i} \{(\tan\theta_{i1} - \tan\theta_{i2})\sin\theta_i$$

$$+ n_{s2}/\cos\theta_{i2} - n_{s1}/\cos\theta_{i1}\} . \qquad \text{(AI-12)}$$

Using eqs. (AI-4)-(AI-6), we obtain

$$\delta_i = \frac{2\pi l}{\lambda_i} \frac{1}{n_c} (n_c \sqrt{n_a^2 - \sin^2\theta_i} - n_b \sqrt{n_c^2 - \sin^2\theta_i})$$

$$\text{(for (A)-set)} . \qquad \text{(AI-13)}$$
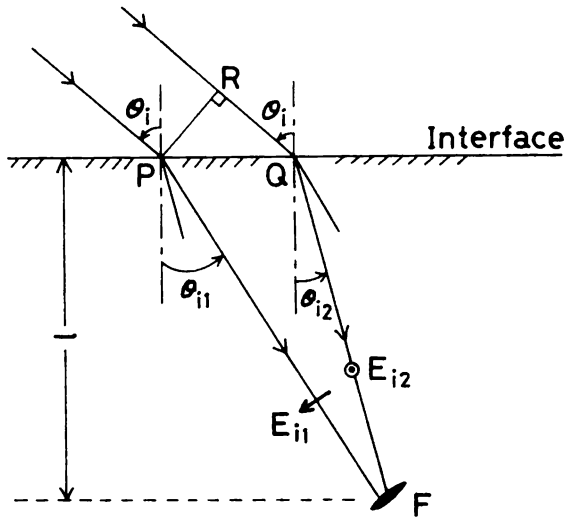
Fig. AI-2. Excitation of a fluorescent molecule (F) existing at a distance 1 from interface by linearly polarized lights vibrating orthogonally to each other.

Similarly, the phase difference, δ_f, between the two rays with their electric fields, $\mathbb{E}_1$ and $\mathbb{E}_2$, of the observed fluorescence coming from a fluorescent molecule which exists at the distance D-1 from the other film surface, can be given by

$$\delta_f = \frac{2\pi(D-1)}{\lambda_f} \frac{1}{n_c} \left(n_c \sqrt{n_a^2 - \sin^2\theta_j} - n_b \sqrt{n_c^2 - \sin^2\theta_j} \right)$$

(for (A)-set) .   (AI-14)

References

1) R. J. Roe, J. Appl. Phys., $\underline{36}$, 2024 (1965).

2) S. Nomura, H. Kawai, I. Kimura, and M. Kagiyama, J. Polym. Sci., A-2, $\underline{8}$, 383 (1970).

3) M. E. Rose, "Elementary Theory of Angular Momentum", John Wiley & Sons, Inc., New York, 1957, Chap. 4.

4) T. Yamanouchi, "Kaiten-gun To Sono Hyogen", Iwanami, Tokyo, 1957, Chap. 3, §. 12.

5) D. I. Bower, J. Polym. Sci., Polym. Phys. Ed., $\underline{10}$, 2135 (1972).

PART II

GENERAL ANALYSIS OF FLUORESCENCE POLARIZATION

IN THE ANISOTROPIC SYSTEM

AND ITS APPLICATION TO POLYMER SOLIDS

CHAPTER 5

General Theory of Polarized Fluorescence Emission

in the Oriented System

with Discussion on Molecular Motions

5-1. Introduction

     In Part I, the theoretical analysis of fluorescence polar-

ization and the calculations for orientation measurement were

carried out under the assumption that fluorescent probes are

fixed in the medium during the fluorescence lifetime. This

assumption can be satisfied when the system is sufficiently

rigid, e.g., as in the case of polymer solid in the glassy state.

However, in the systems such as polymer films in the glass-

transition region and rubbery state, the motions of fluorescent

probes affect the polarization of fluorescence. Therefore, by

analyzing the polarized components of fluorescence intensity,

one can discuss not only the molecular orientation but also the

anisotropy of molecular mobility in oriented polymer systems at

temperatures higher than the glass-transition temperature (T_g).

     In this chapter, the polarized component of fluorescence

intensity is generally formulated for the oriented system in

which the rotational motions of fluorescent molecules are

measurable during the fluorescence lifetime (nanosecond order).
The equation of the polarized component of fluorescence inten-
sity is simplified for the uniaxially symmetrical system.

The theoretical treatment in this chapter is carried out
by modifying the analysis developed in Chapter 2, where the
motions of fluorescent molecules were assumed to be negligible
during the fluorescence lifetime, while here the orientation
angle of a fluorescent molecule excited by incident light changes
to another angle when the molecule is in the process of fluores-
cence emission.

5-2. General Description of Angular Relations among

     Orientation Axes

     First, let us define the coordinate systems, as follows:

     (a) Sample coordinate system O-abc: This is defined as the
coordinate system fixed to an oriented sample (e.g., a stretched
polymer film). The axes a, b, and c are chosen to coincide with
the three optically principal axes. In a uniaxially stretched
polymer film, the c-axis is fixed in the stretched direction.

     (b) Molecular coordinate system O-KLM: This coordinate
is given in a fluorescent molecule which is excited by the
incident polarized light at time t. The M- and L- axes are
defined as the main axis of the molecule and the axis normal to

a plane formed by conjugated double bonds, respectively.

(c) Molecular coordinate system O-K'L'M': This is the coordinate system given for the excited molecule emitting fluorescence at time t'= t + u.

The angular alignments of molecular axes and absorbing and emitting oscillators are shown in Fig. 5-1, which also illustrates the rotation of molecular axes from the position at time t to that at time t'. Figure 5-1a shows the angular alignments of molecular axes and an absorbing oscillator A_i at time t. The orientation of a fluorescent molecule with respect to the sample coordinate system O-abc is specified by the Euler angles $\Omega = (\omega, \varphi, \chi)$. The orientation of an absorbing oscillator A_i, lying in the direction (δ, ε) in the molecular coordinate system O-KLM, can be specified by a set of polar and azimuthal angles (Δ, E) with respect to the O-abc system. Then, the relation among the three sets of angles (Δ, E), (δ, ε), and (ω, φ, χ) is given by eq. (5-1), in terms of the spherical harmonics ($Y_{\ell m}(\Delta, E)$, $Y_{\ell n}(\delta, \varepsilon)$) and the generalized spherical harmonics ($\Phi_{\ell m n}(\Omega)$).

$$Y_{\ell m}{}^{*}(\Delta, E) = 2\pi \left(\frac{2}{2\ell + 1}\right)^{1/2} \sum_{n=-\ell}^{\ell} \Phi_{\ell m n}{}^{*}(\Omega) Y_{\ell n}{}^{*}(\delta, \varepsilon) . \tag{5-1}$$

Figure 5-1b shows the angular alignments of the excited molecule and an emitting oscillator F_i' at time t'= t + u. The orientations of the excited molecule and a unit vector F_i' lying in the

Rotation

(a)

(b)

(c)
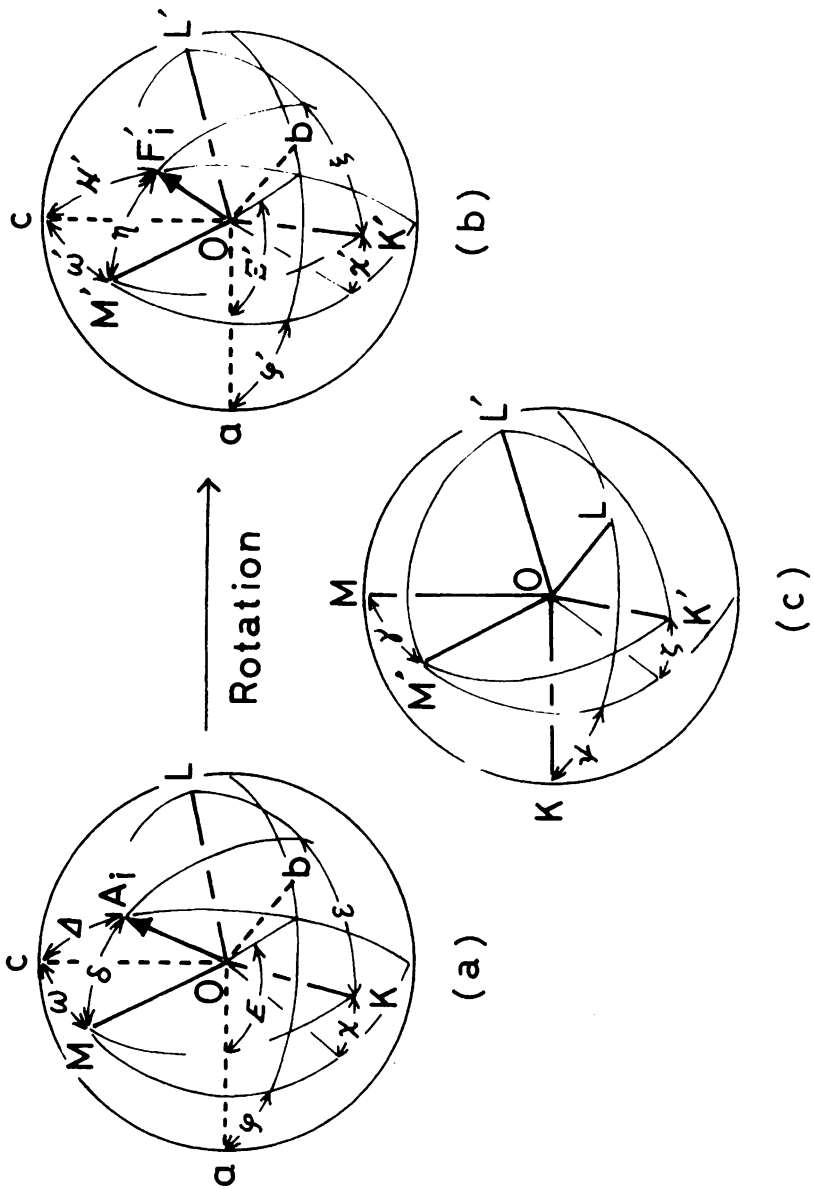
Fig. 5-1. Angular alignments of molecular axes and absorbing and emitting oscillators.

(a) Euler angles $\Omega = (\omega, \varphi, \chi)$ specifying the orientation of the molecular frame O-KLM with respect to the sample coordinate system O-abc at time t, and the two sets of polar and azimuthal angles (δ, ε) and (Δ, E) specifying the direction of an absorbing oscillator A_i with respect to the O-KLM and O-abc systems, respectively, at time t.

(b) Euler angles $\Omega' = (\omega', \varphi', \chi')$ specifying the orientation of the molecular frame O-K'L'M' with respect to the O-abc system at time $t' = t + u$, and the two sets of polar and azimuthal angles (η, ξ) and (H', Ξ') specifying the direction of an emitting oscillator F_i' with respect to the O-K'L'M' and O-abc systems, respectively, at time t'.

(c) Euler angles $\Gamma = (\gamma, \psi, \zeta)$ specifying the rotation of the excited molecule in a period of $u(=t'-t)$.

direction (η,ξ) in the O-K'L'M' system are specified by $\Omega' =$ (ω',φ',χ') and (H',Ξ'), respectively, with respect to the O-abc system. The three sets of angles (H',Ξ'), (η,ξ), and (ω',φ',χ') can also be generally related to one another, as follows;

$$Y_{\ell'm'}{}^{*}(H',\Xi') = 2\pi\left(\frac{2}{2\ell'+1}\right)^{1/2} \sum_{n'=-\ell'}^{\ell'} \Phi_{\ell'm'n'}{}^{*}(\Omega')Y_{\ell'n'}{}^{*}(\eta,\xi) \ .$$

$$(5-2)$$

When the molecule being oriented at the angle Ω at time t rotates to another angle Ω' in a period of $u(=t'-t)$, the rotation angle is specified by the Euler angles $\Gamma = (\gamma,\psi,\zeta)$ as shown in Fig. 5-1c. The three kinds of Euler angles Ω, Ω', and Γ can be generally related to one another by the following equation (see Appendix II).

$$\Phi_{\ell'm'n'}{}^{*}(\Omega') = 2\pi\left(\frac{2}{2\ell'+1}\right)^{1/2} \sum_{p=-\ell'}^{\ell'} \Phi_{\ell'm'p}{}^{*}(\Omega)\Phi_{\ell'pn'}{}^{*}(\Gamma) \ . \qquad (5-3)$$

Next, let us introduce the angular functions as shown below:

(i) $g(\delta,\varepsilon)$ and $h(\eta,\xi)$: These functions are the probability functions of finding absorbing and emitting oscillators, $\mathbb{A}_i$ and $\mathbb{F}_i$, respectively, within the molecular coordinate system O-KLM and characterize the intrinsic photophysical anisotropy of a fluorescent probe, as stated in Chapter 2.

(ii) $q(\Delta,E,t)$: This function is defined as the orientation distribution function at time t, of unit vectors $\mathbb{A}_i$ with respect

to the O-abc system.

(iii) $r(H',\Xi',t'|A)$: This is the probability function of finding an emitting oscillator $\mathbb{F}_i'$ of the excited molecule in the direction (H',Ξ') at time t'.

(iv) $m(\Omega,t)$: This function is defined as the orientation distribution function at time t, of fluorescent probes in the O-abc system.

(v) $P(\Omega,t|\Omega',t')$ (This is also written as $P(\Omega,t|\Gamma,u)$): This function expresses the transition probability from orientation angle Ω to Ω' during the time $u = t'-t$ for a fluorescent probe.

(vi) $K(\Omega,t|\Omega',t')$ (This is also written as $K(\Omega,t|\Gamma,u)$): This is defined as the probability when a fluorescent probe is oriented at Ω at time t and found at Ω' at time t'. Therefore this function can be represented as the product of $m(\Omega,t)$ and $P(\Omega,t|\Omega',t')$, that is,

$$K(\Omega,t|\Omega',t') = m(\Omega,t)P(\Omega,t|\Omega',t') \ . \qquad (5-4)$$

The functions defined in (i)-(vi) are normalized in the following manners.

$$\int_{\delta,\epsilon} g(\delta,\epsilon) \ d(\delta,\epsilon) = 1 \qquad (5-5a)$$

$$\int_{\eta,\xi} h(\eta,\xi) \ d(\eta,\xi) = 1 \qquad (5-5b)$$

$$\int_{\Delta,E} q(\Delta,E,t) \ d(\Delta,E) = 1 \qquad\qquad (5\text{-}5c)$$

$$\int_{H',\Xi'} r(H',\Xi',t'|A) \ d(H',\Xi') = 1 \qquad\qquad (5\text{-}5d)$$

$$\int_{\Omega} m(\Omega,t) \ d\Omega = 1 \qquad\qquad (5\text{-}5e)$$

$$\int_{\Omega'} P(\Omega,t|\Omega',t') \ d\Omega' = \int_{\Gamma} P(\Omega,t|\Gamma,u) \ d\Gamma = 1 \qquad (5\text{-}5f)$$

$$\int_{\Omega}\int_{\Omega'} K(\Omega,t|\Omega',t') \ d\Omega'd\Omega = \int_{\Omega}\int_{\Gamma} K(\Omega,t|\Gamma,u) \ d\Gamma d\Omega = 1 \ , \ (5\text{-}5g)$$

where

$$\int_{\delta,\varepsilon} d(\delta,\varepsilon) = \int_0^{2\pi}\int_0^{\pi} \sin\delta d\delta d\varepsilon$$

$$\int_{\Omega} d\Omega = \int_0^{2\pi}\int_0^{2\pi}\int_0^{\pi} \sin\omega d\omega d\varphi d\chi \ , \ \text{and so on.}$$

Now, multiplying both sides of the equation obtained by the product of eqs. (5-1) and (5-2) by $q(\Delta,E,t)r(H',\Xi',t'|A)g(\delta,\varepsilon)$ $h(\eta,\xi)K(\Omega,t|\Omega',t')$, integrating over the whole range of the angles, we have

$$\int_{\Delta,E}\int_{H',\Xi'} Y_{\ell m}{}^*(\Delta,E)Y_{\ell'm'}{}^*(H',\Xi')q(\Delta,E,t)r(H',\Xi',t'|A)$$

$$\times d(H',\Xi')d(\Delta,E)$$

$$= 8\pi^2\{(2\ell+1)(2\ell'+1)\}^{-1/2} \sum_{n,n'} G_{\ell n}H_{\ell'n'}M_{\ell'm'n'}^{\ell\ m\ n}(t|t') \ , \qquad (5\text{-}6)$$

where

$$G_{\ell n} = \int_{\delta,\varepsilon} Y_{\ell n}{}^{*}(\delta,\varepsilon)g(\delta,\varepsilon) \ d(\delta,\varepsilon) = <[\ Y_{\ell n}{}^{*}(\delta,\varepsilon) \ ]> \qquad (5\text{-}7)$$

$$H_{\ell'n'} = \int_{\eta,\xi} Y_{\ell'n'}{}^{*}(\eta,\xi)h(\eta,\xi) \ d(\eta,\xi) = <[\ Y_{\ell'n'}{}^{*}(\eta,\xi) \ ]> \ (5\text{-}8)$$

$$M_{\ell'm'n'}^{\ell \ m \ n}(t|t') = \int_{\Omega}\int_{\Omega'} \Phi_{\ell mn}{}^{*}(\Omega) \Phi_{\ell'm'n'}{}^{*}(\Omega')K(\Omega,t|\Omega',t') \ d\Omega'd\Omega$$

$$= <[\ \Phi_{\ell mn}{}^{*}(\Omega) \Phi_{\ell'm'n'}{}^{*}(\Omega') \ ]> \ , \qquad (5\text{-}9)$$

in which

$$<[\ X \ ]> = <Re \ X> + i \ <Im \ X>$$

(Re X : real part of X , Im X : imaginary part of X).

Equations (5-7) and (5-8) show that $G_{\ell n}$ and $H_{\ell'n'}$ are the coefficients of the series expansions of $g(\delta,\varepsilon)$ and $h(\eta,\xi)$ in terms of spherical harmonics $Y_{\ell n}(\delta,\varepsilon)$ and $Y_{\ell'n'}(\eta,\xi)$, respectively, and are the angular average values characterizing the intrinsic photophysical anisotropy of a fluorescent probe. Equation (5-9) shows that $M_{\ell'm'n'}^{\ell \ m \ n}(t|t')$ is the coefficient of the series expansion of $K(\Omega,t|\Omega',t')$ in terms of the product of two generalized spherical harmonics, $\Phi_{\ell mn}(\Omega)$ and $\Phi_{\ell'm'n'}(\Omega')$.

By using the transformation relation given by eq. (5-3), eq. (5-9) can be rewritten as follows:

$$M_{\ell'm'n'}^{\ell \, m \, n}(t|t')$$

$$= 2\pi \left(\frac{2}{2\ell'+1}\right)^{1/2} \int_{\Omega}\int_{\Gamma} \Phi_{\ell mn}{}^*(\Omega) \sum_{p} \Phi_{\ell'm'p}{}^*(\Omega)\Phi_{\ell'pn'}{}^*(\Gamma)$$

$$\times\, K(\Omega,t|\Gamma,u)\ d\Gamma d\Omega$$

$$= 2\pi \left(\frac{2}{2\ell'+1}\right)^{1/2} <\{\ \Phi_{\ell mn}{}^*(\Omega) \sum_{p} \Phi_{\ell'm'p}{}^*(\Omega)\Phi_{\ell'pn'}{}^*(\Gamma)\ \}> . \quad (5\text{-}10)$$

Accordingly, it is clear from eq. (5-10) that the coefficient $M_{\ell'm'n'}^{\ell \, m \, n}(t|t')$ is the angular average value characterizing the molecular orientation and the molecular motion.

The left side of eq. (5-6) can be combined with a measurable quantity, i.e., the polarized component of fluorescence intensity, as will be shown in the next section.

5-3. Polarized Component of Fluorescence Intensity

When the sample is irradiated by linearly polarized light with its electric vector $\mathbb{p}_1$, a fluorescent probe which orients at Ω at distance l from the surface of the medium is excited depending on the angular alignment of the absorbing oscillator $\mathbb{A}_i$. The incident polarized light propagates, in general, in two components in the optically anisotropic medium. Hence, the probability of excitation, i_a, can be represented by

$$i_a = k\ \{a_{i1}{}^2(\mathbb{p}_{1-1}\cdot \mathbb{A}_i)^2 + a_{i2}{}^2(\mathbb{p}_{1-2}\cdot \mathbb{A}_i)^2$$

$$+ 2a_{i1}a_{i2}(\mathbb{P}_{1-1} \cdot \mathbb{A}_i)(\mathbb{P}_{1-2} \cdot \mathbb{A}_i)\cos\delta_i\} , \qquad (5-11)$$

where $\mathbb{P}_{1-1}$, $\mathbb{P}_{1-2}$ and a_{i1}, a_{i2} are the vibration axes and the amplitudes of the two components of exciting light, respectively, and δ_i is the phase difference between the two components (see Chapter 2).

Similarly, when the fluorescence light emitted from an oscillator $\mathbb{F}_i{}'$ belonging to the excited molecule is detected through the analyzer with its transmission axis $\mathbb{P}_2$, the intensity is proportional to i_f given by

$$i_f = \phi \{a_{f1}{}^2(\mathbb{P}_{2-1} \cdot \mathbb{F}_i{}')^2 + a_{f2}{}^2(\mathbb{P}_{2-2} \cdot \mathbb{F}_i{}')^2$$

$$+ 2a_{f1}a_{f2}(\mathbb{P}_{2-1} \cdot \mathbb{F}_i{}')(\mathbb{P}_{2-2} \cdot \mathbb{F}_i{}')\cos\delta_f\} , \qquad (5-12)$$

where $\mathbb{P}_{2-1}$ and $\mathbb{P}_{2-2}$ are the vibration axes of two components of fluorescence light propagating in the anisotropic medium, and a_{f1} and a_{f2} are related with the amplitudes of two components passing through the analyzer with the phase difference δ_f between them (see Chapter 2).

Under stationary irradiation of the sample by the exciting light, the total observed fluorescence intensity $I(\begin{smallmatrix}\mathbb{P}_1\\\mathbb{P}_2\end{smallmatrix})$ can be written in the following way;

$$I\left(\begin{matrix} \mathbb{P}_1 \\ \mathbb{P}_2 \end{matrix}\right) = \int_0^\infty \int_0^D \int_{\Delta,E} \int_{H',\Xi'} q(\Delta,E,t)\, i_a\, r(H',\Xi',t'|A)\, i_f\, e^{-u/\tau}$$

$$\times\ d(H',\Xi')d(\Delta,E)dl/D\ du/\tau\ , \qquad (5\text{-}13)$$

where D is the thickness of the anisotropic sample and τ is the fluorescence lifetime. (In this case, the decay of fluorescence emission is taken to be a single exponential.)

Here, let us expand i_a and i_f given by eqs. (5-11) and (5-12) in a series of spherical harmonics, as follows:

$$i_a = k \sum_{\ell=0}^{\infty} \sum_{m=-\ell}^{\ell} S_{\ell m} Y_{\ell m}{}^*(\Delta,E) \qquad (5\text{-}14)$$

with
$$S_{\ell m} = a_{i1}{}^2\, S_{\ell m}^{(1)} + a_{i2}{}^2\, S_{\ell m}^{(2)} + 2a_{i1}a_{i2}\cos\delta_i\, S_{\ell m}^{(3)}$$

$$i_f = \phi \sum_{\ell'=0}^{\infty} \sum_{m'=-\ell'}^{\ell'} T_{\ell'm'} Y_{\ell'm'}{}^*(H',\Xi') \qquad (5\text{-}15)$$

with
$$T_{\ell'm'} = a_{f1}{}^2\, T_{\ell'm'}^{(1)} + a_{f2}{}^2\, T_{\ell'm'}^{(2)} + 2a_{f1}a_{f2}\cos\delta_f\, T_{\ell'm'}^{(3)}\ .$$

By substituting eqs. (5-14) and (5-15) into eq. (5-13) and using eq. (5-6) derived in the preceding section, we obtain

$$I\left(\begin{matrix} \mathbb{P}_1 \\ \mathbb{P}_2 \end{matrix}\right) = 8\pi^2 k\phi \sum_{\substack{\ell\ m\ n \\ \ell'm'n'}} \{(2\ell+1)(2\ell'+1)\}^{-1/2}\, [S_{\ell m} T_{\ell'm'}]_{\text{int}}$$

$$\times\ G_{\ell n} H_{\ell'n'}\, [M_{\ell'm'n'}^{\ell\ m\ n}(t|t')]_s\ , \qquad (5\text{-}16)$$

where

$$[S_{\ell m}T_{\ell'm'}]_{int} = \int_0^D S_{\ell m}T_{\ell'm'}\ d1/D \qquad (5\text{-}17)$$

and

$$[M^{\ell\ m\ n}_{\ell'm'n'}(t|t')]_s = \int_0^\infty M^{\ell\ m\ n}_{\ell'm'n'}(t|t')e^{-u/\tau}\ du/\tau\ , \qquad (5\text{-}18)$$

in which the subscript s is used to denote the time average for the case of stationary irradiation.

The coefficients $G_{\ell n}$, $H_{\ell'n'}$, $S_{\ell m}$, and $T_{\ell'm'}$ have previously been calculated in more condensed form in Chapter 2 (eqs. (2-50)- (2-52)). The coefficient $M^{\ell\ m\ n}_{\ell'm'n'}(t|t')$ will be discussed in detail for the uniaxially oriented system in the next section.

5-4. The Case of Uniaxially Symmetrical System

Let us consider the system in which fluorescent probes are partially uniaxially oriented.

When the orientation distribution of fluorescent probes, referred to the sample coordinate system O-abc, is rotationally symmetrical about the c-axis and the orientation of fluorescent probes themselves is also rotationally symmetrical around the M-axis, the orientation distribution function m(Ω,t) is indepen- dent of φ and χ and the transition probability P(Ω,t$|\Gamma$,u) should satisfy the following conditions;

$$P(\omega,\varphi_1,\chi,t\,|\,\Gamma,u) = P(\omega,\varphi_2,\chi,t\,|\,\Gamma,u) \tag{5-19}$$

(for arbitrary angles φ_1 and φ_2)

and

$$P(\omega,\varphi,\chi,t\,|\,\gamma,\psi,\zeta,u) = P(\omega,\varphi,-\chi,t\,|\,\gamma,-\psi,-\zeta,u) \ . \tag{5-20}$$

Then, by utilizing the symmetrical properties of the generalized spherical harmonics (see Appendix I), the coefficient $M^{\ell\ m\ n}_{\ell'm'n'}(t\,|\,t')$ given by eq. (5-10) has the following symmetrical properties,

$$M^{\ell\ m\ n}_{\ell'm'n'}(t\,|\,t') = 0 \qquad \text{for } m' \neq -m \tag{5-21}$$

and

$$M^{\ell\ m\ n}_{\ell',\overline{m}\ n'}(t\,|\,t') = M^{\ell\ m\ n}_{\ell',\overline{m}\ n'}(t\,|\,t')^* = (-1)^{n+n'} M^{\ell\ \overline{m}\ \overline{n}}_{\ell'm\ n'}(t\,|\,t') \ .$$

$$\tag{5-22} ^{1)}$$

On the other hand, if the photophysical anisotropy of fluorescent probe is quite high and we may take the transition moments of light absorption and emission to be uniaxially symmetrical ellipsoidal dipoles, the coefficients $G_{\ell n}$ and $H_{\ell'n'}$ are zero for $n \neq 0$ and $n' \neq 0$, respectively.

By using the general equation (5-16) under the above mentioned conditions, the polarized component of fluorescence intensity can be represented as

$$I\left(\begin{smallmatrix}\mathbb{P}_1\\\mathbb{P}_2\end{smallmatrix}\right) = 8\pi^2 k\phi \sum_{\ell \ell' m} \{(2\ell + 1)(2\ell'+ 1)\}^{-1/2} [S_{\ell m} T_{\ell' \bar{m}}]_{int}$$

$$\times G_{\ell 0} H_{\ell' 0} [M^{\ell \; m \; 0}_{\ell' \; \bar{m} \; 0}(t|t')]_s \qquad (5\text{-}23)$$

$$(\; -\min(\ell,\ell') \le m \le \min(\ell,\ell') \;, \; \ell \text{ and } \ell' = 0,2 \;) \;,$$

where

$$M^{\ell \; m \; 0}_{\ell' \; \bar{m} \; 0}(t|t') = M^{\ell \; \bar{m} \; 0}_{\ell' \; m \; 0}(t|t')$$

$$= (1/\; 4\pi^2)\,(\frac{2}{2\ell'+ 1})^{1/2} \sum_{p=-\ell'}^{\ell'} < Z_{\ell m 0}(\cos\omega) Z_{\ell' \bar{m} p}(\cos\omega)$$

$$\times Z_{\ell' p 0}(\cos\gamma)\cos p(\chi+\psi) > \;, \quad (5\text{-}24)$$

in which Z is the generalized associated Legendre function.
Right side of eq. (5-24) consists of a sum of terms of angular
average value, and some of them are equivalent to the angular
factors discussed in molecular dynamics by Jarry et al.[2] In
practice, it is difficult to determine all the angular average
values experimentally, since there is a limit to the number of
measurable independent components of polarized fluorescence
intensity.

    If we need not use so a perfect model of molecular dynamics,
we can reasonably assume in the case of uniaxially oriented
system that the molecular motion is rotationally symmetrical
around the initial direction of the molecular axis (M-axis) of
excited molecule, as shown in Fig. 5-2. However, the degree of
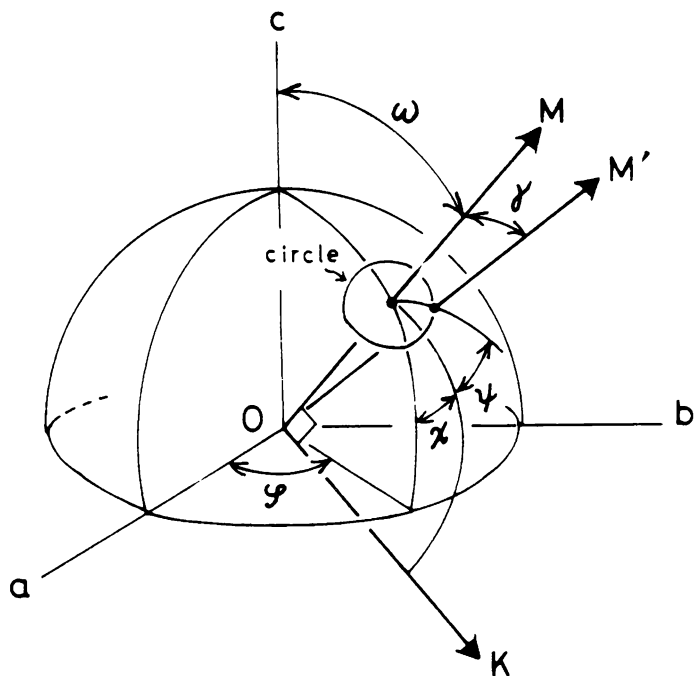
Fig. 5-2. Diagram illustrating a uniaxially symmetric
model of molecular rotational motion. The motion of a
fluorescent probe oriented at angle ω (ω: the polar angle
of the M-axis) is isotropic so far as ψ is concerned.

motion may depend on the orientation angle of the M-axis, i.e.,
the polar angle ω. In such a simple case, eq. (5-24) can be
simplified as

$$M^{\ell\ \ m\ \ 0}_{\ell'\,\bar{m}\ 0}(t|t') = M^{\ell\ \ \bar{m}\ \ 0}_{\ell'\,m\ 0}(t|t')$$

$$= (1/\ 4\pi^2)\,(\frac{2}{2\ell'+1})^{1/2} < Z_{\ell m0}(\cos\omega)\,Z_{\ell'\bar{m}0}(\cos\omega)\,Z_{\ell'00}(\cos\gamma) > .$$

$$(5-25)$$

The above coefficient can be given in more explicit form as

shown below:

$$M_{000}^{000}(t|t') = 1/\ 8\pi^2 \tag{5-26a}$$

$$M_{000}^{200}(t|t') = (\sqrt{5}/\ 8\pi^2)<(3\cos^2\omega - 1)/2> \tag{5-26b}$$

$$M_{200}^{000}(t|t') = (\sqrt{5}/\ 8\pi^2)<(3\cos^2\omega - 1)/2\cdot(3\cos^2\gamma - 1)/2> \tag{5-26c}$$

$$M_{200}^{200}(t|t') = (1/\ 8\pi^2)\{<(3\cos^2\gamma - 1)/2>$$

$$- 5<(3\cos^2\omega - 1)/2\cdot(3\cos^2\gamma - 1)/2>$$

$$+ 9<(5\cos^4\omega - 1)/4\cdot(3\cos^2\gamma - 1)/2>\} \tag{5-26d}$$

$$M_{2\bar{1}0}^{210}(t|t') = M_{210}^{2\bar{1}0}(t|t')$$

$$= (-1/\ 8\pi^2)\{<(3\cos^2\gamma - 1)/2>$$

$$+ 5<(3\cos^2\omega - 1)/2\cdot(3\cos^2\gamma - 1)/2>$$

$$- 6<(5\cos^4\omega - 1)/4\cdot(3\cos^2\gamma - 1)/2>\} \tag{5-26e}$$

$$M_{2\bar{2}0}^{220}(t|t') = M_{220}^{2\bar{2}0}(t|t')$$

$$= (1/\ 8\pi^2)\{<(3\cos^2\gamma - 1)/2>$$

$$- (5/2)<(3\cos^2\omega - 1)/2\cdot(3\cos^2\gamma - 1)/2>$$

$$+ (3/2)<(5\cos^4\omega - 1)/4\cdot(3\cos^2\gamma - 1)/2>\}\ . \tag{5-26f}$$

Consequently, the coefficient $M_{\ell',m}^{\ell\ \ m\ \ 0}(t|t')$ for the uni-
axially symmetrical system is a function of the following

average values; $<(3\cos^2\omega - 1)/2>$, $<(3\cos^2\gamma - 1)/2>$, $<(3\cos^2\omega$
$- 1)/2\cdot(3\cos^2\gamma - 1)/2>$ and $<(5\cos^4\omega - 1)/4\cdot(3\cos^2\gamma - 1)/2>$.
$<(3\cos^2\omega - 1)/2>$ is the second order orientation factor.
$<(3\cos^2\gamma - 1)/2>$ is the average value expressing the molecular
mobility for the total ensemble in the system. $<(3\cos^2\omega - 1)/2$
$\cdot(3\cos^2\gamma - 1)/2>$ and $<(5\cos^4\omega - 1)/4\cdot(3\cos^2\gamma - 1)/2>$ can be
regarded as the factors expressing the orientation dependence
of the molecular mobility. These factors can be analyzed by
using eq. (5-23) from the measurement of polarized components of
fluorescence intensity. For stationary irradiation measurement,
the mobility factor and the orientation-mobility factors con-
taining γ can be obtained not only as an ensemble average, but
also as a time average since the angle γ is a function of time u
in the decay process of fluorescence emission. In this case,
using a subscript s, let us represent the molecular mobility
factor as $<(3\cos^2\gamma - 1)/2>_s$ and represent the orientation-
mobility factors as $<(3\cos^2\omega - 1)/2\cdot(3\cos^2\gamma - 1)/2>_s$ and
$<(5\cos^4\omega - 1)/4\cdot(3\cos^2\gamma - 1)/2>_s$.

In rigid systems, the transition probability $P(\Omega,t|\Gamma,u)$ is
equal to $\underline{\delta}(\Gamma - 0)$ ($\underline{\delta}$: the Dirac delta function), and therefore
eq. (5-26) is applicable to uniaxially oriented rigid systems
by setting as $(3\cos^2\gamma - 1)/2 = 1$. Then, one can find that the
coefficient $M_{\ell'm0}^{\ell m 0}(t|t')$ is a function of the second and fourth

moments ($<\cos^2\omega>$ and $<\cos^4\omega>$) of molecular orientation distribution, as already treated in Chapters 3 and 4.

In isotropic systems, the orientation distribution function $m(\Omega,t)$ and the transition probability $P(\Omega,t|\Gamma,u)$ are both independent of Ω, and therefore the coefficient $[M^{\ell\ m\ 0}_{\ell'\ m\ 0}(t|t')]_s$ is a function of only the mobility factor $<(3\cos^2\gamma - 1)/2>_s$.

Reference and Note

1) These symmetrical properties can be derived by utilizing eq. (AI-2c) and (AI-3) in Appendix I.

2) J. P. Jarry and L. Monnerie, J. Polym. Sci., Polym. Phys. Ed., _16_, 443 (1978).

CHAPTER 6

Orientation, Mobility, and Orientation-Mobility Factors

in Uniaxially Oriented Systems

6-1. Introduction

In Chapter 5, the polarized component of fluorescence inten-
sity was generally described for the anisotropic system in which
the rotational motions of fluorescent probes are measurable
during the fluorescence lifetime. Moreover, the simplified
equation of polarized component of fluorescence intensity was
discussed for the case of uniaxially symmetrical orientation and
motion. Consequently, it turned out in theory that the factors
characterizing the molecular orientation and motion can be
obtained by analyzing the polarized fluorescence intensity.

In this chapter, first, a method for estimating the aniso-
tropy of molecular mobility is discussed in a uniaxially oriented
system, in terms of the orientation, mobility, and orientation-
mobility factors defined in the preceding chapter. Secondly,
the procedure for experimentally determining the factors of
molecular orientation and motion is discussed, and then an
apparatus for measurements is designed in order to study the
molecular orientation, its relaxation mechanism, and the molecu-

lar motion in polymer solids.

6-2. Anisotropy of Molecular Mobility

An oriented system in which fluorescent probes are moving

rotationally is illustrated schematically in Fig. 6-1. The

symbols G, H, S, T, and M are the coefficients characterizing

the intrinsic absorption anisotropy, the intrinsic emission

anisotropy, the excitation probability, the detection proba-

bility of fluorescence, and the orientation and motion of a
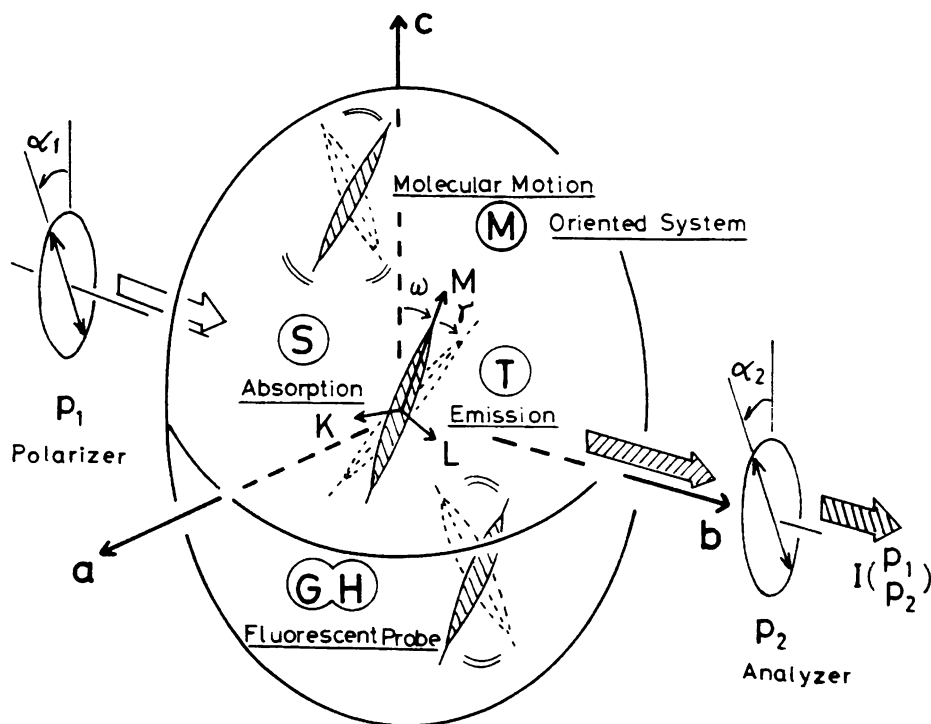
Fig. 6-1. Diagram illustrating an oriented system.

fluorescent molecule, respectively. The polarized fluorescence

intensity from such an anisotropic system depends on the molecu-

lar orientation and motion, the photophysical anisotropy of

fluorescent probe, and the optical system for the measurement.

In uniaxially symmetrical systems, the polarized component of

fluorescence intensity, $I(^{\mathbb{P}_1}_{\mathbb{P}_2})$, can be described by using the

above mentioned coefficients, as follows:

$$I(^{\mathbb{P}_1}_{\mathbb{P}_2}) = 8\pi^2 k\phi \sum_{\ell\,\ell'm} \{(2\ell + 1)(2\ell'+ 1)\}^{-1/2} \underline{[S_{\ell m}T_{\ell'm}]}_{int}$$

$$\times \underline{G_{\ell 0}H_{\ell'0}}\ \underline{[M^{\ell\ \ m\ \ 0}_{\ell'\,m\ \ 0}(t|t')]}_{s} \quad . \quad (6-1)$$

<table>
<tr><td>

Angular alignments

of $\mathbb{P}_1$ and $\mathbb{P}_2$:

  (α_1, β_1)

  (α_2, β_2)

Effect of optical

anisotropy of the

medium.

</td><td>

Photophysical

anisotropy fac-

tors :

$(3<\cos^2\delta> -1)/2$

$(3<\cos^2\eta> -1)/2$

[See eq. (2-52).]

</td><td>

Orientation factor :

  $<(3\cos^2\omega - 1)/2>$

Mobility factor :

  $<(3\cos^2\gamma - 1)/2>_s$

Orientation-mobility

factors :

  $<(3\cos^2\omega - 1)/2$

   $\cdot(3\cos^2\gamma - 1)/2>_s$

  $<(5\cos^4\omega - 1)/4$

   $\cdot(3\cos^2\gamma - 1)/2>_s$

</td></tr>
</table>

[See eqs. (2-50),

 (2-51), and (3-9).]

[See eq. (5-26).]

The factors of molecular orientation and motion are averaged

according to the definition in the preceding chapter (see eqs.

(5-10) and (5-18)), as follows,

$$\langle F(\omega,\gamma)\rangle_s = \int_\Omega \int_0^\infty \int_\Gamma F(\omega,\gamma) P(\Omega,t|\Gamma,u) d\Gamma \; e^{-u/\tau} du/\tau \; m(\Omega,t) d\Omega \;,$$

(6-2)

where $F(\omega,\gamma)$ is a function of ω and γ, and γ is a function of

time u. (The subscript s is used to designate time average.)

Now, let us define $[\overline{(3\cos^2\gamma - 1)/2}]_s$ as

$$[\overline{(3\cos^2\gamma - 1)/2}]_s = \int_0^\infty \overline{(3\cos^2\gamma - 1)/2} \cdot e^{-u/\tau} du/\tau \;,$$

(6-3)

where

$$\overline{(3\cos^2\gamma - 1)/2} = \int_\Gamma (3\cos^2\gamma - 1)/2 \cdot P(\Omega,t|\Gamma,u) d\Gamma \;.$$

(6-4)

Then the mobility and orientation-mobility factors can be written

in the following forms:

$$\langle (3\cos^2\gamma - 1)/2\rangle_s = \int_\Omega [\overline{(3\cos^2\gamma - 1)/2}]_s \; m(\Omega,t) d\Omega$$

(6-5)

$$\langle (3\cos^2\omega - 1)/2 \cdot (3\cos^2\gamma - 1)/2\rangle_s$$
$$= \int_\Omega (3\cos^2\omega - 1)/2 \cdot [\overline{(3\cos^2\gamma - 1)/2}]_s \; m(\Omega,t) d\Omega$$

(6-6)

$$\langle (5\cos^4\omega - 1)/4 \cdot (3\cos^2\gamma - 1)/2\rangle_s$$
$$= \int_\Omega (5\cos^4\omega - 1)/4 \cdot [\overline{(3\cos^2\gamma - 1)/2}]_s \; m(\Omega,t) d\Omega \;.$$

(6-7)

In a simple case of molecular rotation as shown in Appendix

II, $[\overline{(3\cos^2\gamma - 1)/2}]_s$ can be related by eq. (AII-13) to the

relaxation time of rotation of a fluorescent molecule oriented

-130-

at polar angle ω.

Using the factors given by eqs. (6-5)-(6-7) and the orientation factor $<(3\cos^2\omega - 1)/2>$, one can discuss the anisotropy of molecular mobility in uniaxially oriented system, e.g., in a uniaxially stretched polymer film.

When a polymer film, in which fluorescent molecules are dispersed, is drawn uniaxially along the stretching axis (c-axis), let the type of orientation distribution of fluorescent molecules be the ellipsoid of revolution.[1] Then, the molecular orientation distribution function is given by

$$m(\Omega,t) = \frac{1}{8\pi^2} \frac{k^2}{\{k^2 - (k^2-1)\cos^2\omega\}^{3/2}}, \qquad (6-8)$$

where k is the axial ratio of the longer axis to the shorter one of the ellipsoid. If $k = \lambda^{3/2}$ (λ: draw ratio of the film), eq. (6-8) is equivalent to the orientation distribution function of the affine deformation model proposed by Kratky for the orientation of rods floating in a bulk matrix.[2]

Here, let us propose a method for discussion of the anisotropy of molecular mobility in the uniaxially symmetrical system having the molecular orientation distribution function given by eq. (6-8). In Fig. 6-2, different kinds of anisotropy models for molecular mobility are given by describing curves of $[(3\overline{\cos^2\gamma} - 1)/2]_s$ against ω arbitrarily in the range of 0.5 to 0.9

-131-
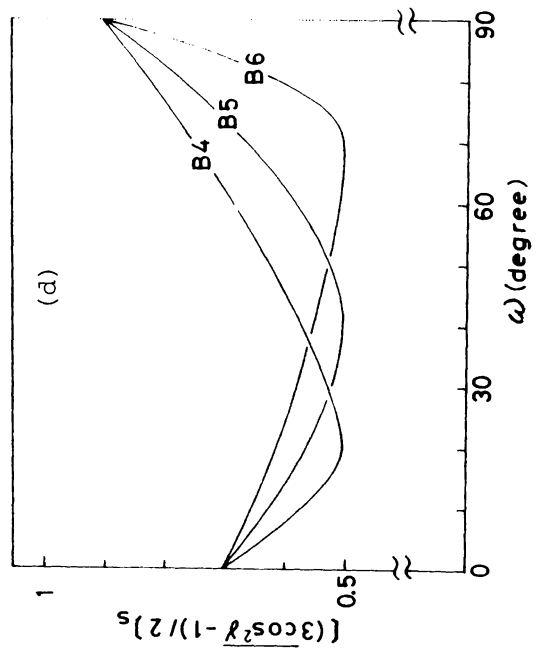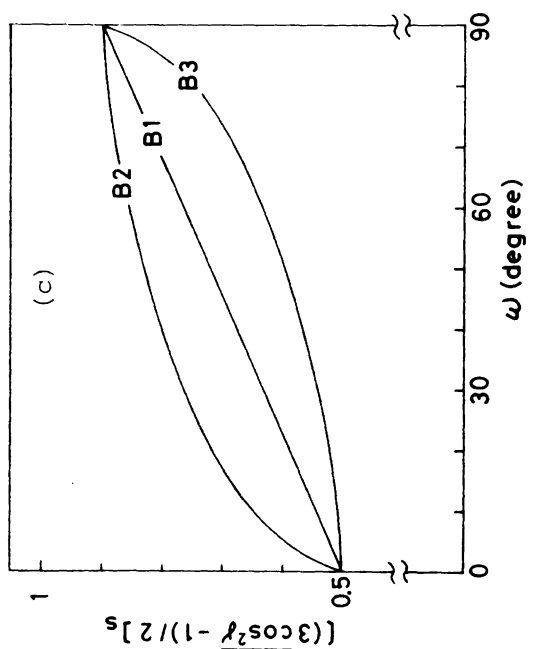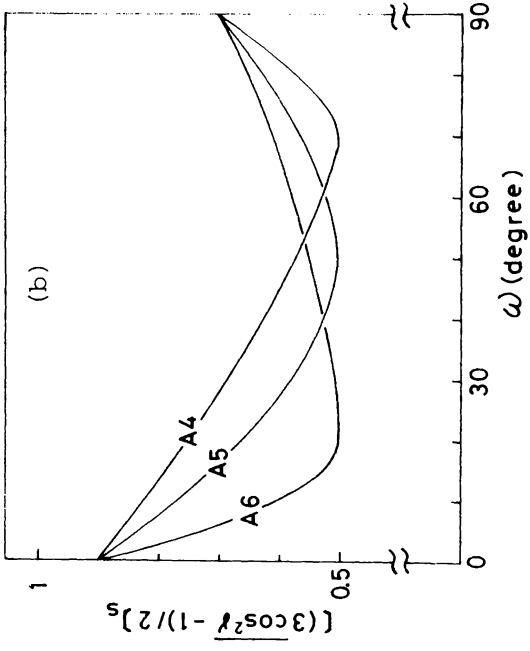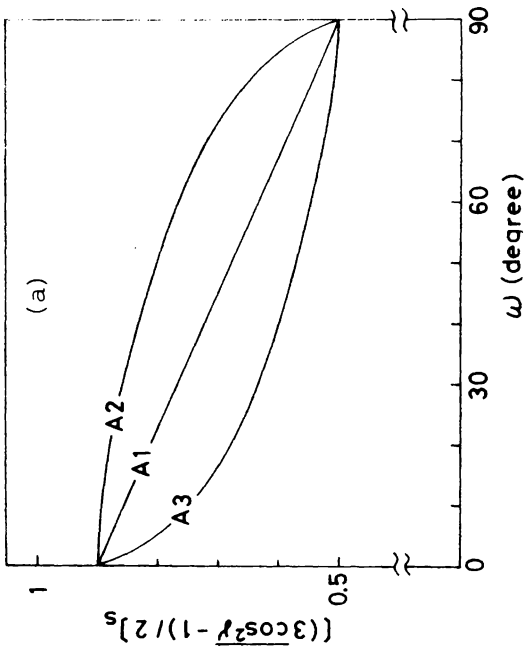
Fig. 6-2. Models of the anisotropy of molecular mobility.

(a) Models A1-A3: The value of $[(3\cos^2\gamma - 1)/2]_s$ decreases monotonously with increasing ω.

(b) Models A4-A6: The curves of A4, A5, and A6 are drawn so that the values of $[(3\cos^2\gamma - 1)/2]_s$ are minimum at $\omega = 70°$, $50°$, and $20°$, respectively.

(c) Models B1-B3: The value of $[(3\cos^2\gamma - 1)/2]_s$ increases monotonously with increasing ω.

(d) Models B4-B6: The curves of B4, B5, and B6 are drawn so that the values of $[(3\cos^2\gamma - 1)/2]_s$ are minimum at $\omega = 20°$, $40°$, and $70°$, respectively.

of $[(3\cos^2\gamma - 1)/2]_s$. The smaller the value of $[(3\cos^2\gamma - 1)/2]_s$, the greater the molecular mobility is. Models A1-A6 are the models for the case that oriented molecules have greater mobility in the direction perpendicular than parallel to the stretched axis (c-axis) of $\omega = 0°$. On the other hand, in Models B1-B6, molecules are movable in the direction of $\omega = 0°$ than in that of $\omega = 90°$. The mobility of oriented molecules increases monotonously in the cases of A1-A3 (Fig. 6-2a) and decreases monotonously in the cases of B1-B3 (Fig. 6-2c) with increasing ω. In the cases of A4-A6 (Fig. 6-2b) and B4-B6 (Fig. 6-2d), the orientation angle at which molecules have the greatest mobility approaches $\omega = 0°$ in the order from A4 to A6 and does $\omega = 90°$ in the order from B4 to B6.

Figures 6-3, 6-4, and 6-5 show the plots of $\langle (3\cos^2\omega - 1)/2 \cdot (3\cos^2\gamma - 1)/2 \rangle_s$ versus $\langle (3\cos^2\gamma - 1)/2 \rangle_s$, $\langle (3\cos^2\omega - 1)/2 \cdot (3\cos^2\gamma - 1)/2 \rangle_s$ versus the product $\langle (3\cos^2\omega - 1)/2 \rangle \langle (3\cos^2\gamma - 1)/2 \rangle_s$, and $\langle (5\cos^4\omega - 1)/4 \cdot (3\cos^2\gamma - 1)/2 \rangle_s$ versus $\langle (3\cos^2\omega - 1)/2 \rangle \langle (3\cos^2\gamma - 1)/2 \rangle_s$, respectively. These factors were calculated from eqs. (6-5)-(6-7) by using the models A1-A6 and B1-B6 shown in Fig. 6-2 and the orientation distribution functions given by eq. (6-8) with k = 1.2, 2, 3, and 5. The solid lines in Figs. 6-3 and 6-4 are the linear lines following the relation that $\langle (3\cos^2\omega - 1)/2 \cdot (3\cos^2\gamma - 1)/2 \rangle_s = \langle (3\cos^2\omega - 1)/2 \rangle \langle (3\cos^2\gamma - 1)/2 \rangle_s$. The solid lines in Fig. 6-5 are the

curves following the relation that $\langle(5\cos^4\omega - 1)/4 \cdot (3\cos^2\gamma - 1)/2\rangle_s$

$= \langle(5\cos^4\omega - 1)/4\rangle\langle(3\cos^2\gamma - 1)/2\rangle_s$, and hence they coincide with

the curve of $\langle(5\cos^4\omega - 1)/4\rangle$ versus $\langle(3\cos^2\omega - 1)/2\rangle$ according

to the orientation distribution of ellipsoid of revolution. If

the molecular mobility is independent of ω, i.e., the anisotropy

of molecular mobility does not exist in the oriented system, the

orientation-mobility factors should be on the solid lines.

From Figs. 6-3 - 6-5, the following tendencies can be found:

In the case that oriented molecules have greater mobility in

directions about perpendicular rather than parallel to the c-axis

(i.e., in such cases as A1-A5 and B6), $\langle(3\cos^2\omega - 1)/2 \cdot (3\cos^2\gamma$

$- 1)/2\rangle_s$ tends to be larger than $\langle(3\cos^2\omega - 1)/2\rangle\langle(3\cos^2\gamma - 1)/2\rangle_s$

and the plot of $\langle(5\cos^4\omega - 1)/4 \cdot (3\cos^2\gamma - 1)/2\rangle_s$ versus $\langle(3\cos^2\omega$

$- 1)/2\rangle\langle(3\cos^2\gamma - 1)/2\rangle_s$ tends to be above the theoretical curve

of $\langle(5\cos^4\omega - 1)/4\rangle$ versus $\langle(3\cos^2\omega - 1)/2\rangle$ for the ellipsoidal

orientation distribution. On the contrary, in the case that

oriented molecules have greater mobility in directions about

parallel rather than perpendicular to the c-axis (i.e., in such

cases as B1-B5 and A6), the relations between the orientation-

mobility factors and the product of orientation and mobility

factors are just opposite to those in such cases as A1-A5 and

B6.
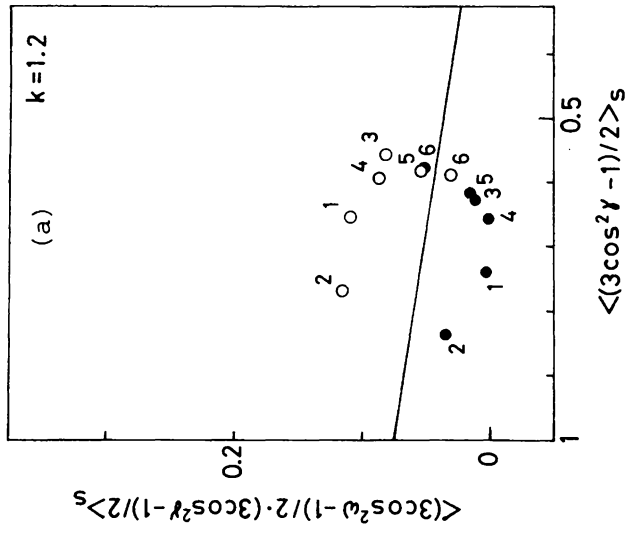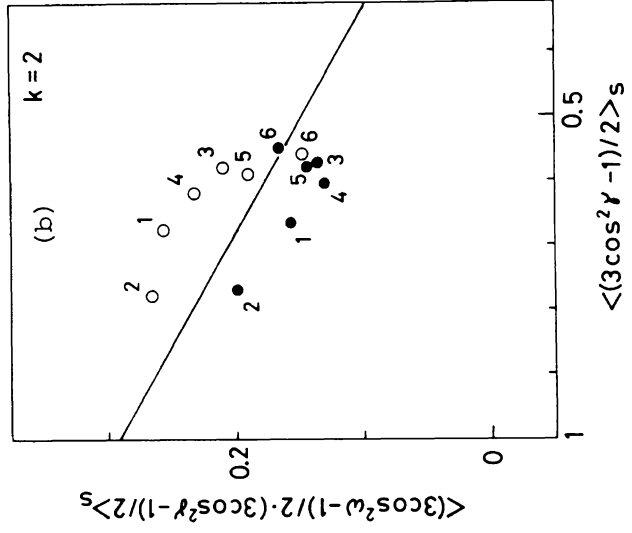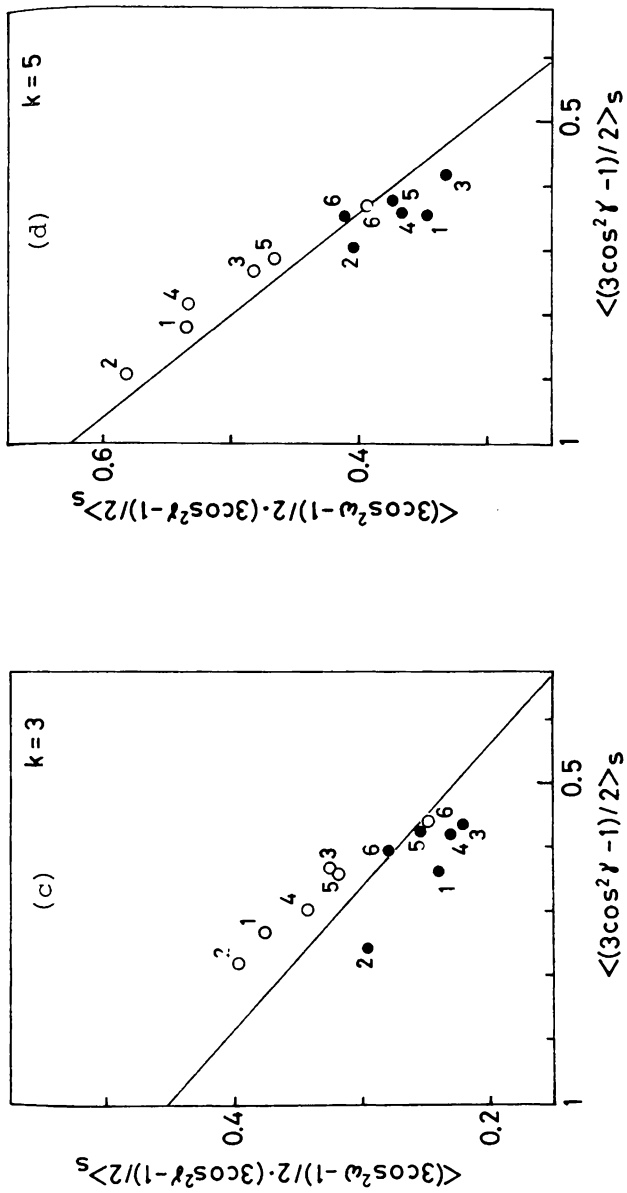
Fig. 6-3. $<(3\cos^2\omega - 1)/2 \cdot (3\cos^2\gamma - 1)/2>_s$ vs. $<(3\cos^2\gamma - 1)/2>_s$, calculated by using the models shown in Fig. 6-2 and the orientation distribution functions given by eq. (6-8) with (a) $k = 1.2$, (b) $k = 2$, (c) $k = 3$, and (d) $k = 5$. ($\bigcirc$): A1-A6, ($\bullet$): B1-B6. (———): $<(3\cos^2\omega - 1)/2 \cdot (3\cos^2\gamma - 1)/2>_s = <(3\cos^2\omega - 1)/2><(3\cos^2\gamma - 1)/2>_s$.
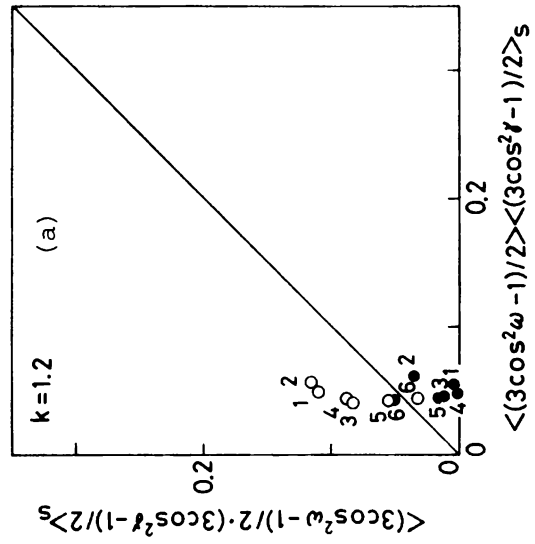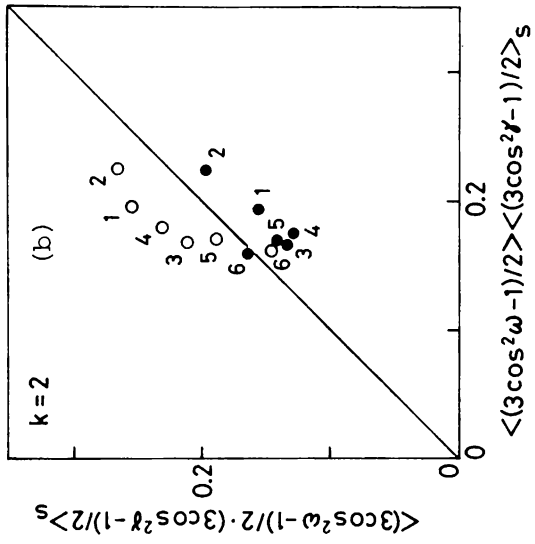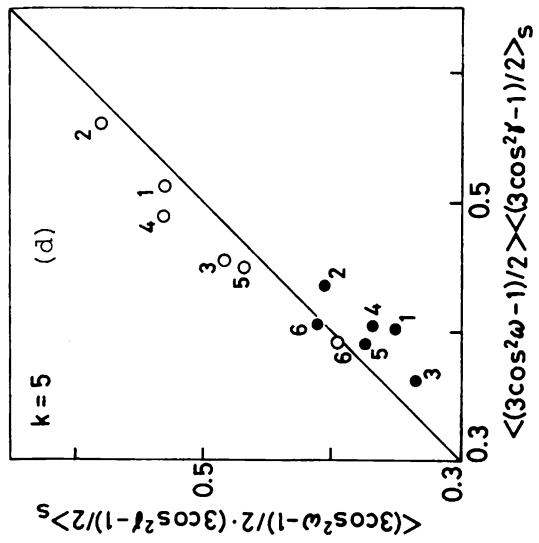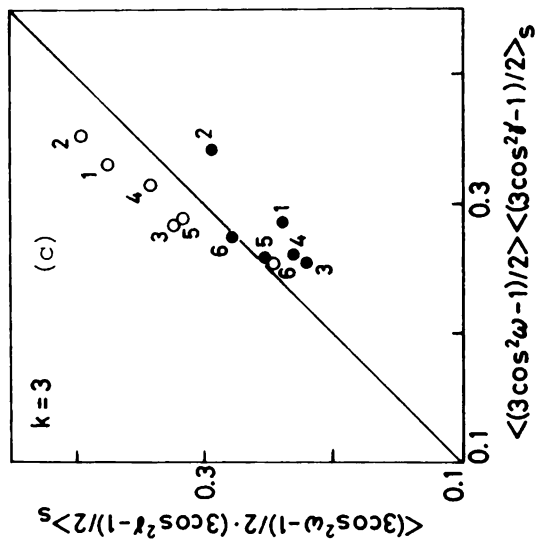
Fig. 6-4. $\langle(3\cos^2\omega - 1)/2 \cdot (3\cos^2\gamma - 1)/2\rangle_s$ vs. $\langle(3\cos^2\omega - 1)/2\rangle\langle(3\cos^2\gamma - 1)/2\rangle_s$, calculated in the same way as in Fig. 6-3.

(———): $\langle(3\cos^2\omega - 1)/2 \cdot (3\cos^2\gamma - 1)/2\rangle_s = \langle(3\cos^2\omega - 1)/2\rangle\langle(3\cos^2\gamma - 1)/2\rangle_s$.

(a) k=1.2

(b) k=2
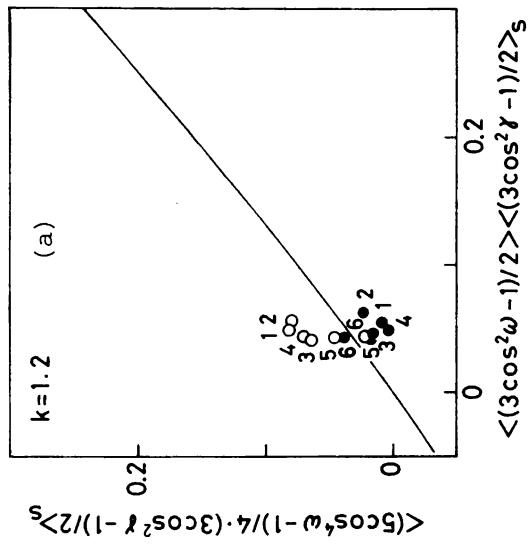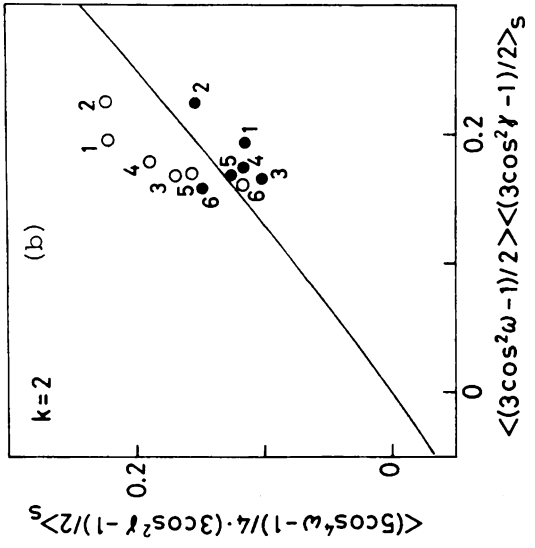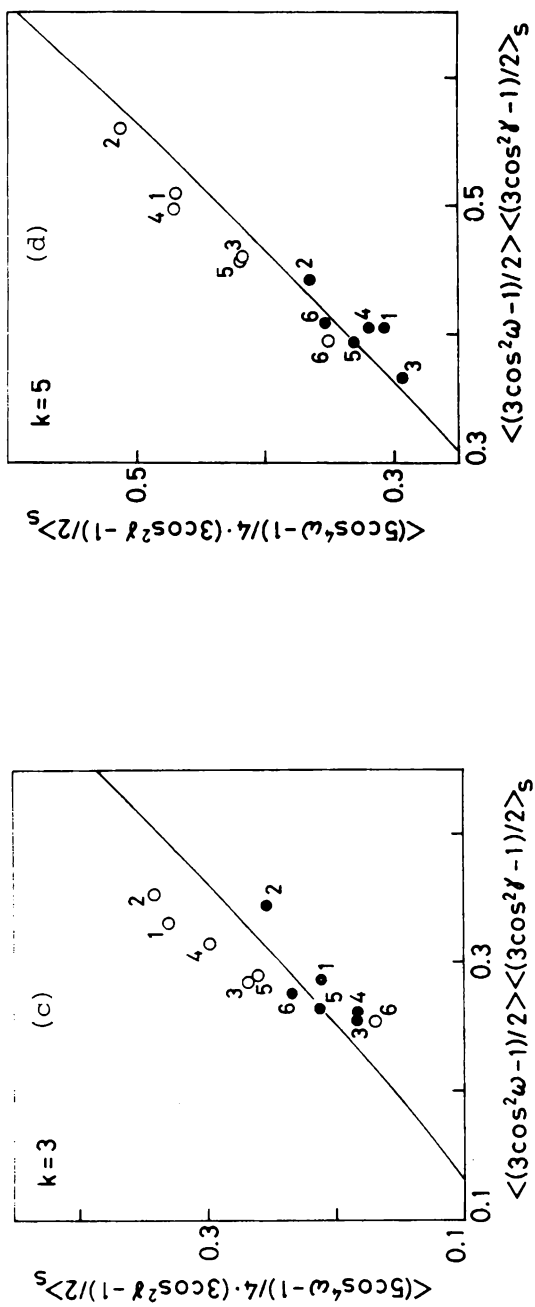
Fig. 6-5. $\langle (5\cos^4\omega - 1)/4 \cdot (3\cos^2\gamma - 1)/2 \rangle_s$ vs. $\langle (3\cos^2\omega - 1)/2 \rangle \langle (3\cos^2\gamma - 1)/2 \rangle_s$, calculated in the same way as in Fig. 6-3.

(————): Theoretical curve of $\langle (5\cos^4\omega - 1)/4 \rangle$ versus $\langle (3\cos^2\omega - 1)/2 \rangle$ for the rotationally ellipsoidal orientation distribution.

6-3. Procedure of Experimental Determination of the Factors

  of Molecular Orientation and Motion

In this section, we consider how the factors of molecular orientation and motion may be dtermined experimentally from the observed components of fluorescence intensity.

First, let the anisotropies of light absorption and emission of the fluorescent probe treated here be nearly equal to each other. Then the following equation holds for the photophysical anisotropy factors constituting eq. (6-1).

$$G_{20} = \sqrt{5/4\pi} \; (3<\cos^2\delta> - 1)/2$$

$$\simeq H_{20} = \sqrt{5/4\pi} \; (3<\cos^2\eta> - 1)/2 \; . \tag{6-9}$$

The factor $(3<\cos^2\delta> - 1)/2$ can be determined from the fluorescence anisotropy ratio[3] of a rigid specimen in which fluorescent probes are randomly oriented.

When the optical system as shown in Fig. 6-6 is used for measuring the polarized fluorescence intensity, the coefficients $[S_{\ell m}T_{\ell'm}^-]_{int}$ constituting eq. (6-1) are represented by eq. (3-9) in Chapter 3. Through use of eq. (3-9), the value of $[S_{\ell m}T_{\ell'm}^-]_{int}$ for several combinations of the angles α_1 and α_2 specifying the alignments of transmission axes of polarizer and analyzer are listed in Table 6-1. By utilizing the values in Table 6-1, several components of polarized fluorescence intensity, $I\binom{\alpha_1}{\alpha_2}$,
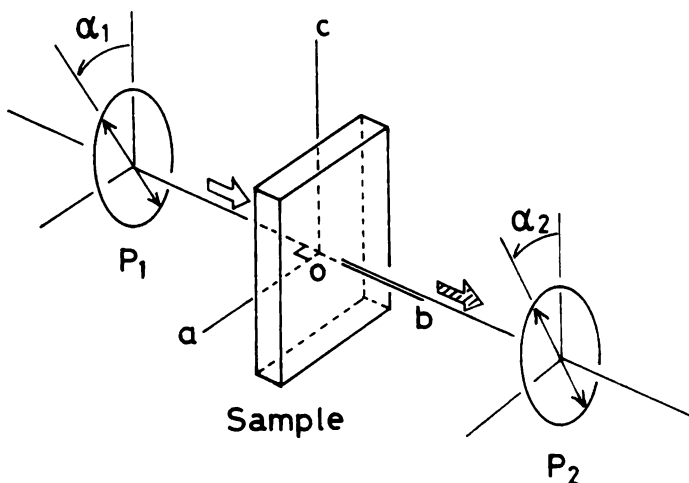
Fig. 6-6. Optical system for measuring polarized fluorescence intensity. The planes of polarizer (P_1) and analyzer (P_2) are both parallel to the ac-plane of the sample.

can be calculated in the following explicit form:

Two independent components of fluorescence intensity observed under the set of $\alpha_2 = 0°$ are

$$I\binom{0}{0} = (k\phi/9)\ \{1 + 2AX_1 + 2AX_2 + (4/5)A^2X_3\} \qquad (6\text{-}10a)$$

$$I\binom{90}{0} = (k\phi/9)\ \{1 - AX_1 + 2AX_2 - (2/5)A^2X_3\}\ , \qquad (6\text{-}10b)$$

where

$$A = (3<\cos^2\delta> - 1)/2 \qquad (6\text{-}11)$$

$$X_1 = <(3\cos^2\omega - 1)/2> \qquad (6\text{-}12a)$$

-143-

Table 6-1. Coefficients $[S_{\ell m}T_{\ell',\bar{m}}]_{int}$ for the optical system as shown in Fig. 6-6.

$\binom{\alpha_1}{\alpha_2}$ (degree)	$[S_{00}T_{00}]_{int}$	$[S_{20}T_{00}]_{int}$	$[S_{00}T_{20}]_{int}$	$[S_{20}T_{20}]_{int}$	$[S_{2\bar{1}}T_{2\bar{1}}]_{int}$ $=[S_{21}T_{21}]_{int}$	$[S_{22}T_{2\bar{2}}]_{int}$ $=[S_{22}T_{22}]_{int}$
$\binom{0}{0}$	$4\pi/9$	$8\pi/(9\sqrt{5})$	$8\pi/(9\sqrt{5})$	$16\pi/45$	0	0
$\binom{90}{0}$	$4\pi/9$	$-4\pi/(9\sqrt{5})$	$8\pi/(9\sqrt{5})$	$-8\pi/45$	0	0
$\binom{0}{45}$	$4\pi/9$	$8\pi/(9\sqrt{5})$	$2\pi/(9\sqrt{5})$	$4\pi/45$	0	0
$\binom{45}{45}$	$4\pi/9$	$2\pi/(9\sqrt{5})$	$2\pi/(9\sqrt{5})$	$\pi/45$	$-(2\pi/15)\int_0^D \cos\delta_i$ $\times \cos\delta_f \, dl/D$	$\pi/30$
$\binom{90}{45}$	$4\pi/9$	$-4\pi/(9\sqrt{5})$	$2\pi/(9\sqrt{5})$	$-2\pi/45$	0	$\pi/15$
$\binom{0}{90}$	$4\pi/9$	$8\pi/(9\sqrt{5})$	$-4\pi/(9\sqrt{5})$	$-8\pi/45$	0	0
$\binom{90}{90}$	$4\pi/9$	$-4\pi/(9\sqrt{5})$	$-4\pi/(9\sqrt{5})$	$4\pi/45$	0	$2\pi/15$

$$X_2 = \langle (3\cos^2\omega - 1)/2 \cdot (3\cos^2\gamma - 1)/2 \rangle_s \qquad (6\text{-}12\text{b})$$

$$X_3 = \langle (3\cos^2\gamma - 1)/2 \rangle_s - 5\langle (3\cos^2\omega - 1)/2 \cdot (3\cos^2\gamma - 1)/2 \rangle_s$$

$$+ 9\langle (5\cos^4\omega - 1)/4 \cdot (3\cos^2\gamma - 1)/2 \rangle_s \; . \qquad (6\text{-}12\text{c})$$

Three independent components of fluorescence intensity observed under the set of $\alpha_2 = 45°$ are

$$I\binom{0}{45} = (k\phi/9)\,\{1 + 2AX_1 + (1/2)AX_2 + (1/5)A^2X_3\} \qquad (6\text{-}10\text{c})$$

$$I\binom{45}{45} = (k\phi/9)\,\{1 + (1/2)AX_1 + (1/2)AX_2 + (1/20)A^2X_3$$

$$+ (3/5)A^2X_4\int_0^D \cos\delta_i \cos\delta_f \, dl/D + (3/20)A^2X_5\} \qquad (6\text{-}10\text{d})$$

$$I\binom{90}{45} = (k\phi/9)\,\{1 - AX_1 + (1/2)AX_2 - (1/10)A^2X_3 + (3/10)A^2X_5\}, \qquad (6\text{-}10\text{e})$$

where

$$X_4 = \langle (3\cos^2\gamma - 1)/2 \rangle_s + 5\langle (3\cos^2\omega - 1)/2 \cdot (3\cos^2\gamma - 1)/2 \rangle_s$$

$$- 6\langle (5\cos^4\omega - 1)/4 \cdot (3\cos^2\gamma - 1)/2 \rangle_s \qquad (6\text{-}12\text{d})$$

$$X_5 = \langle (3\cos^2\gamma - 1)/2 \rangle_s - (5/2)\langle (3\cos^2\omega - 1)/2 \cdot (3\cos^2\gamma - 1)/2 \rangle_s$$

$$+ (3/2)\langle (5\cos^4\omega - 1)/4 \cdot (3\cos^2\gamma - 1)/2 \rangle_s$$

$$= (1/2)(X_3 + X_4 - 5X_2) \; . \qquad (6\text{-}12\text{e})$$

Two independent components of fluorescence intensity observed under the set of $\alpha_2 = 90°$ are

-145-

$$I\left(^0_{90}\right) = (k\phi/9)\ \{1 + 2AX_1 - AX_2 - (2/5)A^2X_3\}$$

$$= 2I\left(^0_{45}\right) - I\left(^0_0\right) \tag{6-10f}$$

$$I\left(^{90}_{90}\right) = (k\phi/9)\ \{1 - AX_1 - AX_2 + (1/5)A^2X_3 + (3/5)A^2X_5\}$$

$$= 2I\left(^{90}_{45}\right) - I\left(^{90}_0\right) \ . \tag{6-10g}$$

There are now five unknown quantities; the orientation factor, the mobility factor, the two orientation-mobility factors, and a proportional constant $k\phi$. Accordingly , the four unknown factors of molecular orientation and motion can be determined by analyzing five components of fluorescence intensity, for example, $I\left(^0_0\right)$, $I\left(^{90}_0\right)$, $I\left(^0_{45}\right)$, $I\left(^{45}_{45}\right)$, and $I\left(^{90}_{45}\right)$. For this purpose, it is necessary to evaluate the birefringence factor $\int_0^D \cos\delta_i \cos\delta_f \, dl/D$ (described in Chapter 3, eq. (3-12)) from the measurement of the retardation of anisotropic medium, since some components of polarized fluorescence intensity are affected by the optical anisotropy of the medium.

6-4. Apparatus for Measurements of Molecular Orientation
      and Motion

In order to study the molecular orientation, its relaxation mechanism, and the molecular motion in polymer solids by the fluorescence polarization method, an apparatus for measurement has been designed and constructed.

Figure 6-7 shows the diagram of the apparatus for measurement. Light from a source (LS: mercury-arc lamp) is rendered parallel by a lens system (L). The parallel light beam is made monochromatic by a filter system (F_1), which is chosen to transmit the light with a desired wavelength for the excitation of used fluorescent probe. Then the exciting light is linearly polarized by a polarizer (P_1) and falls on the sample (O). The polarized components of fluorescence intensity are detected by a multiplier phototube (PM) through an analyzer (P_2) and a cut-off filter (F_3). The filter F_3 is chosen to transmit only the fluorescence light. A part of transmitted exciting light is detected through an analyzer and a monochromatic filter (F_2) for the purpose of measuring the retardation of the anisotropic sample. The polarizer can be rotated at a proper constant speed and the transmission axes of three analyzers can be fixed in the appropriate directions. In the experiments described in the following chapters, the transmission axes of two analyzers for the measurement of fluorescence were set at angles of 0° and 45° to the vertical axis parallel to the c-axis of the oriented sample, i.e., $\alpha_2 = 0$° and 45°, and that of analyzer for the measurement of transmitted exciting light was set at an angle of −45° to the c-axis. The sample is held in the thermo-regulated box attached to a tensile machine, and it can also be drawn to the vertical direction.
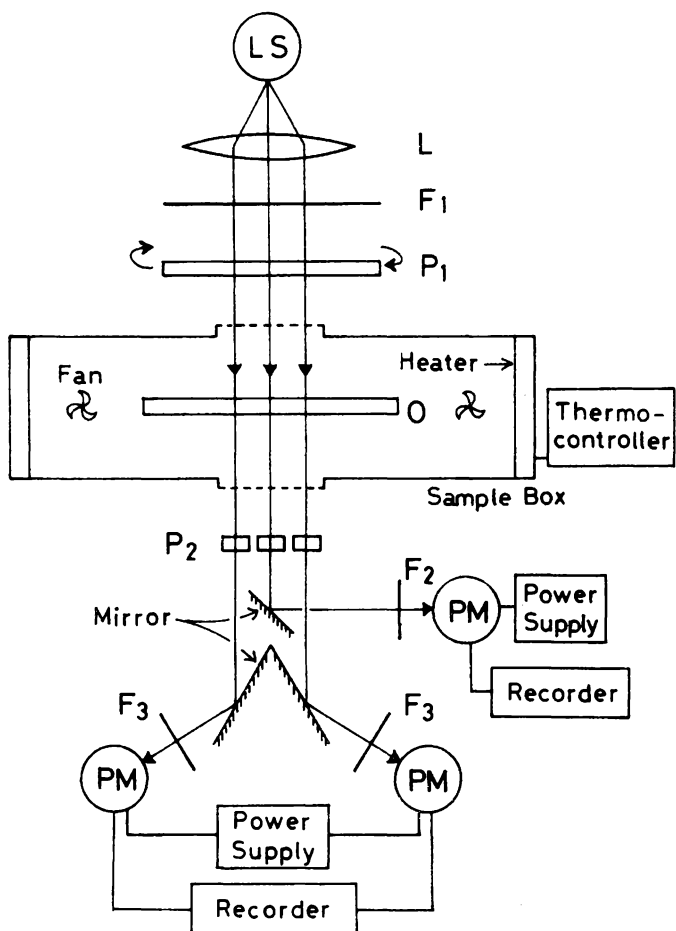
Fig. 6-7. Diagram of the apparatus for measurements.

(The vertical direction is normal to the plane of this

figure.)

By using this apparatus, five independent components of fluorescence intensity and the retardation of the anisotropic medium can be continuously measured, and hence it is possible to analyze the factors of molecular orientation and motion.

References and Note

1) In Chapter 3, it was confirmed that the molecular orientation distribution in stretched PVA-RP films is this type. In Chapter 7, it is to be shown that the type of orientation distribution of fluorescent probes (Diphenyloctatetraene) in stretched poly(vinyl chloride) films is also the ellipsoid of revolution.

2) O. Kratky, Kolloid-Z., <u>64</u>, 213 (1933).

3) See eq. (3-17) and Note (2) in Chapter 3.

CHAPTER 7

Application to Uniaxial Stretching of Polymer Solids

in the Glass-transition Region

7-1. Introduction

In the previous chapters, the theory of fluorescence polar-
ization in the anisotropic system, in which the rotational
motions of fluorescent probes exist, was developed and, conse-
quently, this fluorescence polarization technique was proposed
for studies on the molecular orientation and motion in oriented
polymer solids in the glass-transition region and in the rubbery
state.

In the present and following chapters, the molecular orien-
tation and its relaxation mechanism in uniaxially stretched
polymer films are discussed in relation to the molecular mobility.
The estimation is carried out from the orientation and mobility
factors obtained separately by analyzing the observed components
of fluorescence intensity. Moreover, the anisotropy of the
mobility of fluorescent probes oriented in the stretched polymer
film is discussed in terms of the orientation, mobility, and
orientation-mobility factors.

In this chapter, an example of the experimental result is

shown for uniaxially oriented polymer films in the glass-transition region.

7-2. Experimental

The experiment was carried out for poly(vinyl chloride) (PVC) films in which fluorescent probes, 1,8-Diphenyl-1,3,5,7-octa-tetraene (DPOT; see Fig. 7-1), are dispersed.

Sample Preparation

The film specimen was prepared by casting the cyclohexanone solution of PVC (SG-1100, Nihon Carbide Co.) containing DPOT onto a glass plate at about 40 °C. After evaporating the solvent, the cast film was dried in vacuo at 55 °C. The concentration of DPOT in the film thus prepared was controlled at about 10^{-4} mol/l.[1]

Photophysical Properties of DPOT in PVC Film

The absorption, emission, excitation, and excitation polarization spectra of DPOT in PVC film were measured in order to select the wavelength for excitation of the fluorescent probe and the filter system for transmitting only fluorescence light. These spectra are shown in Fig. 7-2.

The photophysical anisotropy factors of DPOT were estimated as $\langle\cos^2\delta\rangle \approx \langle\cos^2\eta\rangle = 0.960$ from the value of fluorescence aniso-tropy ratio R_0 of an unstretched PVC-DPOT film.[2]

The fluorescence lifetime (τ) of DPOT in PVC film was 7.0 ±
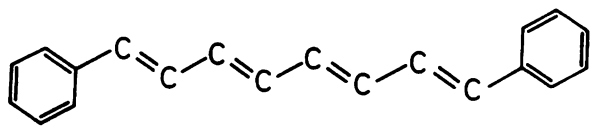
Fig. 7-1. 1,8-Diphenyl-1,3,5,7-octatetraene (DPOT).
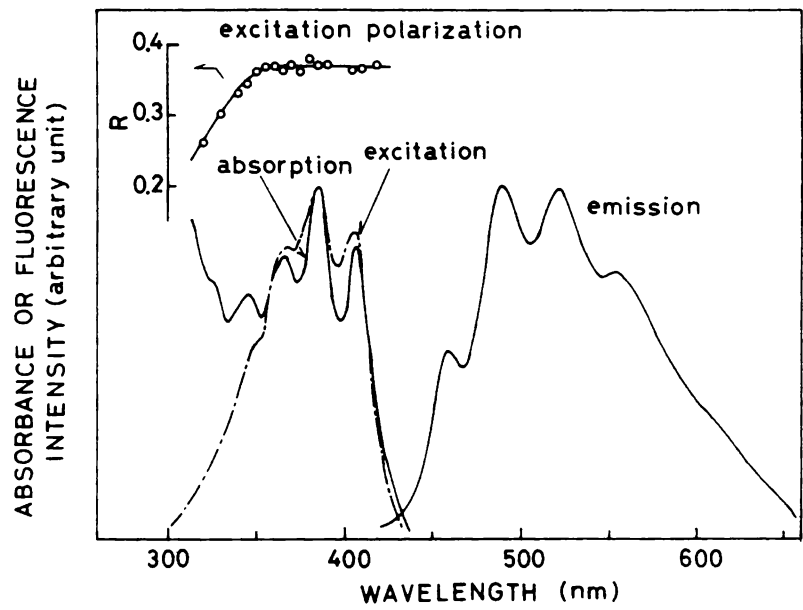
Fig. 7-2. Absorption, emission, excitation, and excitation polarization spectra of DPOT in PVC film.

0.5 ns, which was obtained from the fluorescence decay curve measured by the single photon counting method.[3]

Measurements

Measurement (A): Orientation Relaxation by Heat Treatment (measured at room temperature).

The molecular orientation relaxation by heat treatment of stretched PVC-DPOT films was investigated. The measurement was carried out at room temperature after heat-treating of samples stretched uniaxially at various draw ratios and at various temperatures. As the sample films are sufficiently rigid at room temperature (see Fig. 7-7 shown later), it can be assumed that the molecular motions are restrained in the film specimens used for this experiment. Accordingly, the estimation of molecular orientation relaxation treated here was carried out by using values of the second and fourth moments of the molecular orientation distribution in the stretched and the heat-treated samples, in the same manner as described in Chapter 4. The angular distributions of polarized components of fluorescence intensity (i.e., polar diagram representation) were also used for this estimation. In this case, the diagram should be represented by correcting the birefringence effect as described in Chapter 3.

Measurement (B): Molecular Orientation and Molecular Mobility.

The measurements of molecular orientation and molecular mobility were carried out by analyzing the observed components of fluorescence intensity which were obtained by means of the apparatus described in the preceding chapter (Fig. 6-7), in the following processes; 1) the heating process of a film specimen being in unstretched state, 2) the drawing process of the film, 3) the relaxing process in which the stretched film is kept at a constant length and temperature, and 4) the temperature changing process at a constant length.

Filter Systems for Measurements.

A monochromatic glass filter UV-DIA (UV-D36A at present, Toshiba Elc. Co.) was used as the excitation filter system (F_1) to transmit 365 nm mercury line and a sharp cut-off filter SC-46 (Fuji Photo Film Co.) was used as the observation filter system (F_3) to transmit only fluorescence light. In the case of measurement (B) mentioned above, a monochromatic filter UV-DIA was also used as the filter system (F_2) to transmit exciting light for measuring the retardation of anisotropic sample.

Birefringence Effect.

As the fluorescent probe DPOT was excited by 365 nm mercury line and the fluorescence spectral band of DPOT in PVC film observed through the cut-off filter SC-46 has the maximum peak at 520 nm, the values of λ_i = 365 nm and λ_f = 520 nm were adopted

for the calculation of the birefringence term $\int_0^D \cos\delta_i \cos\delta_f \, dl/D$. ($\lambda_i$ and λ_f are the wavelengths of exciting light and fluorescence; see Chapter 3, eq. (3-12)-(3-14).) The retardations of oriented samples were determined by means of a polarizing microscope (Nikon POH, Nihon Kogaku Co.) for the case of measurement (A), and those for the case of measurement (B) were calculated by using the intensity of transmitted exciting light.

<u>Estimation of Anisotropy of Molecular Mobility</u>

The anisotropy of molecular mobility in the oriented PVC-DPOT film was estimated from the orientation, mobility, and orientation-mobility factors, according to the method discussed in Chapter 6.

7-3. Results and Discussion

7-3, 1. Orientation Relaxation by Heat Treatment (Measured at Room Temperature)

In fig. 7-3, the second moment ($<\cos^2\omega>$) of the orientation distribution of DPOT in PVC films stretched uniaxially at 65 °C, 85 °C, and 110 °C and that of the samples treated at 85 °C and 110 °C at a constant length for about 20 min are plotted against the per cent elongation. These values were all obtained from the measurement at room temperature ($\sim$20 °C) after the stretching or the heat-treating followed by quick cooling. A solid
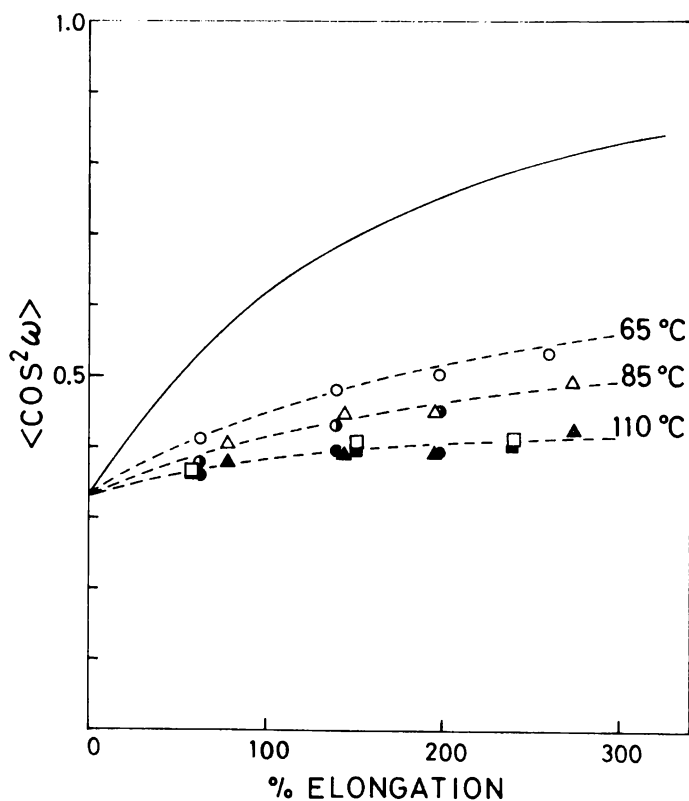
Fig. 7-3. Plot of $<\cos^2\omega>$ versus per cent elongation for PVC-DPOT films.

(a) A series of samples stretched at 65 °C: (O) stretched at 65 °C, (◐) treated at 85 °C for 23 min, (●) treated again at 110 °C for 20 min. (b) A series of samples stretched at 85 °C: (△) stretched at 85 °C, (▲) treated at 110 °C for 20 min.

(c) A series of samples stretched at 110 °C: (□) stretched at 110 °C, (■) treated at 110 °C for 18 min.

Solid line (———): Theoretical curve according to the Kratky type affine deformation model.

line in this figure shows the theoretical curve according to the Kratky type affine deformation mechanism.[4] It turns out from this figure that the degree of orientation depends on the drawing temperature. That is, the lower the drawing temperature, the higher the degree of orientation is observed. (However, a sample film tended to be opaque when it was elongated in the lower temperature range below 60 °C, and a break of film often took place on the drawing when it was elongated in the higher temperature range above 120 °C.) Figure 7-3 also shows a temperature dependence of the orientation relaxation by the heat treatment of stretched samples. The molecular orientation in the sample stretched at 65 °C tends to relax (○→◑) when it was treated at 85 °C, and then this sample treated at 85 °C tends to relax further (◑→●) when it was treated again 110 °C. The similar orientation relaxation phenomena can be observed when the sample stretched at 85 °C was treated at 110 °C (△→▲). However, the orientation of the sample stretched at 110 °C shows no appreciable change when it was treated at 110 °C.

In Fig. 7-4, the relationships between the second moment ($<\cos^2 \omega>$), the fourth moment ($<\cos^4 \omega>$), and the per cent elongation of PVC-DPOT films are shown three-dimensionally in order to reveal the transformation mechanism of the type of molecular orientation distribution. Solid lines in this figure are the theoretical curves according to the Kratky type affine deforma-
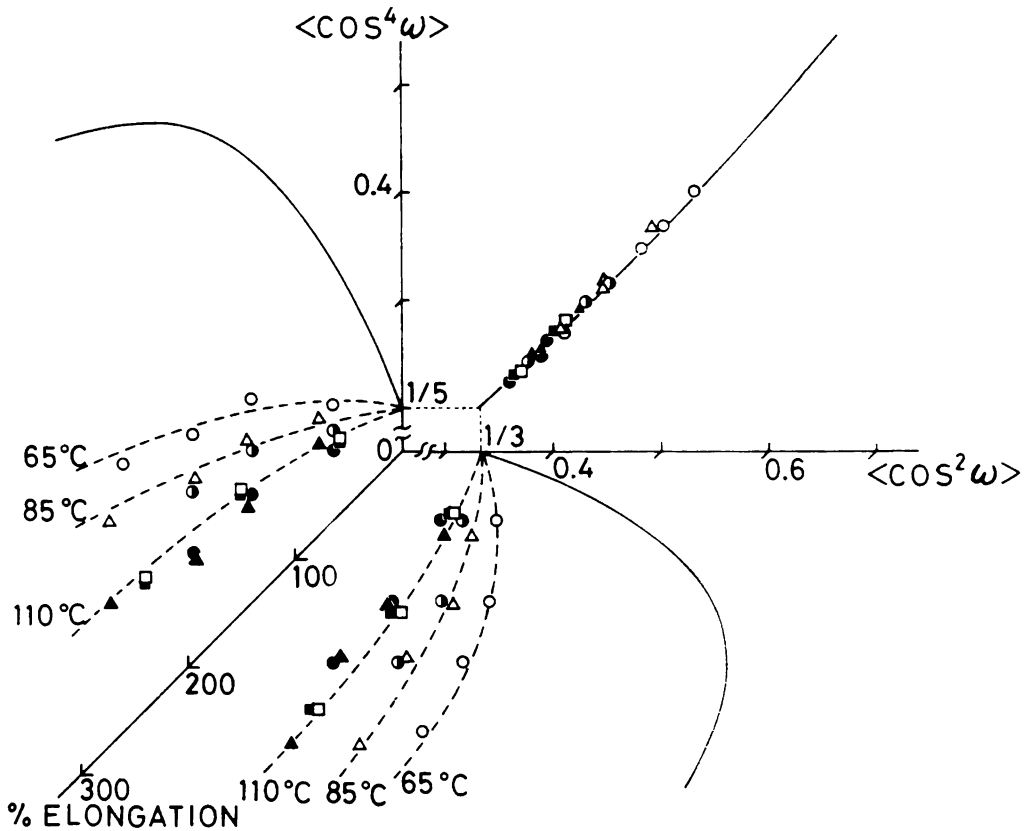
Fig. 7-4. Three-dimensional representation of the relationships

between $\langle \cos^2 \omega \rangle$, $\langle \cos^4 \omega \rangle$, and per cent elongation for PVC-DPOT

films. The symbol marks are the same as in Fig. 7-3.

Solid lines (———): Theoretical curves according to the Kratky

type affine deformation mechanism. The theoretical curve of

$\langle \cos^4 \omega \rangle$ versus $\langle \cos^2 \omega \rangle$ coincides with the relationship assuming

the type of orientation distribution to be the prolate ellipsoid

of revolution.

tion mechanism, and the theoretical curve of $<\cos^4\omega>$ against $<\cos^2\omega>$ also coincides with the relationship assuming the type of orientation distribution to be the prolate ellipsoid of revolution. While the molecular orientation is delayed compared with the affine deformation mechanism for all the series of sample films stretched at three different temperatures, the plots of $<\cos^4\omega>$ against $<\cos^2\omega>$ fit the solid line curve. Therefore, the type of orientation distribution of the molecular axes of fluorescent probes DPOT in PVC film can be explained to be a prolate ellipsoidal distribution, though the deformation mechanism is not exactly the same as the affine transformation mechanism. On the other hand, the type of orientation distribution in samples treated at higher temperature above the drawing temperature remains unchanged as the stretched film were not heat-treated, in spite of the relaxation of the degree of orientation.

The angular distributions of polarized components of fluorescence intensity from PVC-DPOT films are shown in Fig. 7-5, where $I_{\parallel}$ ($-\!\!\bigcirc\!\!-$) and $I_{\perp}$ ($-\!\!\bullet\!\!-$) were obtained by rotating the

Fig. 7-5. Polar diagram representation of the angular distribution of polarized components of fluorescence intensity from the same samples as in Figs. 7-3 and 7-4.

Elongation	60 %	140 %	195 %	255 %
drawn at 65 °C				
heated at 85 °C for 23 min				
heated at 110 °C for 20 min				

Elongation	75 %	144 %	195 %	270 %
drawn at 85 °C				
heated at 110 °C for 20 min				

Elongation	60 %	150 %	240 %
drawn at 110 °C			
heated at 110 °C for 18 min			

sample under the sets of parallel Nicols and crossed Nicols, respectively, of polarizer and analyzer. These polar diagrams are described by correcting the birefringence effect on the fluorescence intensity. At a sight of Fig. 7-5, one can understand the transformation mechanism of molecular orientation distribution.

7-3, 2.   Molecular Orientation and Relaxation Mechanism

in Relation to Molecular Mobility

Unstretched Sample

The temperature dependence of the fluorescence anisotropy ratio (R) of unstretched PVC-DPOT sample is shown in Fig. 7-6. The value of R is constant in the temperature range below ca. 60 °C, whereas it decreases with temperature in the range above ca. 70 °C. This decrease of R is the consequence of the fluorescence depolarization due to the rotational motions of DPOT. In a system of random orientation (i.e., isotropic system), the polarized component of fluorescence intensity depends on the only mobility factor $<(3\cos^2\gamma - 1)/2>_s$, as stated in Chapter 5, and the fluorescence anisotropy ratio can be given in the following form;

$$R = \frac{2}{5} A^2 <(3\cos^2\gamma - 1)/2>_s ,\qquad\qquad (7-1)$$

where
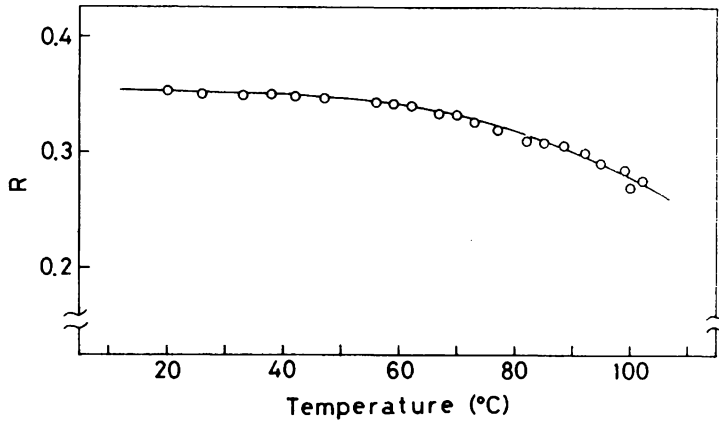
Fig. 7-6. Fluorescence anisotropy ratio, R, versus temperature for unstretched PVC-DPOT film.
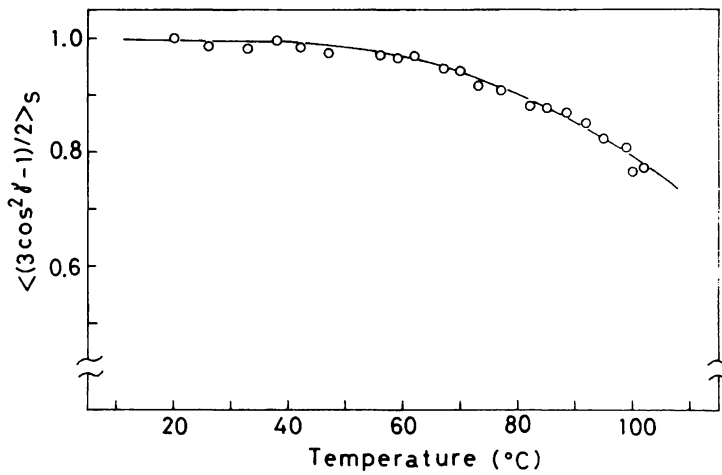
Fig. 7-7. Temperature dependence of the mobility factor, $<(3\cos^2\gamma - 1)/2>_S$, for unstretched PVC-DPOT film.

$$A = (3<\cos^2\delta> - 1)/2 \simeq (3<\cos^2\eta> - 1)/2 \; .$$

Figure 7-7 shows the plot of the mobility factor obtained by using eq. (7-1) against temperature. It is clear that the molecular motions are restrained in the lower temperature range ca. 60 °C and that the molecular mobility increases monotonously in the higher temperature range above 60 °C.

Drawing Process

The experimental results of the drawing process of PVC-DPOT films are shown in Fig. 7-8, where the orientation factor $<(3\cos^2\omega - 1)/2>$, the mobility factor $<(3\cos^2\gamma - 1)/2>_s$, and tensile stress $\tilde{f}$ are plotted against draw ratio during uniaxial stretching at a deformation rate of 40 mm/min at 75 °C and at 100 °C. (The stress $\tilde{f}$ was evaluated by using the value of a cross section of unstretched film.) The value of $<(3\cos^2\omega - 1)/2>$ increases with increasing extent of elongation. Comparing the two molecular orientation behaviors at 75 °C and at 100 °C, the fluorescent probes orient more highly in the sample drawn at 75 °C than that at 100 °C. This result is consistent with that of the measurements in the frozen state (see Fig. 7-3). On the other hand, the molecular mobility is greater at 100 °C than at 75 °C, comparing the values of $<(3\cos^2\gamma - 1)/2>_s$ of the two samples drawn to the same extent.

In both drawings at 75 °C and at 100 °C, the value of

-164-
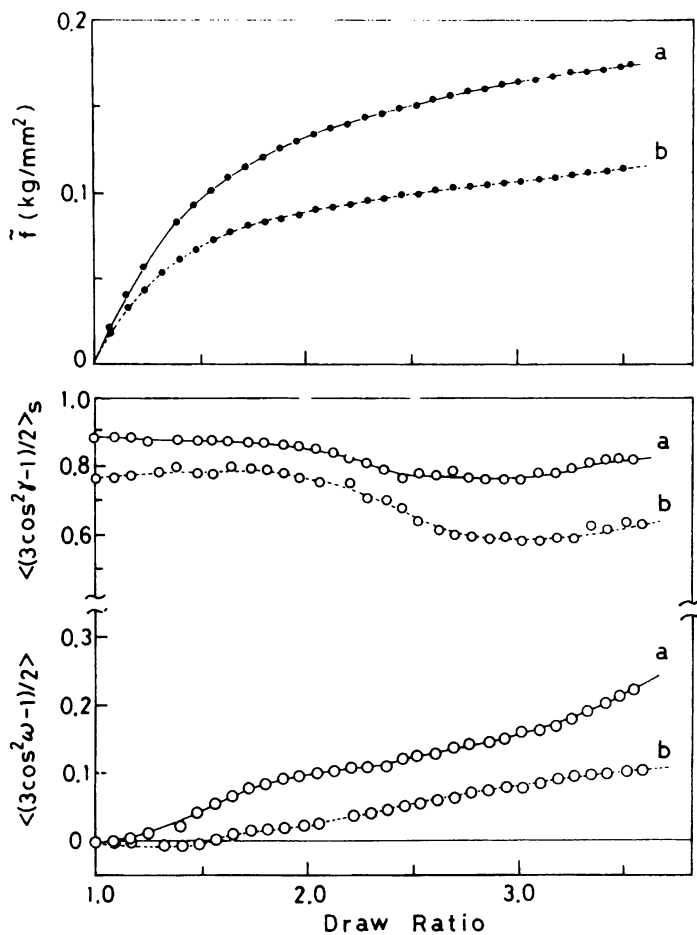
Fig. 7-8. Orientation factor $<(3\cos^2\omega - 1)/2>$, mobility factor $<(3\cos^2\gamma - 1)/2>_s$, and tensile stress $\tilde{f}$ against draw ratio during stretching of PVC-DPOT film at 75 °C (a) and at 100 °C (b).

$<(3\cos^2\gamma - 1)/2>_s$ tends to decrease at a relatively early stage of drawing, then to saturate with increasing of elongation. This implies that the fluorescent probes in PVC film move more actively in the stretched state than in the unstretched state. In the sample film, some regions must exist in which polymer chains can not be oriented without the destruction of the initial structure. Accordingly, the fluorescent probes in such regions can move more easily in PVC film on the drawing process.

Relaxing Process

The experimental results of the relaxing process, in which the stretched samples are kept at a constant length and temperature, are shown in Fig. 7-9. In this figure, f is the stress evaluated by using a cross section of the stretched film after the following temperature changing process. The molecular orientation rapidly relaxes to some extent with time in the range of 20 - 200 sec after drawing, then remains approximately constant. The value of $<(3\cos^2\gamma - 1)/2>_s$ tends to increase slightly with time in the range above 100 sec, that is, the molecular motions seem to be slightly restrained in this relaxing process. The stress decreases monotonously and approaches a constant value with time. Comparing the two results at 75 °C and 100 °C, the degree of orientation relaxation and that of stress relaxation are both somewhat smaller at 100 °C than at 75 °C. However,
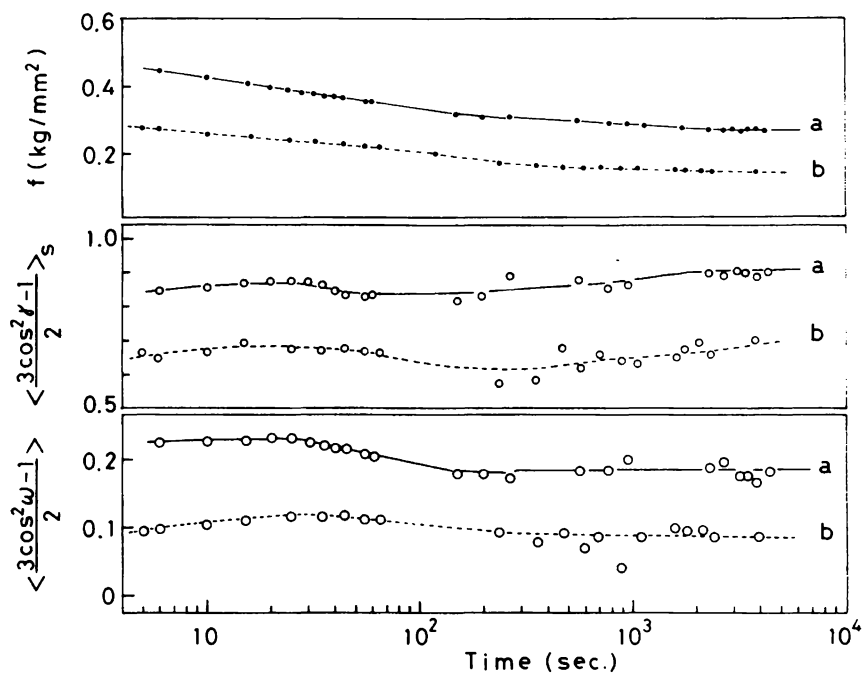
Fig. 7-9. Plots of $<(3\cos^2\omega - 1)/2>$, $<(3\cos^2\gamma - 1)/2>_s$,

and f against time after drawing of PVC-DPOT film at

75 °C (a) and at 100 °C (b).

the orientation relaxation phenomena is not so remarkable at

either temperature. It may be thought that the orientation

mechanism depending on temperature coexisted with the molecular

orientation mechanism at about equiliblium on the drawing process.

Temperature Changing Process

The temperature dependences of orientation factor, mobility

factor, and stress were examined for the stretched PVC-DPOT

samples which had been kept at a constant length and temperature
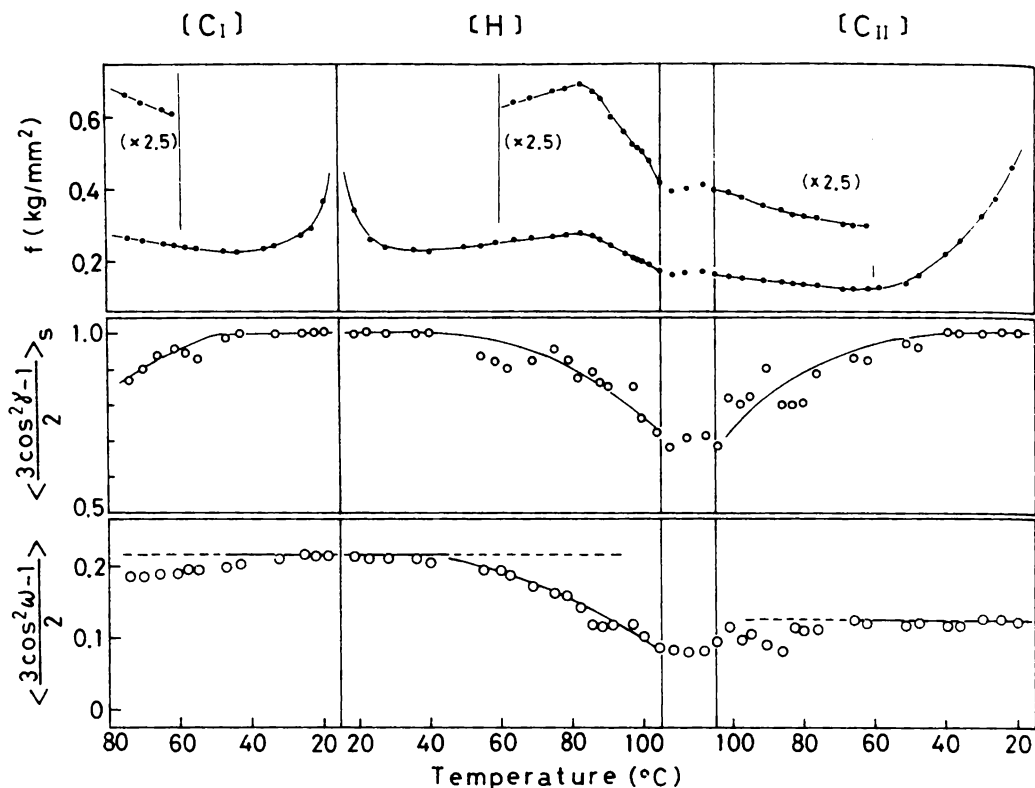
Fig. 7-10a. Temperature dependence of $<(3\cos^2\omega - 1)/2>$, $<(3\cos^2\gamma - 1)/2>_s$, and f for PVC-DPOT sample stretched at 75 °C. $[C_I]$: First cooling process, $[H]$: Heating process, and $[C_{II}]$: Second cooling process. In the stage between the processes $[H]$ and $[C_{II}]$, the sample was kept at about 100 °C for 25 min.

for about 1.5 hours after drawing. The results for the samples drawn at 75 °C and at 100 °C are shown in Figs. 7-10a and 7-10b, respectively.

It is clear from the temperature dependence of $<(3\cos^2\gamma - 1)/2>_s$ that the molecular motions are restrained in the lower

-168-
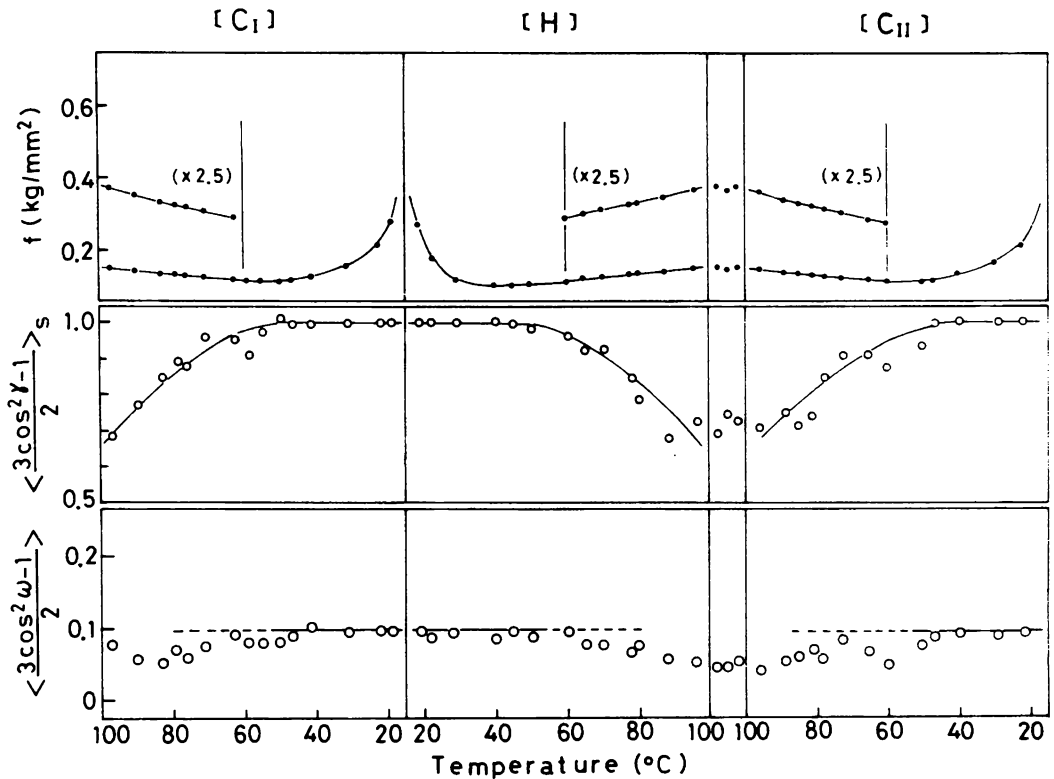
Fig. 7-10b. The same as Fig. 7-10a, but for PVC-DPOT sample stretched at 100 °C.

temperature range and are greater in the higher temperature range for both the samples drawn at 75 °C and 100 °C. It is interesting that the increase of stress according to the increase of entropy, i.e., a so-called 'entropy elasticity' can be observed in the temperature ranges where the value of $<(3\cos^2\gamma - 1)/2>_s$ decreases, except for the range of 80 - 100 °C on the heating process [H] of the sample drawn at 75 °C.

The molecular orientation of PVC-DPOT sample drawn at 100 °C

remains unchanged in lower temperature ranges, however tends to relax to some extent in higher temperature ranges in spite of the increase of the stress with increasing temperature. In Fig. 7-10b, comparing the value of orientation factor at 20 °C on the process $[C_{II}]$ with that at 20 °C on the process $[C_I]$, one can find no appreciable change of the degree of molecular orientation. Accordingly, it can be said that the above mentioned small orientation relaxation in the higher temperature range is reversible for the heat change in this experiment (20 - 100 °C), and that this orientation relaxation occurs only due to the increase of molecular mobility.

On the other hand, the molecular orientation of PVC-DPOT sample drawn at 75 °C remains unchanged in lower temperature ranges for all the processes, but decreases to a considerable extent with increasing temperature on the heating process [H]. In the range of 80 - 100 °C on this process [H], the stress also relaxes notably. In higher temperature ranges except for that of the process [H], a small decrease of $<(3\cos^2\omega - 1)/2>$ can be observed with increasing temperature. This small decrease of molecular orientation is the same reversible relaxation due to the molecular motions as stated for the sample drawn at 100 °C. In Fig. 7-10a, comparing the value of orientation factor at 20 °C on the process $[C_{II}]$ with that at 20 °C on the process $[C_I]$, one can find the molecular orientation remarkably relaxed. This

orientation relaxation can be regarded as an irreversible relax-
ation caused by a large structural change during the stage of
stress relaxation in the range above drawing temperature on the
heating process [H].

From these experimental results of the temperature changing
process, it can be concluded as follows: The oriented structure
of PVC-DPOT film remains stable below the drawing temperature
(D.T.) though the small relaxation occurs due to molecular
motions. However, the orientation decreases remarkably as the
temperature is raised above D.T. Once the film is treated at a
temperature above D.T., the oriented structure is stable again
for the heat change below the treating temperature.

Figure 7-11 shows the relationship between the fourth
moment ($<\cos^4 \omega>$) and the second moment ($<\cos^2 \omega>$) of molecular
orientation distribution obtained at 20 °C on the processes [C_I]
and [C_{II}] for the samples given in Fig. 7-10. It turns out that
the type of molecular orientation distribution is the prolate
ellipsoid of revolution for all the samples. This result is
consistent with that shown in Fig. 7-4.

7-3, 3. Estimation of Anisotropy of Molecular Mobility

Figure 7-12 shows the plots of orientation-mobility factors
against the product of the orientation factor and the mobility
factor for PVC-DPOT sample on the drawing process at 75 °C.

-171-
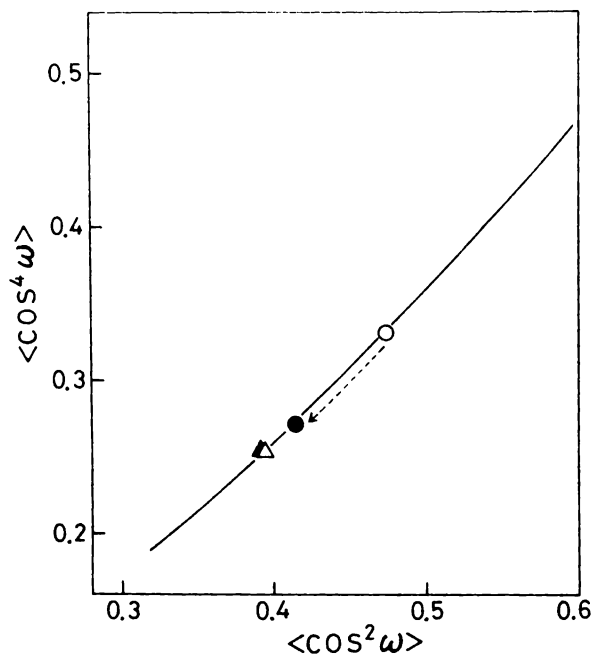
Fig. 7-11. $<\cos^4 \omega>$ versus $<\cos^2 \omega>$, obtained at 20 °C on the processes [C_I] (○,△) and [C_II] (●,▲). Circle: PVC-DPOT stretched at 75 °C, Triangle: PVC-DPOT stretched at 100 °C, Solid line: Theoretical curve according to the rotationally ellipsoidal orientation distribution.

When the molecular mobility is isotropic in the stretched system, the rotational angle γ is independent of the orientation angle ω and hence $<(3\cos^2\omega - 1)/2 \cdot (3\cos^2\gamma - 1)/2>_s$ is equal to $<(3\cos^2\omega - 1)/2><(3\cos^2\gamma - 1)/2>_s$. However, as can be seen from Fig. 7-12a, the anisotropy of molecular motions exists in the stretched sample. The obtained values of $<(3\cos^2\omega - 1)/2 \cdot (3\cos^2\gamma - 1)/2>_s$ are above the diagonal line in Fig. 7-12a. The obtained values

-172-
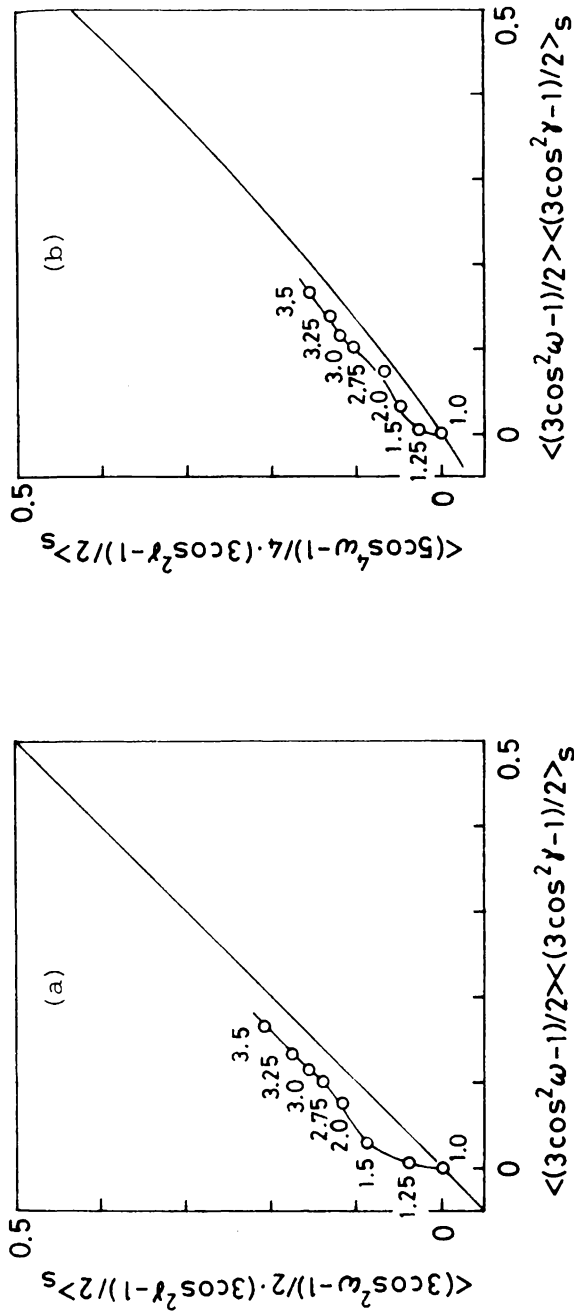
Fig. 7-12. Plots of orientation-mobility factors against the product of orientation and mobility factors for PVC-DPOT sample in the drawing process at 75 °C. Numbers denote the values of draw ratio. (a) $\langle (3\cos^2\omega - 1)/2 \cdot (3\cos^2\gamma - 1)/2 \rangle_s$ vs. $\langle (3\cos^2\omega - 1)/2 \rangle \langle (3\cos^2\gamma - 1)/2 \rangle_s$. Solid line: $\langle (3\cos^2\omega - 1)/2 \cdot (3\cos^2\gamma - 1)/2 \rangle_s = \langle (3\cos^2\omega - 1)/2 \rangle \langle (3\cos^2\gamma - 1)/2 \rangle_s$. (b) $\langle (5\cos^4\omega - 1)/4 \cdot (3\cos^2\gamma - 1)/2 \rangle_s$ vs. $\langle (3\cos^2\omega - 1)/2 \rangle \langle (3\cos^2\gamma - 1)/2 \rangle_s$. Solid line: Theoretical curve of $\langle (5\cos^4\omega - 1)/4 \rangle$ versus $\langle (3\cos^2\omega - 1)/2 \rangle$ for the rotationally ellipsoidal orientation distribution.

of $\langle (5\cos^4\omega - 1)/4 \cdot (3\cos^2\gamma - 1)/2 \rangle_s$ are above the theoretical curve of $\langle (5\cos^4\omega - 1)/4 \rangle$ versus $\langle (3\cos^2\omega - 1)/2 \rangle$ according to the rotationally ellipsoidal orientation distribution in Fig. 7-12b. Comparing these results with those of calculations using models for anisotropic molecular mobility (see Figs. 6-4 and 6-5 in Chapter 6), it can be concluded that fluorescent probes have greater mobility in the directions about perpendicular rather than parallel to the stretching axis.

Figure 7-13 shows the same plots as in Fig. 7-12, but for the sample on the drawing process at 100 °C. In the range where the draw ratio is less than 2, the tendency of anisotropy is the same as in the case of drawing at 75 °C. However, when the draw ratio is larger than 2, the anisotropy tends to disappear with increasing extent of elongation. Because, the molecular mobility is greater at 100 °C than at 75 °C and besides the fluorescent probes overall move more actively and more freely as the deformation of the film progresses.

Figure 7-14 shows the plots of the orientation-mobility factors against the product of the orientation factor and the mobility factor measured in the temperature changing process of PVC-DPOT sample stretched at 75 °C. In the higher temperature ranges where the molecular motions are measurable, the obtained values are above the solid lines in both Figs. 7-14a and 7-14b. Accordingly, it can be said that the motions of fluorescent
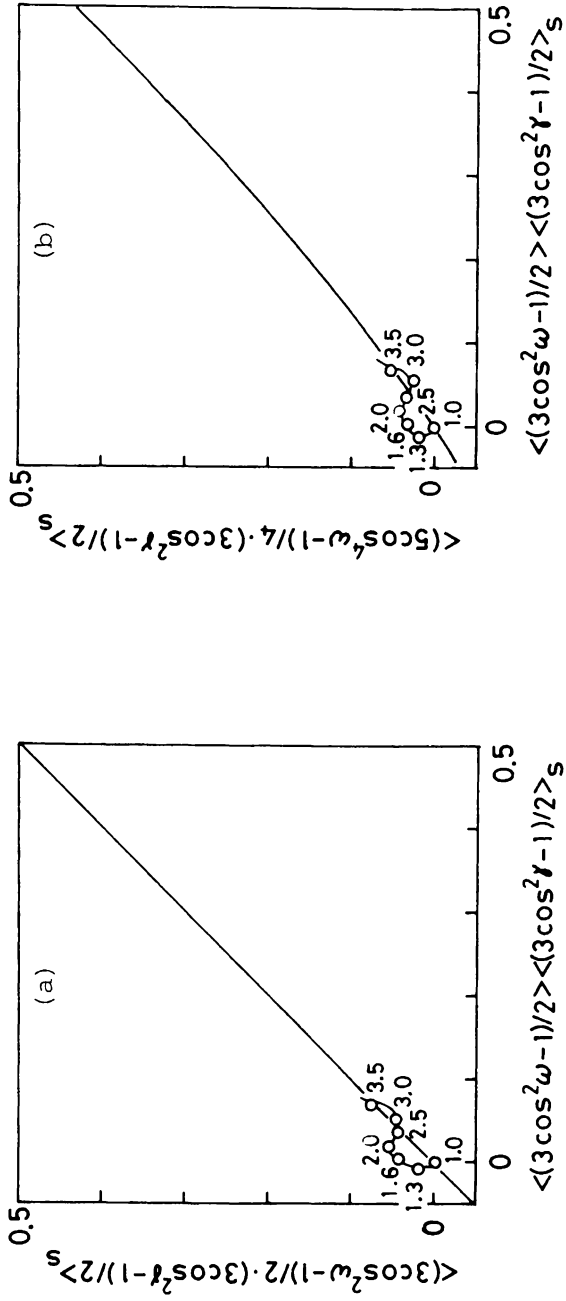
Fig. 7-13. The same as Fig. 7-12, but for the sample in the drawing process at 100 °C.
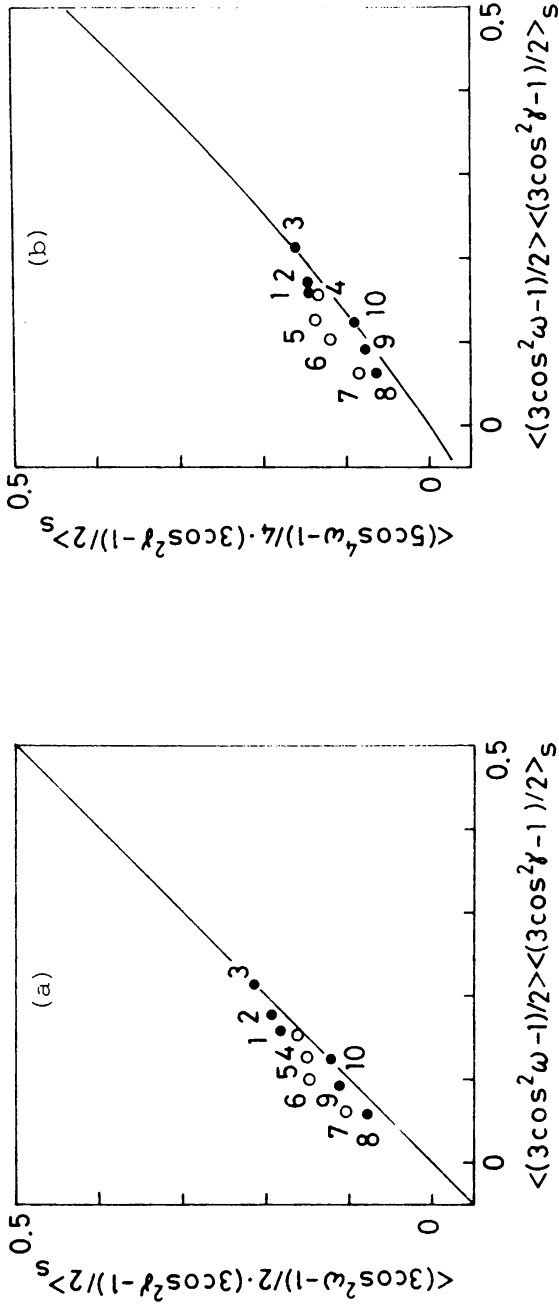
Fig. 7-14. The same as Fig. 7-12, but for the temperature changing process of
PVC-DPOT sample stretched at 75 °C. (1) 74 °C, (2) 61 °C, and (3) 20 °C on the
process [C$_I$]. (4) 69 °C, (5) 82 °C, (6) 92 °C, and (7) 101 °C on the process [C$_{II}$].
(8) 104 °C, (9) 76 °C, and (10) 20 °C on the process [H].

probes oriented parallel to the stretched axis are more restricted, in comparison with those of fluorescent probes oriented perpendicular to the stretched axis. In these figures, the difference between the value obtained at 20 °C on the process $[C_I]$ (● 3) and that at 20 °C on the process $[C_{II}]$ (● 10) corresponds to the irreversible orientation relaxation shown in Fig. 7-11 (O→●).

Figure 7-15 shows the same plots as in Fig. 7-14, but for the temperature changing process for the sample stretched at 100 °C. In these figures (7-15a and 7-15b), the obtained values of the orientation-mobility factors lie in the region where the values obtained on the process $[C_{II}]$ of the sample stretched at 75 °C lie in Fig. 7-14. Because, once the sample drawn at 75 °C is treated at 100 °C, the molecular orientation and motion of the treated sample are almost identical with those of the sample drawn at 100 °C, as discussed previously.

In this chapter, the molecular orientation and its relaxation mechanism in uniaxially stretched PVC-DPOT films have been discussed in relation to the molecular mobility. By using the separately obtained factors characterizing molecular orientation and motion, the orientation and its relaxation phenomena were examined on the drawing process, the relaxing process, and the temperature changing process of PVC-DPOT films. It is interesting that two kinds of orientation relaxation mechanism were observed,
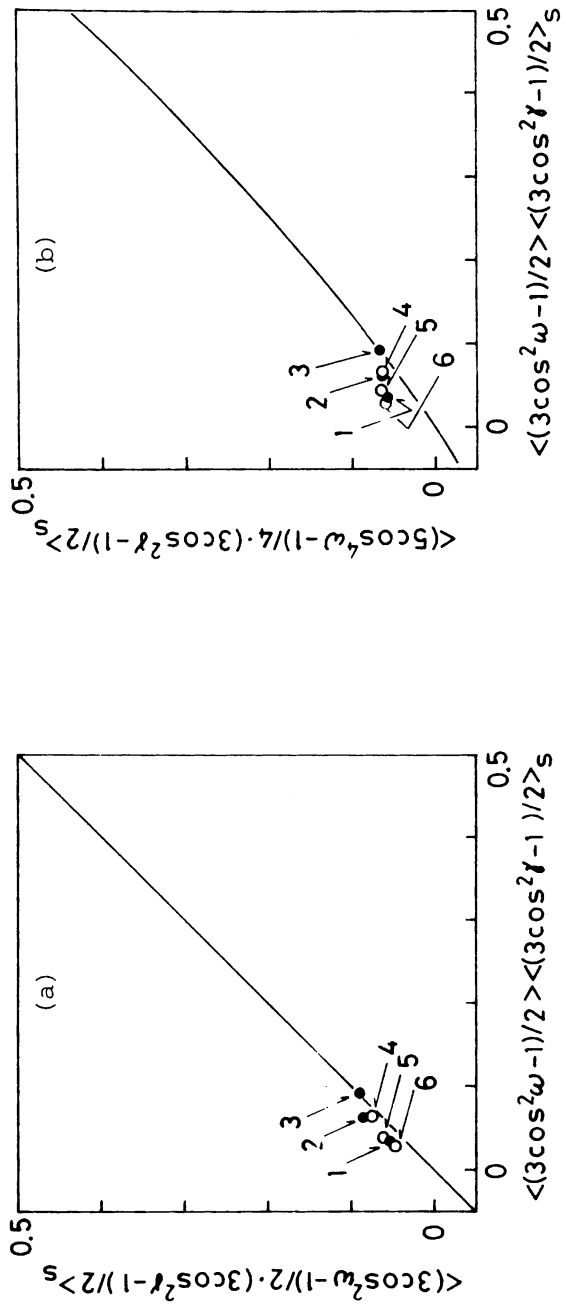
Fig. 7-15. The same as Fig. 7-14, but for the sample stretched at 100 °C.

(1) 90 °C, (2) 79 °C, and (3) 20 °C on the process [C$_I$]. (4) 70 °C, (5) 88 °C,

and (6) 96 °C on the process [H].

that is, one is an irreversible relaxation which occurs remark-
ably in the temperature range above drawing temperature and the
other is a reversible relaxation which occurs due to the molecular
motions. And, the fomer was larger and the latter was smaller in
PVC-DPOT films. Moreover, the anisotropy of molecular mobility
in the oriented system could be discussed in terms of the orien-
tation, mobility, and orientation-mobility factors.

In the following chapter, the experiment is carried out for
crosslinked rubber films. Somewhat different phenomena of the
molecular orientation and its relaxation from those in PVC-DPOT
are expected.

References and Notes

1) The depolarization mechanism caused by energy transfer due
    to high concentration effect is absent in the film specimens
    used here, because values of fluorescence anisotropy ratio
    of unstretched PVC-DPOT films were nearly constant ($\sim$0.36 at
    room temperature) in the concentration range below 3×10^{-4}
    mol/l.

2) When values of parameter B defined in Chapter 3 (see eqs. (3-
    15) and (3-16)) were measured at room temperature for PVC-
    DPOT samples stretched uniaxially at various draw ratios,
    they were independent of the extent of elongation and nearly

equal to unity. Hence the anisotropies of light absorption

and emission of the fluorescent molecule DPOT are nearly

equal to each other. Then, the photophysical anisotropy

factor can be estimated from eq. (3-17).

3) The fluorescence decay curve of DPOT in PVC film is shown in

Fig. 7-16, where the fluorescence intensity (photon counts)

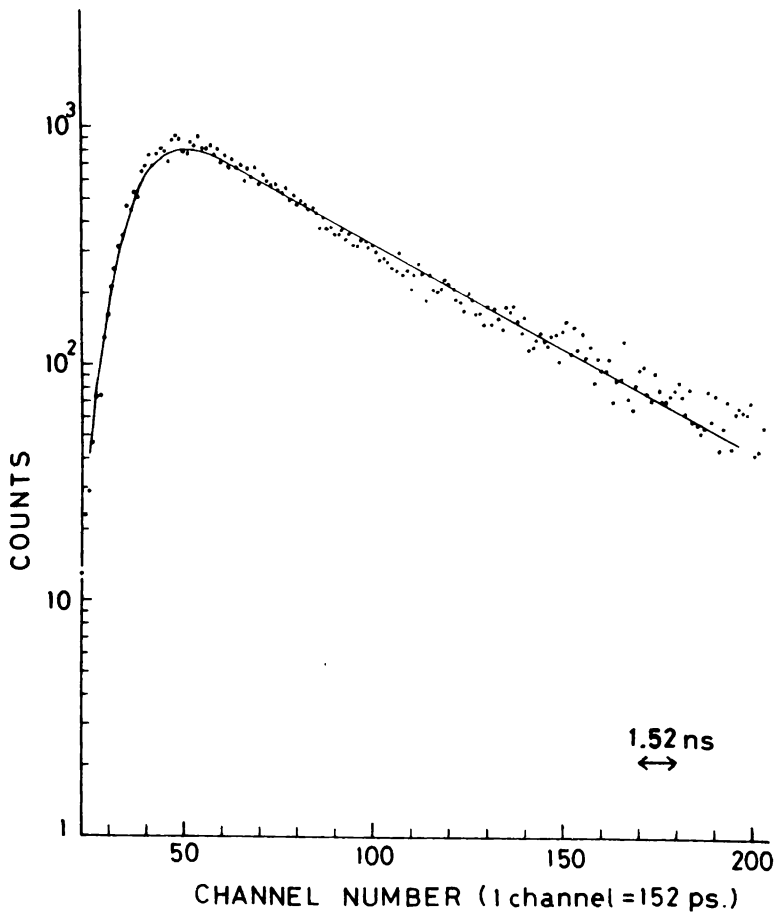is plotted against time. This decay curve was measured by

Fig. 7-16. Decay curve of fluorescence from DPOT in PVC film.

A solid line is the simulated curve of $\tau = 7.0$ ns.

the sigle photon counting method[*)] (Halfwidth of the excitation light pulse $\simeq$ 3.0 ns) using Ortec Inc. system with Hitachi multi-channel analyzer.

*) S. Nishimoto and Y. Nishijima, Ann. Rept. Res. Inst. Chem. Fibers, <u>32</u>, 41 (1975).

4) O. Kratky, Kolloid-Z., <u>64</u>, 213 (1933).

See Chapter 4 of this thesis.

CHAPTER 8

Application to Uniaxial Stretching of Rubber Films

8-1. Introduction

     In Chapters 5 and 6, the fluorescence polarization method
was proposed for studies on the molecular orientation and motion
in anisotropic polymer systems in the glass-transition region
and in the rubbery state. An example of experimental result was
shown for uniaxially oriented PVC-DPOT films in the glass-
transition region in the preceding chapter. In this chapter,
the molecular orientation and its relaxation mechanism are dis-
cussed in relation to the molecular mobility for the case of
natural rubber films.

8-2. Experimental

     Natural rubber films containing stilbene derivative SW (see
Fig. 8-1) as the fluorescent probe were used in the experiment.

Sample Preparation

     Sample films of natural rubber (NR-SW film) were made by
casting the solution of natural rubber in benzene containing
dicumyl peroxide (4 wt% for rubber) and fluorescent probe SW,

then crosslinked by treating at about 130 °C for 15 min under the pressure of 100 kg/cm^2. The concentration of the fluorescent probes in natural rubber film (NR film) was controlled at about 5×10^{-5} mol/l.

Photophysical Properties of SW

The absorption, emission, excitation, and excitation polarization spectra of SW in NR film were measured in order to select the filter systems of the apparatus for measurements. These spectra are shown in Fig. 8-2.

As the values of the photophysical anisotropy factors of this probe, $<\cos^2\delta> \simeq <\cos^2\eta> = 0.957$ was adopted. This value was estimated from the fluorescence anisotropy ratio of unstretched PVC-SW film.[1]

The fluorescence lifetime (τ) of SW is about 1 ns.

Measurements

The measurements of molecular orientation and molecular mobility were carried out in the same way as described in Chapter 7, in the following processes; 1) the temperature changing process of unstretched NR-SW film, 2) the drawing process of NR-SW film, 3) the relaxing process in which the stretched film is kept at a constant length and temperature, and 4) the temperature changing process at a constant length.

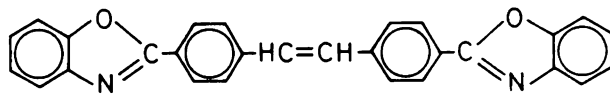The filter systems for the measurements are the same as in

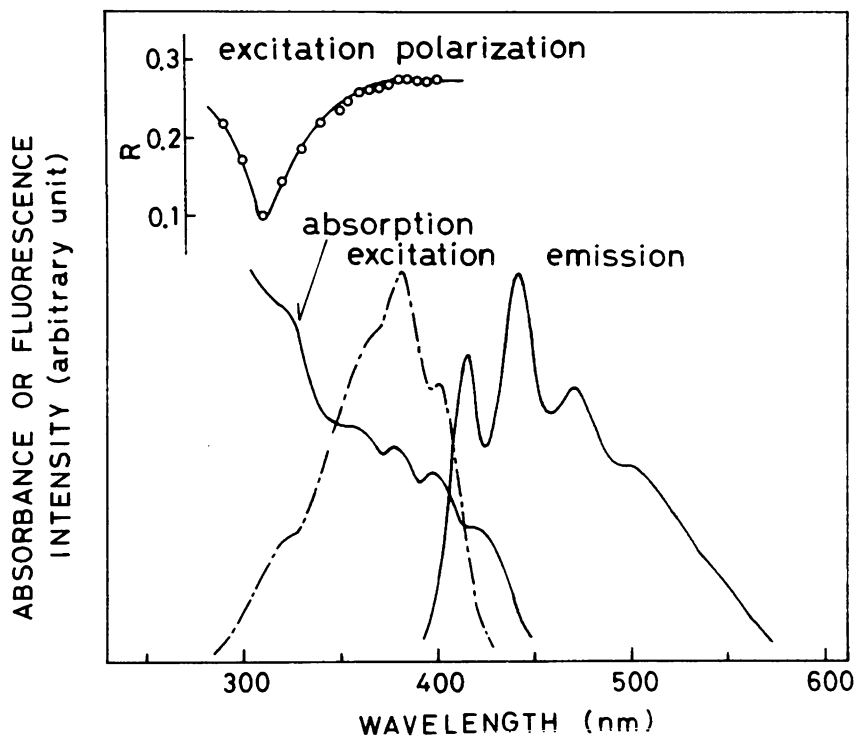Fig. 8-1. Stilbene derivative SW.

Fig. 8-2. Absorption, emission, excitation, and
excitation polarization spectra of SW in NR film.

Chapter 7, except for the use of SC-42 (Fuji Photo Film Co.) with a cut-off wavelength of 420 nm as the observation filter system (F_3). The values of λ_i and λ_f used for the calculation of the birefringence term are 365 nm and 442 nm, respectively. (λ_i and λ_f are the wavelengths of exciting light and observed fluorescence, respectively.)

Estimation of Anisotropy of Molecular Mobility

The anisotropy of molecular mobility in the oriented NR-SW film was estimated by using the orientation, mobility, and orientation-mobility factors, in the same way as in Chapter 7.

8-3.   Results and Discussion

8-3, 1.   Molecular Orientation and Relaxation Mechanism
        in Relation to Molecular Mobility

Unstretched Sample

The temperature dependence of the fluorescence anisotropy ratio (R) and that of the mobility factor ($<(3\cos^2\gamma - 1)/2>_s$) are shown in Figs. 8-3 and 8-4, respectively, for unstretched NR-SW sample. It is clear from these figures that the motions of fluorescent probes SW in NR film become progressively greater as the temperature is raised.
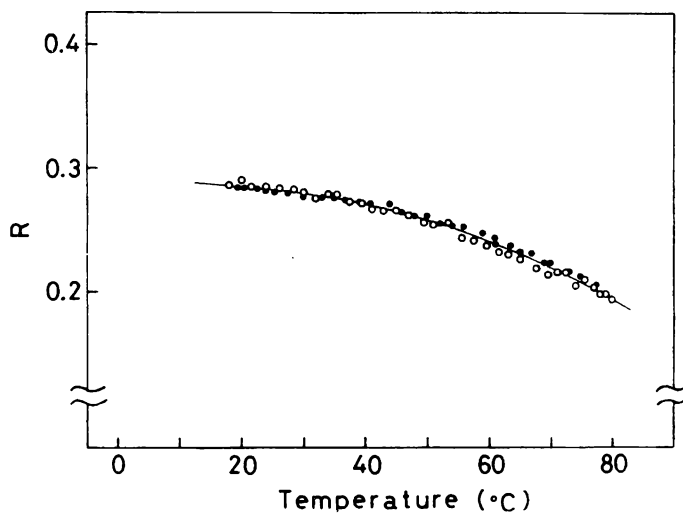
Fig. 8-3. Fluorescence anisotropy ratio versus temperature for unstretched NR-SW film.

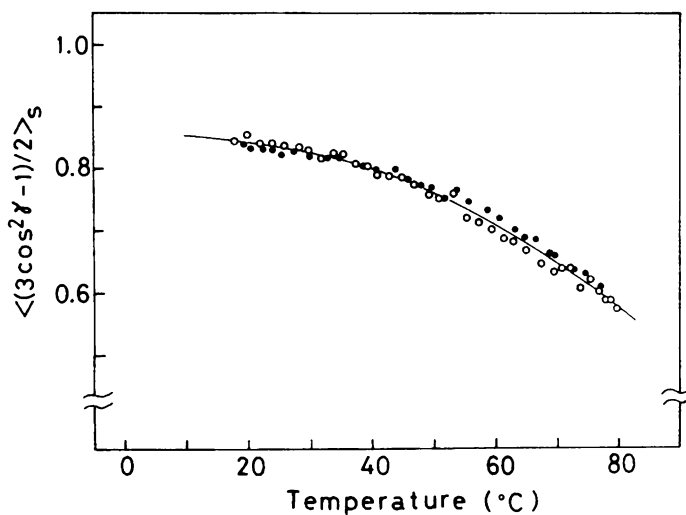(O): heating process, (●): cooling process.

Fig. 8-4. Temperature dependence of the mobility factor for unstretched NR-SW film.

(O): heating process, (●): cooling process.

Drawing Process

The orientation factor $\langle (3\cos^2\omega - 1)/2 \rangle$, the mobility factor $\langle (3\cos^2\gamma - 1)/2 \rangle_s$, and tensile stress of NR-SW film are plotted against draw ratio during uniaxial stretching at a deformation rate of 40 mm/min at 17 °C in Fig. 8-5. In this figure, $\tilde{f}$ and f are the stresses evaluated by using the values of A_0 and $A_0\lambda^{-1}$, respectively (where A_0 is a cross section of the unstretched sample and λ is draw ratio). The plot of tensile stress $\tilde{f}$ versus draw ratio displays the ordinary behavior of crosslinked rubber. At higher draw ratio than 4, the tensile stress $\tilde{f}$ increases rapidly because of the extension of network chains or a crystallization due to the orientation of segments. The value of orientation factor $\langle (3\cos^2\omega - 1)/2 \rangle$ gradually increases with increasing extent of elongation when the draw ratio is less than 3.5, then increases remarkably as it becomes higher than 3.5. On the other hand, the value of mobility factor $\langle (3\cos^2\gamma - 1)/2 \rangle_s$ tends to decrease with increasing extent of elongation in the range of $\lambda < 4$, then gradually increases when the draw ratio is higher than 4. That is to say, the fluorescent probes move more actively on the drawing process of $\lambda < 4$, whereas beyond $\lambda = 4$ the molecular motions seem to be gradually restrained with a remarkable increase of the degree of orientation. It is interesting that the behaviors of molecular orientation and mobility on the drawing process of rubber film have a close
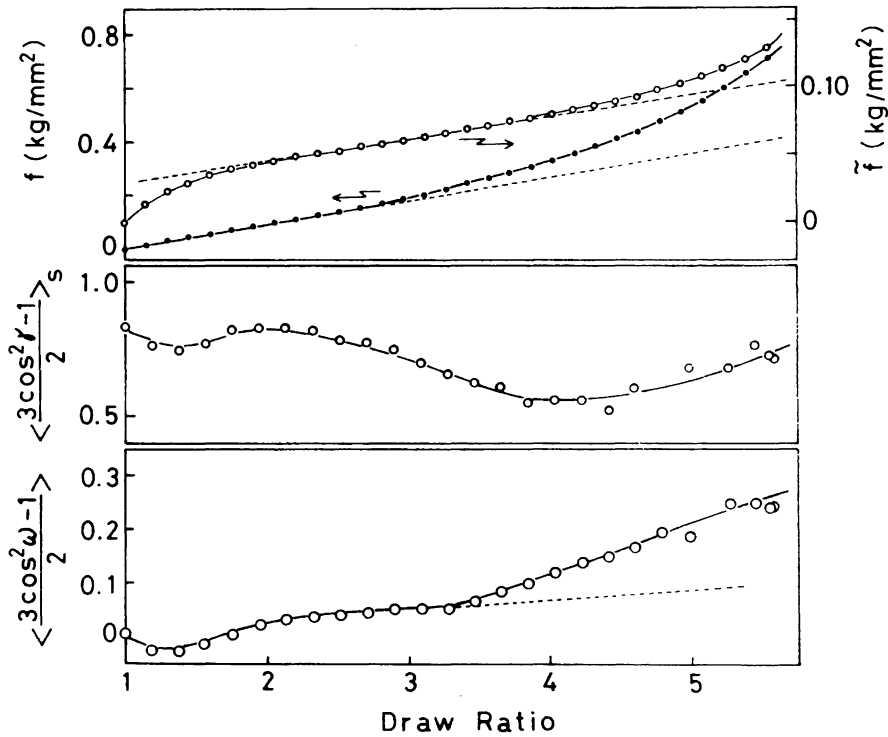
Fig. 8-5. Orientation factor, mobility factor, and tensile stress versus draw ratio during stretching of NR-SW film at 17 °C.

relationship with that of the tensile stress versus draw ratio.

An experimental result of uniaxial stretching of NR-SW film at 65 °C is shown in Fig. 8-6. An increase of molecular orientation with increasing draw ratio at 65 °C is far smaller than at 17 °C. The value of the mobility factor versus draw ratio scarcely changes. Moreover, the tensile stress $\tilde{f}$ versus draw ratio does not increase rapidly even at $\lambda = 5$. It turns out that
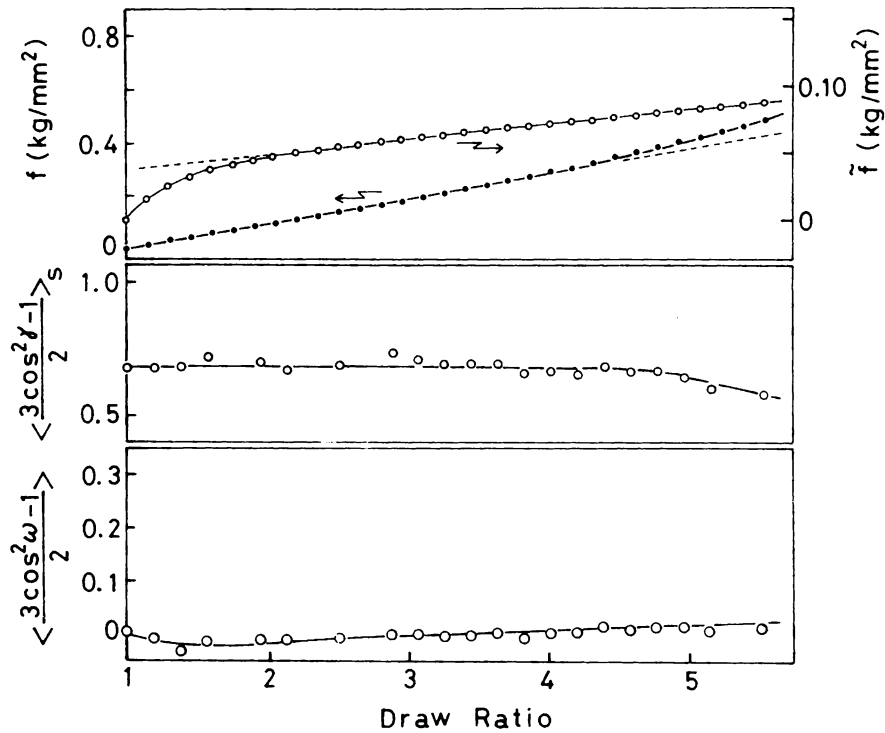
Fig. 8-6. The same as Fig. 8-5, but for NR-SW film

on the drawing process at 65 °C.

network chains in rubber film become more flexible and fluores-

cent probes also become more movable at higher temperature.

This effect of greater mobility of fluorescent probes results

in a scarcely increased molecular orientation.

Relaxing Process

The experimental result of the relaxation process after

drawing at 17 °C is shown in Fig. 8-7. In spite of the decrease

of stress with time, a gradual increase of orientation and a gradual decrease of molecular mobility are observed. This result suggests that the molecular motions are restrained with time by some structural change (e.g., development of oriented crystallization) of deformed network chains.
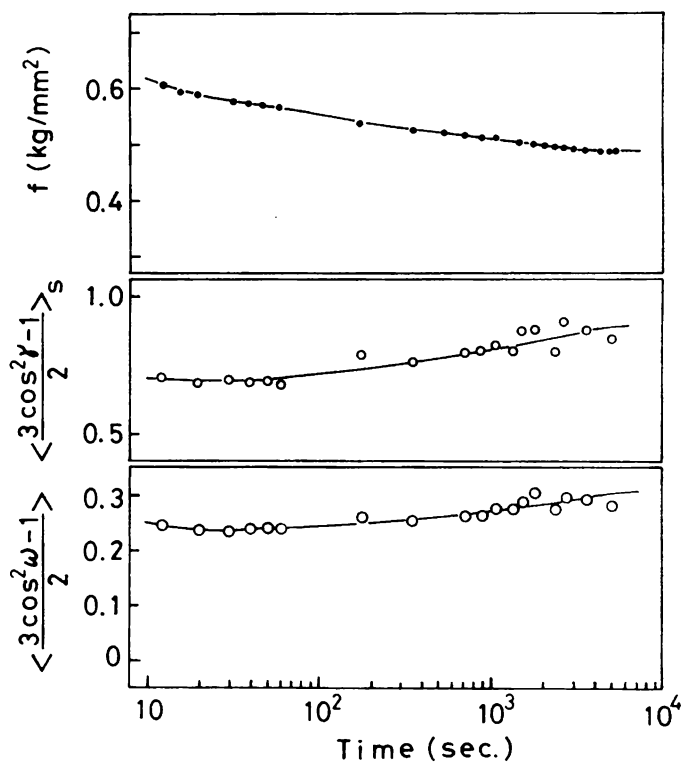

Fig. 8-7. Plots of orientation factor, mobility factor, and stress against time after drawing of NR-SW film at 17 °C.

Figure 8-8 shows the experimental result of the relaxation process after drawing at 65 °C. The molecular orientation and mobility remain almost unchanged during this measurement. Moreover, the stress relaxes only to a small extent compared with that of NR-SW sample drawn at 17 °C. Accordingly, it can be said that the natural rubber film was deformed in a structural equiliblium state during stretching at 65 °C.
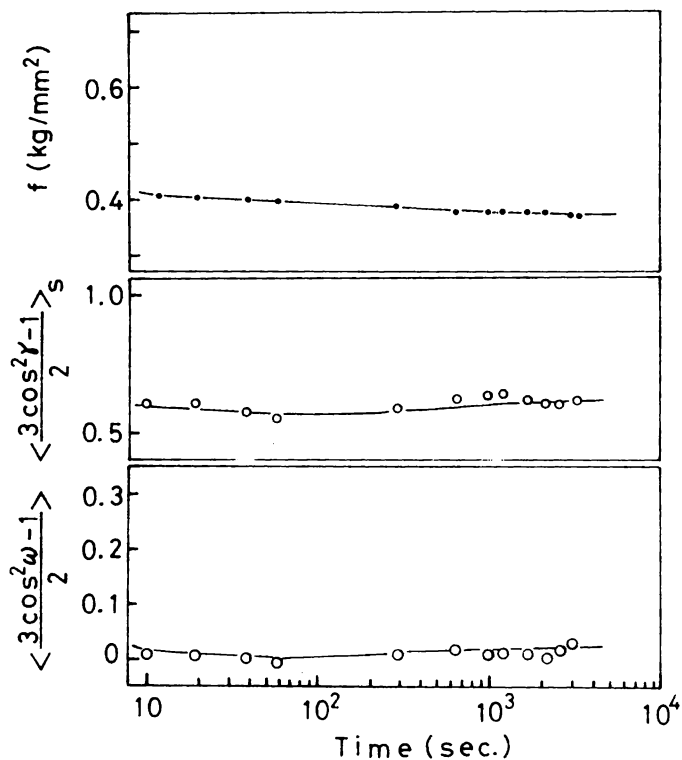

Fig. 8-8. The same as Fig. 8-7, but for NR-SW sample stretched at 65 °C.

Temperature Changing Process

Figure 8-9 shows the result of the temperature changing process of NR-SW sample which was kept at a constant length for about 1.5 hours after drawing at 17 °C. The further relaxation of stress can be observed on the heating process [H]. On the cooling process [C], the decrease of stress according to the decrease of entropy can be observed. On the other hand, the molecular orientation decreases and the molecular mobility increases with increasing temperature on the heating process [H], and the former increases and the latter decreases with decreasing temperature on the cooling process [C]. The flexibility of molecular chains in polymer network such as crosslinked rubber becomes greater with increasing temperature. Therefore, it seems that such an environmental effect on oriented fluorescent probes results in a promotion of their unrestrained motions and, consequently, even in a decrease of the degree of orientation. In this figure, comparing the value of the orientation factor in the initial state of this measurement with that in the final state, one can find that the molecular orientation relaxed to a small extent. This molecular orientation relaxation can be regarded as an irreversible relaxation caused during the earlier stage of stress relaxation on the heating process [H]. The orientation change except for this irreversible relaxation can be regarded as a reversible relaxation which occurs only due to the molecular
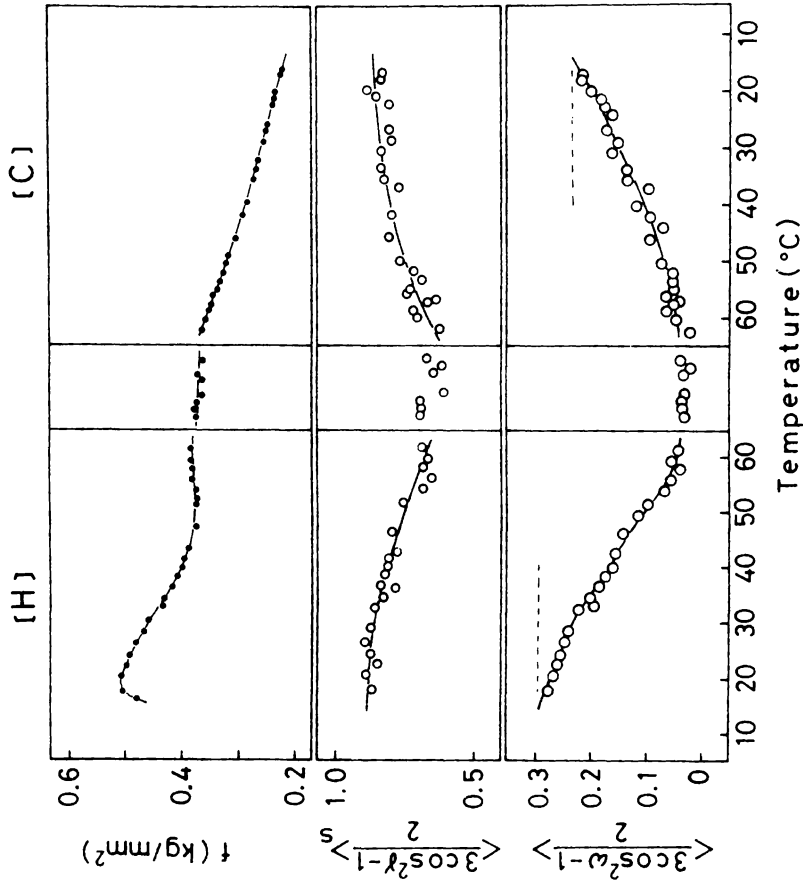
Fig. 8-9. Temperature dependence of orientation factor, mobility factor, and stress for NR-SW sample stretched at 17 °C. [H]: Heating process, [C]: Cooling process. In the stage between the processes [H] and [C], the sample was kept at about 60 °C for 50 min.
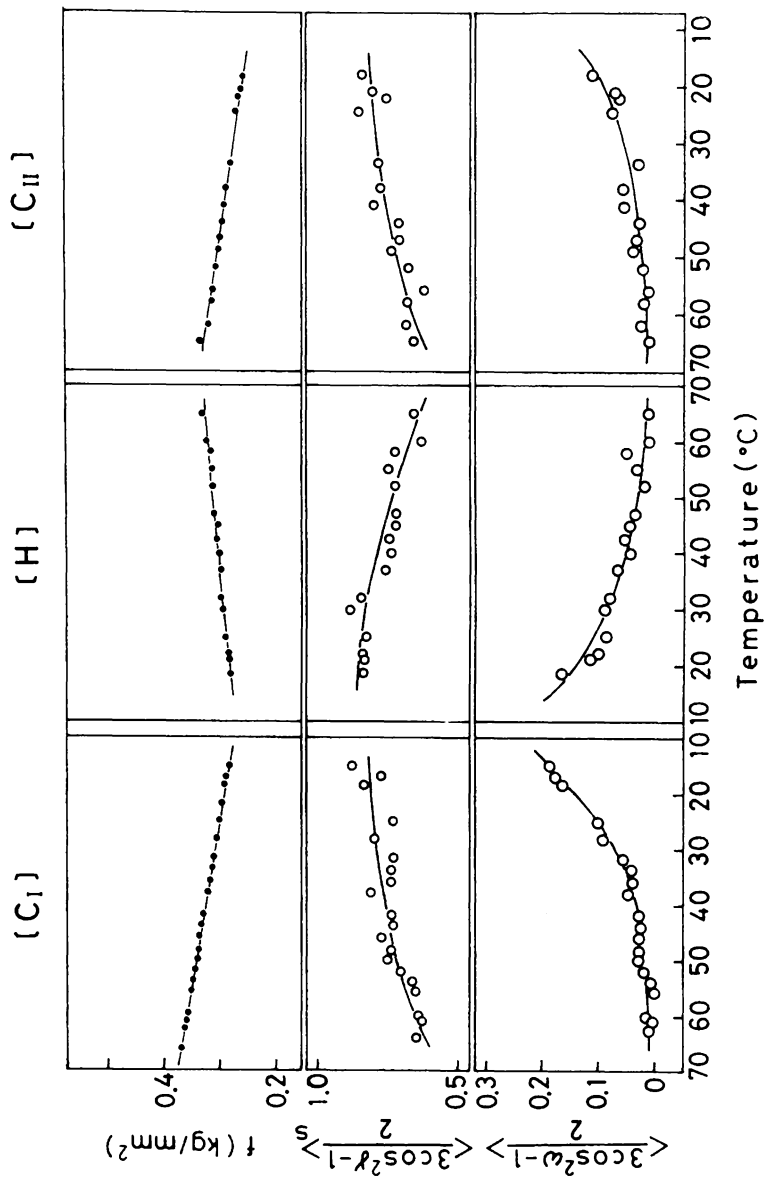
Fig. 8-10. Temperature dependence of orientation factor, mobility factor, and stress

for NR-SW sample stretched at 65 °C. [C_I]: First cooling process, [H]: Heating process,

[C_{II}]: Second cooling process.

motions.

In Fig. 8-10, the plots similar to those in Fig. 8-9 are
shown for NR-SW sample stretched at 65 °C. In all the processes
of heat change, one can find the same tendency of temperature
dependence of orientation, mobility, and stress as shown on the
cooling process [C] in Fig. 8-9. That is to say, the stress
decreases and the molecular orientation increases with a decrease
of molecular mobility, and the former increases and the latter
decreases with an increase of molecular mobility. Such behaviors
of molecular orientation and stress are reversible in the tem-
perature range of this experiment.

Comparing the results of the temperature changing process
of NR-SW films with those in the case of PVC-DPOT films (see
Fig. 7-10 in Chapter 7), it can be said that a reversible orien-
tation relaxation is characteristic of rubber films and an
irreversible orientation relaxation is observed notably in PVC-
DPOT films.

8-3, 2. Estimation of Anisotropy of Molecular Mobility

Orientation-mobility factors are plotted against the product
of the orientation factor and the mobility factor in Fig. 8-11
for NR-SW film in the drawing process at 17 °C. Since the
obtained values are plotted above the solid lines in these
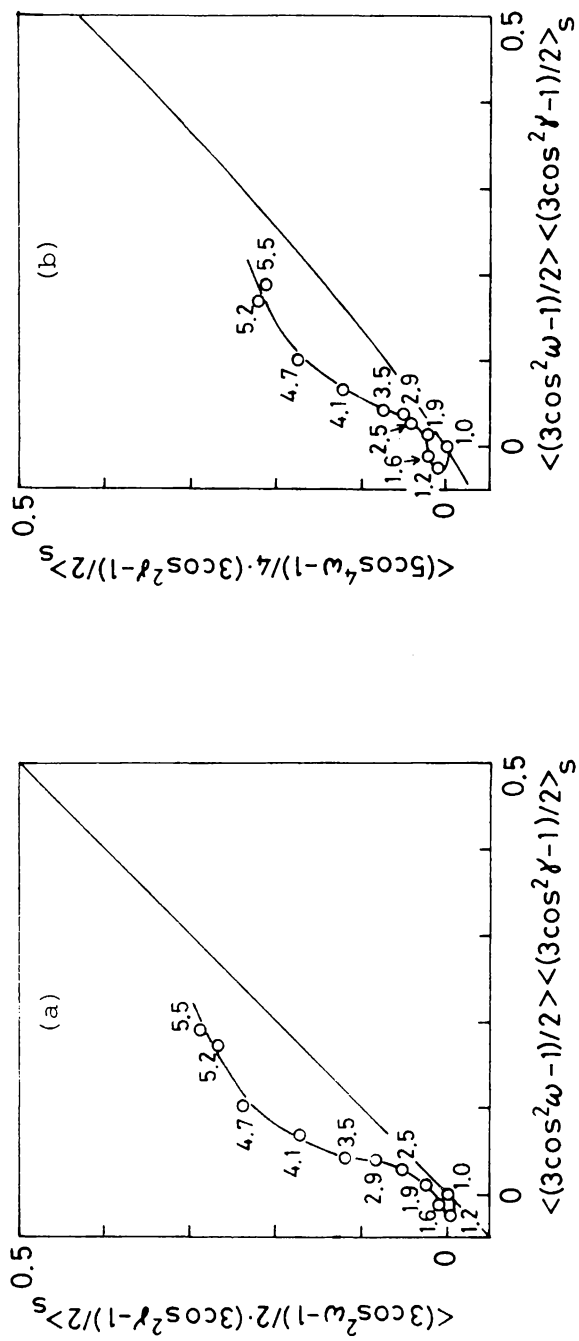figures, the anisotropy of molecular mobility exists in the

Fig. 8-11. Plots of orientation-mobility factors against the product of orientation and mobility factors on the drawing process of NR-SW film at 17 °C. Numbers denote the values of draw ratio (λ). (a) $<(3\cos^2\omega - 1)/2 \cdot (3\cos^2\gamma - 1)/2>_s$ vs. $<(3\cos^2\omega - 1)/2> \cdot <(3\cos^2\gamma - 1)/2>_s$. Solid line: $<(3\cos^2\omega - 1)/2 \cdot (3\cos^2\gamma - 1)/2>_s = <(3\cos^2\omega - 1)/2> \cdot <(3\cos^2\gamma - 1)/2>_s$. (b) $<(5\cos^4\omega - 1)/4 \cdot (3\cos^2\gamma - 1)/2>_s$ vs. $<(3\cos^2\omega - 1)/2> \times <(3\cos^2\gamma - 1)/2>_s$. Solid line: Theoretical curve of $<(5\cos^4\omega - 1)/4>$ versus $<(3\cos^2\omega - 1)/2>_s$ for the rotationally ellipsoidal orientation distribution.
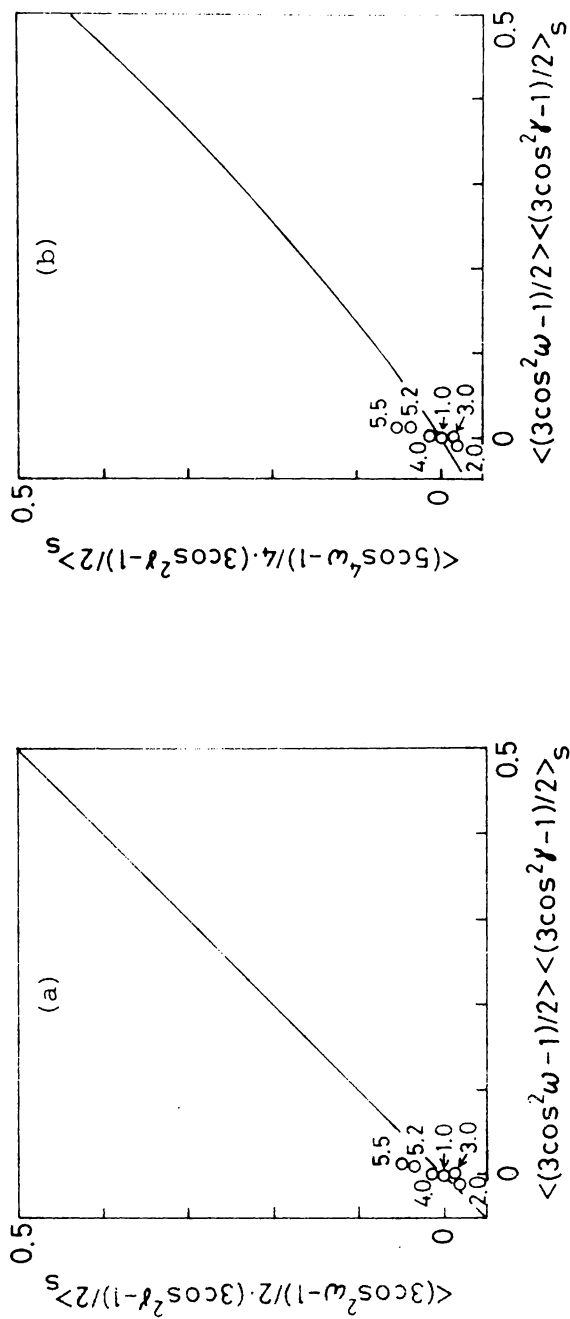
Fig. 8-12. The same as Fig. 8-11, but for the sample in the drawing process at 65 °C.

stretched sample.[2]   Comparing this result with that of calcula-

tions using models for anisotropic molecular mobility,[2] it is

concluded that fluorescent probes in NR film have greater mobility

in the directions about perpendicular rather than parallel to the

stretching axis. The degree of anisotropy is relatively small

in the range of λ < 3.5, however becomes much greater beyond λ =

3.5. That is, especially at the draw ratio of λ > 3.5, the

motions of fluorescent probes oriented parallel to the stretching

axis are more restricted in comparison with those of probes

oriented about perpendicular to the stretching axis. It is

thought that this remarkable anisotropy at the draw ratio above

3.5 results in a gradual increase of $<(3\cos^2\gamma - 1)/2>_s$ in the

range of λ > 4 in Fig. 8-5.

Figure 8-12 shows the same plots as in Fig. 8-11, but for

the sample on the drawing process at 65 °C. The anisotropy of

molecular mobility is scarcely observed in the range of λ < 5.

Because, the molecular mobility is too great at 65 °C for the

fluorescent probes to orient highly, as described in the preced-

ing section.

Figures 8-13 and 8-14 show the plots of orientation-mobility

factors against the product of the orientation factor and the

mobility factor for the temperature changing process of NR-SW

samples stretched at 17 °C and at 65 °C, respectively. The

obtained values lie above the solid lines in these figures for
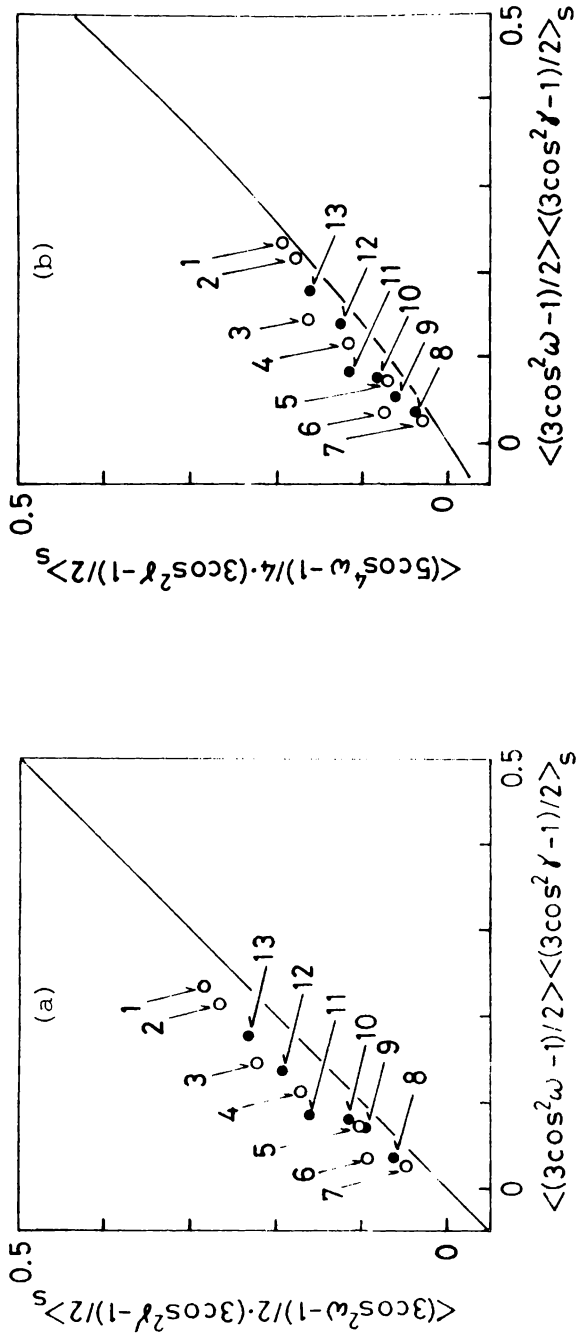
-199-

Fig. 8-13. The same as Fig. 8-11, but for the temperature changing process of NR-SW sample stretched at 17 °C. (1) 18 °C, (2) 23 °C, (3) 35 °C, (4) 43 °C, (5) 51 °C, (6) 56 °C, and (7) 62 °C on the heating process [H]. (8) 55 °C, (9) 42 °C, (10) 37 °C, (11) 32 °C, (12) 27 °C, and (13) 18 °C on the cooling process [C].
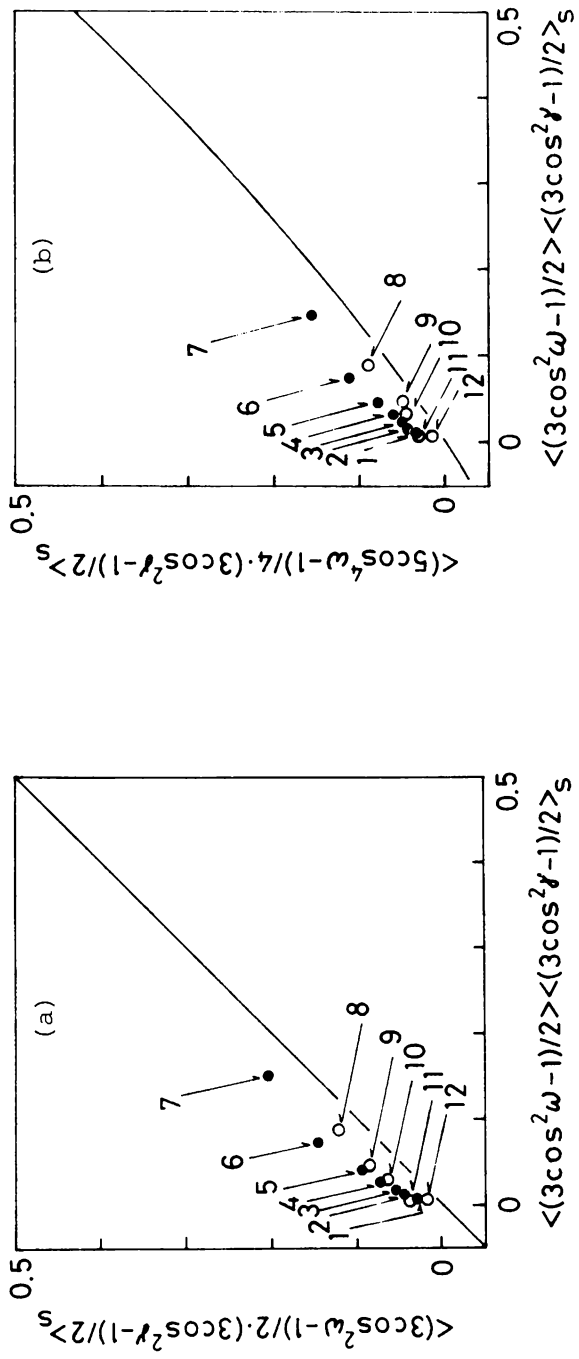
Fig. 8-14. The same as Fig. 8-13, but for the sample stretched at 65 °C.

(1) 62 °C, (2) 52 °C, (3) 42 °C, (4) 36 °C, (5) 32 °C, (6) 25 °C, and (7) 16 °C

on the cooling process $[C_I]$.   (8) 21 °C,   (9) 37 °C,   (10) 40 °C,   (11) 60 °C, and

(12) 65 °C on the heating process [H].

both samples. Hence the molecular motions are more restricted in the direction parallel rather than perpendicular to the stretching axis. However, the degree of anisotropy tends to decrease with increasing temperature. It is clearly shown here that, as the temperature is raised, the molecular motions become more active and freer and besides the molecular orientation relaxes to a considerable extent (see Fig. 8-10).

In this chapter, the theory of fluorescence polarization in the anisotropic system, in which the rotational motions of fluorescent molecules are measurable, has been applied for analyzing molecular orientation and motion in uniaxially oriented natural rubber films. By using the separately obtained factors characterizing molecular orientation and molecular motion, the orientation and its relaxation mechanism in NR-SW films were examined. Moreover, by utilizing the orientation-mobility factors, the anisotropy of molecular mobility could be discussed. Consequently, it was shown that the molecular orientation and its relaxation phenomena in crosslinked rubber films are closely related to the anisotropic molecular mobility. And, a reversible molecular orientation relaxation was observed more remarkably in NR-SW film compared with PVC-DPOT film.

References

1) See Note 3) in Chapter 3 of this thesis.

2) See Chapters 6 and 7 of this thesis.

AII- 1.   Generalization of Transformation Relation

         among Coordinate Systems

     Let us define a direction of a unit vector $\mathbf{v}$ in the O-KLM,

O-K'L'M', and O-abc systems by the sets of polar and azimuthal

angles, (κ,λ), (κ',λ'), and (K,Λ), respectively. The orientations

of the O-KLM and O-K'L'M' frames with respect to the O-abc system

can be specified by the Euler angles $\Omega = (\omega,\varphi,\chi)$ and $\Omega' = (\omega',\varphi',$

$\chi')$, respectively. Let the Euler angles $\Gamma = (\gamma,\psi,\zeta)$ be the

rotation angles of the O-K'L'M' with respect to the O-KLM system.

     Then, the relations among (K,Λ), (κ,λ), and (ω,φ,χ), among

(K,Λ), (κ',λ'), and (ω',φ',χ'), and among (κ,λ), (κ',λ'), and

(γ,ψ,ζ) can be given by eqs. (AII-1), (AII-2), and (AII-3),

respectively, from the expanded Legendre addition theorem.[1,2]

$$Y_{\ell m}(K,\Lambda) = \left(\frac{8\pi^2}{2\ell+1}\right)^{1/2} \sum_{p=-\ell}^{\ell} \Phi_{\ell m p}(\Omega) Y_{\ell p}(\kappa,\lambda) \qquad \text{(AII-1)}$$

$$Y_{\ell m}(K,\Lambda) = \left(\frac{8\pi^2}{2\ell+1}\right)^{1/2} \sum_{n=-\ell}^{\ell} \Phi_{\ell m n}(\Omega') Y_{\ell n}(\kappa',\lambda') \qquad \text{(AII-2)}$$

$$Y_{\ell p}(\kappa,\lambda) = \left(\frac{8\pi^2}{2\ell+1}\right)^{1/2} \sum_{n=-\ell}^{\ell} \Phi_{\ell p n}(\Gamma) Y_{\ell n}(\kappa',\lambda') \ . \qquad \text{(AII-3)}$$

Comparing the equation obtained by substituting eq. (AII-3) into

eq. (AII-1) with eq. (AII-2), we find

$$\Phi_{\ell mn}(\Omega') = \left(\frac{8\pi^2}{2\ell + 1}\right)^{1/2} \sum_{p=-\ell}^{\ell} \Phi_{\ell mp}(\Omega)\, \Phi_{\ell pn}(\Gamma) \ . \qquad \text{(AII-4)}$$

Next, let us consider the case that an excited fluorescent molecule with O-KLM frame oriented at Ω at time t reorients at Ω' at time t' = t + u after k times of small rotation. For each rotation, the transformation relation similar to eq. (AII-4) can be applied. That is,

$$\Phi_{\ell mq_1}(\Omega_1) = \left(\frac{8\pi^2}{2\ell + 1}\right)^{1/2} \sum_{p} \Phi_{\ell mp}(\Omega)\, \Phi_{\ell pq_1}(\Gamma_1) \qquad \text{(AII-5,1)}$$

$$\Phi_{\ell mq_2}(\Omega_2) = \left(\frac{8\pi^2}{2\ell + 1}\right)^{1/2} \sum_{q_1} \Phi_{\ell mq_1}(\Omega_1)\, \Phi_{\ell q_1 q_2}(\Gamma_2) \qquad \text{(AII-5,2)}$$

$$\cdot$$
$$\cdot$$
$$\cdot$$

$$\Phi_{\ell mq_{k-1}}(\Omega_{k-1}) = \left(\frac{8\pi^2}{2\ell + 1}\right)^{1/2} \sum_{q_{k-2}} \Phi_{\ell mq_{k-2}}(\Omega_{k-2})\, \Phi_{\ell q_{k-2} q_{k-1}}(\Gamma_{k-1})$$

$$\text{(AII-5,k-1)}$$

$$\Phi_{\ell mn}(\Omega') = \left(\frac{8\pi^2}{2\ell + 1}\right)^{1/2} \sum_{q_{k-1}} \Phi_{\ell mq_{k-1}}(\Omega_{k-1})\, \Phi_{\ell q_{k-1} n}(\Gamma_k) \ , \quad \text{(AII-5,k)}$$

where Ω_j (j=1,2,$\cdots$,k-1; $\Omega_k = \Omega'$) denotes the Euler angles $(\omega_j, \varphi_j, \chi_j)$ of the molecular coordinate system at t+jΔu (Δu= u/k) with respect to the sample coordinate system O-abc and Γ_j (j=1,2,$\cdots$,k) denotes the Euler angles $(\gamma_j, \psi_j, \zeta_j)$ of the molecular coordinate

system at $t+j\Delta u$ with respect to that at $t+(j-1)\Delta u$.

Repeating substitution of eq. (AII-5,j) into eq. (AII-5,j+1) (j=1,2,$\cdots$,k-1), we obtain

$$\Phi_{\ell mn}(\Omega') = (\frac{8\pi^2}{2\ell + 1})^{k/2} \sum_{p} \sum_{q_1} \cdots \sum_{q_{k-1}} \Phi_{\ell mp}(\Omega) \Phi_{\ell pq_1}(\Gamma_1) \cdots$$

$$\times \Phi_{\ell q_{k-2}q_{k-1}}(\Gamma_{k-1}) \Phi_{\ell q_{k-1}n}(\Gamma_k) . \qquad \text{(AII-6)}$$

By comparing eq. (AII-6) with eq. (AII-4), the following equation can be found:

$$\Phi_{\ell pn}(\Gamma) = (\frac{8\pi^2}{2\ell + 1})^{(k-1)/2} \sum_{q_1} \sum_{q_2} \cdots \sum_{q_{k-1}} \Phi_{\ell pq_1}(\Gamma_1) \Phi_{\ell q_1 q_2}(\Gamma_2) \cdots$$

$$\times \Phi_{\ell q_{k-2}q_{k-1}}(\Gamma_{k-1}) \Phi_{\ell q_{k-1}n}(\Gamma_k) . \qquad \text{(AII-7)}$$

AII-2. Simple Model of Molecular Rotational Motion

For the jth rotation of a fluorescent molecule as mentioned in the preceding section AII-1, let us write the probability of transition from Ω_{j-1} to Ω_j in a concise form, as follows;

$$P(\Omega|\Omega_1) \qquad \text{for the 1st rotation}$$

$$P(\Omega_1|\Omega_2) \qquad \text{for the 2nd rotation}$$

$$\begin{array}{c} \cdot \\ \cdot \\ \cdot \end{array}$$

$$P(\Omega_{k-1}|\Omega') \qquad \text{for the } \underline{k}\text{th rotation.}$$

Then, the probability of transition from Ω to Ω' of the molecule,
$P(\Omega,t|\Omega',t')$, can be represented as

$$P(\Omega,t|\Omega',t')\,d\Omega' = P(\Omega,t|\Gamma,u)\,d\Gamma$$

$$= \int_{\Omega_{k-1}} d\Omega_{k-1} \cdots \int_{\Omega_2} d\Omega_2 \int_{\Omega_1} d\Omega_1\, P(\Omega|\Omega_1)\, P(\Omega_1|\Omega_2) \cdots P(\Omega_{k-1}|\Omega')\ d\Omega'\ .$$

$$\text{(AII-8)}$$

Now, let us suppose that the $\underline{j}$th rotation is independent
of the $\underline{i}$th rotation $(i=1,2,\cdots,j-1)$ and, consequently, that
$P(\Omega_{j-1}|\Omega_j)$ depends solely on the rotation angle Γ_j, i.e.,
$P(\Omega_{j-1}|\Omega_j)\,d\Omega_j = P(\Gamma_j)\,d\Gamma_j$. Moreover, for simplicity, if we treat
the case in which the transition probability depends solely on
the rotation angle γ_j of the M-axis, eq. (AII-8) becomes

$$P(\Omega,t|\Gamma,u)\,d\Gamma = \int_{\Gamma_{k-1}} d\Gamma_{k-1} \cdots \int_{\Gamma_2} d\Gamma_2 \int_{\Gamma_1} d\Gamma_1\, P(\gamma_1)\, P(\gamma_2) \cdots P(\gamma_k)\, d\Gamma_k .$$

$$\text{(AII-9)}$$

By using eqs. (AII-9) and (AII-7), $(3\overline{\cos^2\gamma} - 1)/2$ defined
by eq. (6-4) in Chapter 6 can be reformed in the following
ways;

$$(\overline{3\cos^2\gamma - 1})/2 = \int_\Gamma 2\pi(2/5)^{1/2} \Phi_{200}(\Gamma)P(\Omega,t|\Gamma,u)d\Gamma$$

$$= \prod_{j=1}^{k} \int_{\Gamma_j} 2\pi(2/5)^{1/2} \Phi_{200}(\Gamma_j)P(\gamma_j)d\Gamma_j$$

$$= \prod_{j=1}^{k} (\overline{3\cos^2\gamma_j - 1})/2 \ . \qquad\qquad \text{(AII-10)}$$

In the limit $k \to \infty$,

$$(\overline{3\cos^2\gamma - 1})/2 = \lim_{k\to\infty}\{(\overline{3\cos^2\Delta\gamma - 1})/2\}^k$$

$$\simeq \lim_{k\to\infty} (1 - 3\overline{\Delta\gamma^2}/2)^k \ , \qquad\qquad \text{(AII-11)}$$

where $\qquad\qquad \Delta\gamma = (\sum_{j=1}^{k} \gamma_j)/k$.

By replacing $\overline{\Delta\gamma^2}$ by $2\Delta u/\rho_\omega$,[3)]

$$(\overline{3\cos^2\gamma - 1})/2 = \exp(-3u/\rho_\omega) \ , \qquad\qquad \text{(AII-12)}$$

where ρ_ω is the relaxation time of the rotation of the M-axis orienting at ω.

Consequently, $[(\overline{3\cos^2\gamma - 1})/2]_S$ defined by eq. (6-3) in Chapter 6 becomes

$$[(\overline{3\cos^2\gamma - 1})/2]_S = (1 + 3\tau/\rho_\omega)^{-1} \ . \qquad\qquad \text{(AII-13)}$$

Accordingly, eqs. (6-5), (6-6), and (6-7) can also be reformed
as

$$<(3\cos^2\gamma - 1)/2>_s = <(1 + 3\tau/\rho_\omega)^{-1}> \qquad \text{(AII-14)}$$

$$<(3\cos^2\omega - 1)/2 \cdot (3\cos^2\gamma - 1)/2>_s$$
$$= <(3\cos^2\omega - 1)/2 \cdot (1 + 3\tau/\rho_\omega)^{-1}> \qquad \text{(AII-15)}$$

$$<(5\cos^4\omega - 1)/4 \cdot (3\cos^2\gamma - 1)/2>_s$$
$$= <(5\cos^4\omega - 1)/4 \cdot (1 + 3\tau/\rho_\omega)^{-1}> . \qquad \text{(AII-16)}$$

References and Notes

1) See section 2-3 in Chapter 2. The explicit form of the
    generalized spherical harmonics $\Phi_{\ell mn}$ is given in Appendix I.
    The normalized spherical harmonics $Y_{\ell m}$ is defined as
    $Y_{\ell m} = (2\pi)^{1/2}\Phi_{\ell m0}$ (eq. (2-13)).

2) R. J. Roe, J. Appl. Phys., 36, 2024 (1965).

    M. E. Rose, "Elementary Theory of Angular Momentum", John
    Wiley & Sons, Inc., New York, 1957, Chap. 4.

3) The molecular rotation treated here is assumed to obey the
    'random process', so that the ratio of $\overline{\Delta\gamma^2}$ to Δu is, in
    general, independent of time u.[*)]

*) Y. Nishijima, Ann. Rept. Res. Inst. Chem. Fibers, <u>31</u>, 13 (1974).

SUMMARY

The results of the studies collected in this thesis are
summarized below.

PART I

Chapter 2.

The intrinsic photophysical anisotropy of fluorescent mole-
cules was described by using the probability functions of finding
abosorbing and emitting oscillators in the molecular coordinate
system. Considering the birefringence effect of optically aniso-
tropic medium and using the photophysical **anisotropy** of the
fluorescent probe, the equation for the polarized component of
fluorescence intensity in the molecular oriented system was
derived in the generalized form.

Chapter 3.

The general equation of polarized component of fluorescence
intensity derived in Chapter 2 was applied for the cases of
uniaxially and biaxially oriented systems. Uniaxially stretched
poly(vinyl alcohol) (PVA) and poly(vinyl chloride) (PVC) films
containing stilbene derivative -RP and -SW as the fluorescent
probe, respectively, were used in order to check the validity

of the equation of polarized component of fluorescence intensity

for the optically anisotropic system of uniaxial orientation.

PVA-RP films were also biaxially stretched and used as the aniso-

tropic samples, in order to check the validity of the equation

of polarized component of fluorescence intensity for the opti-

cally anisotropic system of biaxial orientation. The observed

polarized components of fluorescence intensity from the bire-

fringent films were in good agreement with those calculated by

using the equations. As a result of these verifications, we can

obtain the angular distribution of polarized components of

fluorescence intensity exactly corrected for the birefringence

effect.

Chapter 4.

In this chapter, the quantitative estimation of molecular

orientation was carried out, using the second and fourth order

moments obtained by the fluorescence polarization method. The

samples used here are PVA-RP films stretched in four ways; free

width uniaxial stretching, simultaneous biaxial stretching,

successive biaxial stretching, and fixed width uniaxial stretch-

ing. In all the series of samples stretched in the above-

mentioned four ways, the type of orientation distribution of

molecular axes of fluorescent probes in PVA film was explained

to be an ellipsoidal distribution, though the deformation

mechanism is not exactly the same as the affine transformation mechanism. This result suggests that the orientation distribution of polymer chains in the non-crystalline region in PVA film does not show a peculiar type either for the uniaxial or the biaxial deformations. Furthermore, the degree of molecular orientation about the principal axes (a-, b-, and c- axes) of anisotropic sample was also fully discussed. It is an advance that the molecular orientation in biaxially anisotropic systems could be quantitatively estimated by evaluating five moments.

PART II

Chapter 5.

In Part I, the polarized component of fluorescence intensity was calculated under an assumption that fluorescent probes are fixed in the medium during the fluorescence lifetime. This assumption can be satisfied for a sufficiently rigid medium, e.g., as in the case of polymer solids in the glassy state. However, at higher temperatures than T_g, the motions of fluorescent molecules affect the polarized component of fluorescence intensity. In this chapter, the equation for the polarized component of fluorescence intensity was generally described, introducing a function (i.e., the transition probability $P(\Omega, t | \Gamma, u)$) characterizing the rotational motions of fluorescent probes. In order to

analyze the molecular orientation and motion in uniaxially

oriented systems, the simplified equations were discussed and

the following angular factors were defined; the orientation fac-

tor ($<(3\cos^2\omega - 1)/2>$), the mobility factor ($<(3\cos^2\gamma - 1)/2>_s$),

and the orientation-mobility factors ($<(3\cos^2\omega - 1)/2 \cdot (3\cos^2\gamma

- 1)/2>_s$, $<(5\cos^4\omega - 1)/4 \cdot (3\cos^2\gamma - 1)/2>_s$).

Chapter 6.

A method for qualitatively estimating the anisotropy of

molecular mobility from the orientation, mobility, and orien-

tation-mobility factors was proposed. In this chapter, the

procedure for experimentally determining the angular factors

of molecular orientation and motion was also considered and,

consequently, an apparatus for the measurements was designed

and constructed in order to study the molecular orientation,

its relaxation mechanism and molecular motions in deformed

polymer films.

Chapter 7.

Fluorescence polarization technique was applied to studies

on the molecular orientation and its relaxation mechanism in

polymer solids. Poly(vinyl chloride) (PVC) films containing

1,8-Diphenyl-1,3,5,7-octatetraene (DPOT) as the fluorescent

probe were used in the experiment. First, the orientation

relaxation by heat treatment of uniaxially stretched PVC-DPOT films was examined. It was shown that the degree of orientation was dependent on the temperatures for stretching and heat-treating. The type of orientation distribution was a rotational ellipsoid in all the stretched and the heat-treated samples. Secondly, the molecular orientation and its relaxation mechanism were discussed in relation to molecular mobility, by using the orientation factor and the mobility factor. Moreover, the anisotropy of molecular mobility in stretched films was estimated from the orientation, mobility, and orientation-mobility factors. The measurements were carried out on the drawing process, the relaxing process, and the temperature changing process. Some interesting results were obtained: 1) On the drawing process, the molecular mobility which is averaged over all fluorescent probes in the stretched sample became greater than in the unstretched state. This result suggests the existence of some regions in which polymer chains can not be oriented without the destruction of the initial structure. Such a structural change influences the motions of fluorescent probes as a local environmental effect. 2) Two kinds of orientation relaxation phenomena were observed on the temperature changing process. That is, one is an irreversible relaxation which occurs remarkably in the high temperature range above the drawing temperature, and the other is a reversible relaxation which occurs only due to the increase of

molecular mobility. The former was more remarkable than the

latter in PVC-DPOT. 3) The anisotropic molecular mobility was

measured in the higher temperature range in oriented PVC-DPOT

film. Fluorescent molecules have greater mobility in the direc-

tions about perpendicular rather than parallel to the stretching

axis.

Chapter 8.

The fluorescence polarization technique was applied to the

studies on molecular orientation and relaxation phenomena in

rubber films. The molecular orientation and its relaxation

mechanism in crosslinked natural rubber (NR) films were inves-

tigated in relation to the molecular mobility, by using stilbene

derivative SW as the fluorescent probe. The anisotropy of

molecular mobility was also studied, using the orientation,

mobility, and orientation-mobility factors. The measurements

were carried out on the uniaxial drawing process, the relaxing

process, and the temperature changing process. The experimental

results shows that there is a close relationship among molecular

orientation behavior, molecular mobility, and tensile stress.

In stretched NR-SW films, an increase of stress according to

the increase of entropy was notably observed in the temperature

range where the molecular mobility became greater with increasing

temperature. A reversible orientation relaxation, which occurs

only due to the increase of molecular mobility, was more remark-
ably observed in the rubber system than the case of PVC-DPOT films.
It was clarified that the molecular orientation and its relaxa-
tion phenomena in crosslinked NR films are closely related to the
anisotropic molecular mobility.

LIST OF PUBLICATIONS

Intramolecular Exciplex Formation in Oriented Polymer Solid
Matrix

Yoshiyuki Nishio, Masahide Yamamoto, and Yasunori Nishijima

Repts. Progr. Polymer Phys. Japan, 21, 389 (1978).

General Analysis of Fluorescence Polarization in the Anisotropic
System (I) Theoretical Treatment

Yoshiyuki Nishio, Yoshihiko Onogi, and Yasunori Nishijima

Repts. Progr. Polymer Phys. Japan, 22, 465 (1979).

General Analysis of Fluorescence Polarization in the Anisotropic
System (II) Experimental Verification for the Case of
Uniaxially Oriented Polymer Films

Yoshiyuki Nishio, Hideo Tanaka, Yoshihiko Onogi, and
Yasunori Nishijima

Repts. Progr. Polymer Phys. Japan, 22, 469 (1979).

Studies on Molecular Orientation Relaxation and Molecular
Motion in Polymer Solid System by the Fluorescence Polarization
Method (I)

Yoshiyuki Nishio, Hideo Tanaka, and Yasunori Nishijima

Repts. Progr. Polymer Phys. Japan, 22, 473 (1979).

Studies on Molecular Orientation Relaxation and Molecular
Motion in Polymer Solid System by the Fluorescence Polarization
Method (II)

Hideo Tanaka, Yoshiyuki Nishio, Yoshihiko Onogi, and
Yasunori Nishijima

Repts. Progr. Polymer Phys. Japan, 23, 563 (1980).

Studies on Molecular Orientation Relaxation and Molecular
Motion in Polymer Solid System by the Fluorescence Polarization
Method (III)

Yoshiyuki Nishio, Yoshihiko Onogi, and Yasunori Nishijima

Repts. Progr. Polymer Phys. Japan, 24, 485 (1981).

Structural Analysis of Polymer Solids by the Fluorescence
Polarization: (I) Characterization of Molecular Orientation
in Stretched Polymer Films.

Yoshiyuki Nishio, Yoshihiko Onogi, and Yasunori Nishijima

in preparation

Structural Analysis of Polymer Solids by the Fluorescence
Polarization: (II) Characterization of Molecular Motion and
Orientation Relaxation in Strethced Polymer Films.

Yoshiyuki Nishio, Yoshihiko Onogi, and Yasunori Nishijima

in preparation

collaboration.

The author wishes to thank his colleagues in the Nishijima Laboratory for their kind help in many ways.

Finally, the author would like to express his thanks to his wife, Keiko, for her constant encouragement during the course of this work.

September 1981   Yoshiyuki NISHIO

Errata

page	line	printed	should read
ii	8	Strethced	Stretched
iv	2	Strethcing	Stretching
xii	20	time	Time.
	21	time	Time
77	18	thse	these
83	3	fifferent	different
90	3	firure	figure
100	5	correspnd	correspond
	14	light	lights
142	4	dtermined	determined
156	16	fig.	Fig.
160	14	film	films
167	2-3	orientation mechanism	orientation relaxation mechanism
	4	equiliblium	equilibrium
179	4	fomer	former
181	1	sigle	single
192	7	equiliblium	equilibrium
213	8	abosorbing	absorbing